
Electronic Thesis and Dissertation Repository

12-16-2016 12:00 AM

Evidence of a Role for G Protein Signaling Modulator 3 in Cell Division

Drew C. Wallace
The University of Western Ontario

Supervisor
Dr. Peter Chidiac
The University of Western Ontario Joint Supervisor
Dr. Greg Kelly
The University of Western Ontario

Graduate Program in Developmental Biology
A thesis submitted in partial fulfillment of the requirements for the degree in Master of Science
© Drew C. Wallace 2016

Follow this and additional works at: <https://ir.lib.uwo.ca/etd>



Part of the [Cell Biology Commons](#), and the [Developmental Biology Commons](#)

Recommended Citation

Wallace, Drew C., "Evidence of a Role for G Protein Signaling Modulator 3 in Cell Division" (2016).
Electronic Thesis and Dissertation Repository. 4279.
<https://ir.lib.uwo.ca/etd/4279>

This Dissertation/Thesis is brought to you for free and open access by Scholarship@Western. It has been accepted for inclusion in Electronic Thesis and Dissertation Repository by an authorized administrator of Scholarship@Western. For more information, please contact wlsadmin@uwo.ca.

ABSTRACT

Components of G protein-mediated signaling are associated with positioning and orienting the mitotic spindle in the process of cell division. However, a functional role for G protein signaling modulator 3 (GPSM3) in cell division has yet to be defined. The purpose of this study was to investigate a potential role for GPSM3 in cell division. Vascular smooth muscle cells (VSMCs) from Wistar-Kyoto (WKY) and spontaneously hypertensive (SHR) rats, that are known to express GPSM3, were used as a model system. Here I report that GPSM3 mRNA and protein levels varied during different stages of the cell cycle in SHR VSMCs. In HEK-293 cells, overexpressing GPSM3 resulted in an increased rate of proliferation. Finally, during metaphase, anaphase, and telophase, GPSM3 and β -tubulin co-localize at the mitotic spindle and midbody. Overall, this study provides evidence of a role for GPSM3 in cell division, likely via an interaction with the mitotic spindle.

KEYWORDS

G protein-mediated signaling, G protein signaling modulator 3 (GPSM3), cell division, proliferation, mitotic spindle, vascular smooth muscle cell (VSMC)

ACKNOWLEDGEMENTS

I would like to sincerely thank my supervisor, Dr. Peter Chidiac, who has been a great mentor and friend during the pursuit of this degree. I will never forget the advice and direction you provided during my research, the many life lessons you taught me, or the difference between media and medium. I am also thankful for my co-supervisor, Dr. Greg Kelly, and my advisory committee members, Drs. Kathleen Hill, John Di Guglielmo, and Jim Karagiannis.

I would like to thank the members of the Chidiac Lab – Katherine Lee, Patrick Stockwell, Jenny Wang, Anette Surmanski, Brandon Kim, Nicole Arseneau, Abby Tong, Yue Zhao, and Alexey Pereverzev – who have helped get me to where I am today. I also want to thank Eddie Chan, Dr. Sharon Lu, Christie Vanderboor, Pierre Thibeault, Dr. Robert Gros, Magda Dragan, Lin Zhao, and the staff of both the Biology and the Physiology and Pharmacology offices for all of their help over the years. It has been a pleasure working with all of you.

Finally, I would like to thank my family for always supporting me and making sure there is never a dull moment in my life. Reid – who always goes his own way and inspires me to do the same. Margot – who is the strongest person I know. Mom – who is the bravest person I know. Dad – who always tries his hardest. And Mickey – who always has our best interests in her heart.

Thank you all so much.

TABLE OF CONTENTS

Abstract.....	ii
Acknowledgements.....	iii
Table of Contents.....	iv
List of Figures.....	viii
List of Tables.....	xi
List of Appendices.....	xii
List of Abbreviations.....	xiii
Chapter 1 – Introduction.....	1
1.1 G PROTEIN SIGNALING.....	1
1.1.1 G PROTEIN SIGNALING OVERVIEW.....	1
1.1.2 G PROTEIN COUPLED RECEPTORS.....	3
1.1.3 DIVERSITY OF G α PROTEINS AND SIGNALING.....	4
1.1.4 STRUCTURAL BASIS OF G α PROTEIN ACTIVATION.....	7
1.1.5 DIVERSITY OF G $\beta\gamma$ SIGNALING.....	10
1.1.6 STRUCTURAL BASIS OF G $\beta\gamma$ SIGNALING.....	11
1.1.7 KINETIC REGULATION OF G PROTEIN ACTIVITY.....	12
1.2 GPSM MOTIF-CONTAINING PROTEINS.....	15
1.2.1 IDENTIFICATION AND CHARACTERIZATION OF GPSM MOTIF- CONTAINING PROTEINS.....	15
1.2.2 DIVERSITY OF GPSM MOTIF-CONTAINING PROTEINS.....	17

1.2.3 MOLECULAR BASIS FOR THE GDI ACTIVITY OF GPSM MOTIF-CONTAINING PROTEINS.....	19
1.2.4 REGULATION OF GPSM MOTIF FUNCTION.....	22
1.2.5 CELLULAR FUNCTIONS OF GPSM MOTIF-CONTAINING PROTEINS.....	24
1.3 ASYMMETRIC CELL DIVISION.....	25
1.3.1 ASYMMETRIC CELL DIVISION OVERVIEW.....	25
1.3.2 G PROTEINS AND THEIR ACCESSORY PROTEINS IN ASYMMETRIC CELL DIVISION.....	27
1.4 G PROTEIN SIGNALING MODULATOR 3 (GPSM3).....	32
1.4.1 IDENTIFICATION AND CHARACTERIZATION OF GPSM3.....	32
1.4.2 FUNCTIONAL ROLES OF GPSM3.....	34
1.4.3 GPSM3 DISEASE ASSOCIATION.....	37
1.4.4 GPSM3 IN VASCULAR SMOOTH MUSCLE CELLS.....	39
1.5 RESEARCH PURPOSE AND AIMS.....	40
Chapter 2 – Methods.....	42
2.1 TISSUE SAMPLE COLLECTION.....	42
2.2 AORTIC VASCULAR SMOOTH MUSCLE CELL ISOLATION.....	42
2.3 SERUM STARVATION AND REPLACEMENT.....	43
2.3.1 SERUM STARVATION AND REPLACEMENT PRIOR TO RNA AND PROTEIN EXTRACTION.....	43
2.3.2 SERUM STARVATION AND REPLACEMENT PRIOR TO IMMUNOFLUORESCENT LABELING.....	44

2.4 RNA EXTRACTION.....	44
2.5 REVERSE TRANSCRIPTION (RT-PCR) AND QUANTITATIVE POLYMERASE CHAIN REACTION (QPCR).....	45
2.6 PROTEIN ISOLATION.....	47
2.7 IMMUNOBLOTTING.....	47
2.8 TRANSFECTION.....	48
2.8.1 TRANSFECTION FOR MTT ASSAY AND CELL COUNTING.....	49
2.8.2 TRANSFECTION FOR MAMMALIAN TWO-HYBRID ASSAY.....	49
2.9 MTT ASSAY.....	50
2.10 CELL COUNT ASSAY.....	51
2.11 IMMUNOFLUORESCENT LABELING.....	51
2.12 MAMMALIAN TWO-HYBRID SYSTEM.....	52
2.13 DNA CONSTRUCTS.....	54
2.14 LUCIFERASE ASSAY SYSTEM.....	58
2.15 STATISTICAL ANALYSES.....	59
Chapter 3 – Results.....	60
3.1 DIFFERENTIAL EXPRESSION OF GPSM3 IN WKY AND SHR RATS.....	60
3.2 GPSM3 EXPRESSION AND RATE OF CELL DIVISION.....	63
3.3 GPSM3 LOCALIZATION DURING MITOSIS IN VASCULAR SMOOTH MUSCLE CELLS.....	73
3.4 MAMMALIAN TWO-HYBRID ASSAY FOR GPSM3 PROTEIN INTERACTORS.....	82
Chapter 4 – Discusssion.....	100
4.1 SUMMARY OF NOVEL FINDINGS.....	100

4.2 CONTRIBUTION OF RESEARCH TO CURRENT STATE OF KNOWLEDGE.....	101
4.2.1 CONTRIBUTION TO OUR GENERAL KNOWLEDGE OF GPSM3.....	102
4.2.2 CONTRIBUTION TO OUR KNOWLEDGE OF HYPERTENSION.....	105
4.2.3 CONTRIBUTION TO OUR KNOWLEDGE OF CELL DIVISION.....	106
4.3 EXPERIMENTAL METHODS: NOTES AND LIMITATIONS.....	109
4.3.1 SERUM STARVATION.....	109
4.3.2 EYFP-TAGGED GPSM3.....	109
4.3.3 MAMMALIAN TWO-HYBRID ASSAY.....	110
4.4 FUTURE DIRECTIONS.....	112
4.5 CONCLUSIONS.....	114
Chapter 5 – References.....	115
Chapter 6 – Appendix 1.....	135
5.1 SUPPLEMENTAL FIGURES.....	135
5.2 ANIMAL PROTOCOL APPROVAL FORM.....	137
5.3 FIGURE REPRINTING PERMISSIONS.....	138
Curriculum Vitae.....	140

List of Figures

Figure 1.1 Receptor-mediated activation of heterotrimeric G proteins.....	2
Figure 1.2 Regulation of systemic functions by signaling through G protein pathways.....	6
Figure 1.3 Structural features of heterotrimeric G proteins.....	8
Figure 1.4 Regulation of G protein cycle.....	14
Figure 1.5 Diversity of GPSM motif-containing proteins.....	18
Figure 1.6 The GPSM motif of RGS14 interacts with Gai1.....	20
Figure 1.7 Symmetric versus asymmetric cell division.....	26
Figure 1.8 Orientation of the mitotic spindle by GPSM2.....	28
Figure 1.9 Amino acid sequence of GPSM3.....	33
Figure 2.1 Checkmate™ Mammalian Two-Hybrid System vectors.....	53
Figure 3.1 GPSM3 mRNA levels in WKY-derived and SHR-derived VSMCs.....	61
Figure 3.2 GPSM3 mRNA levels in different WKY and SHR rat tissue types.....	62
Figure 3.3 Effect of serum deprivation and serum replacement on GPSM3 mRNA levels in WKY-derived VSMCs.....	64
Figure 3.4 Effect of serum deprivation and serum replacement on GPSM3 mRNA levels in SHR-derived VSMCs.....	65
Figure 3.5 Effect of serum deprivation and serum replacement on GPSM3 protein levels in WKY-derived VSMCs.....	66
Figure 3.6 Effect of serum deprivation and serum replacement on GPSM3 protein levels in SHR-derived VSMCs.....	68
Figure 3.7 Effect of EYFP-tagged GPSM3 transfection on cell proliferation in HEK-293 cells as measured by MTT assay.....	71

Figure 3.8 Effect of EYFP-tagged GPSM3 transfection on cell proliferation in HEK-293 cells as measured by cell counting.....	72
Figure 3.9 Localization of GPSM3 and β -tubulin during interphase in WKY and SHR vascular smooth muscle cells.....	75
Figure 3.10 Co-localization of GPSM3 and β -tubulin during metaphase in WKY and SHR vascular smooth muscle cells.....	76
Figure 3.11 Co-localization of GPSM3 and β -tubulin during anaphase in WKY and SHR vascular smooth muscle cells.....	78
Figure 3.12 Co-localization of GPSM3 and β -tubulin during telophase in WKY and SHR vascular smooth muscle cells.....	80
Figure 3.13 Localization of GPSM3 and β -tubulin during metaphase in HEK-293 cells.....	83
Figure 3.14 Localization of GPSM3 during metaphase and telophase in WKY vascular smooth muscle cells.....	84
Figure 3.15 Localization of β -tubulin during metaphase and telophase in WKY vascular smooth muscle cells.....	85
Figure 3.16 Localization of secondary antibodies during metaphase and telophase in WKY vascular smooth muscle cells.....	86
Figure 3.17 Mammalian Two-Hybrid luciferase assay results between GPSM3 and heterotrimeric G proteins.....	87
Figure 3.18 Mammalian Two-Hybrid luciferase assay results of heterotrimeric G protein vector controls.....	89

Figure 3.19 Mammalian Two-Hybrid luciferase assay results between GPSM3 and mitosis-related proteins of interest.....	92
Figure 3.20 Mammalian Two-Hybrid luciferase assay results of mitosis-related gene of interest vector controls.....	94
Figure 3.21 Mammalian Two-Hybrid luciferase assay results between GPSM3 and online database-predicted interactors.....	96
Figure 3.22 Mammalian Two-Hybrid luciferase assay results of online database-predicted interactor vector controls.....	98
Figure 5.1 Localization of EYFP-tagged GPSM3 during mitosis in HEK-293 cells.....	136

List of Tables

Table 1.1 Classes of G α subunits, their expression pattern, and their effectors.....	5
Table 1.2 GPSM3 protein-protein interaction partners.....	35
Table 2.1 Primers for qPCR.....	46
Table 2.2 Genes of interest and the restriction enzymes used for subcloning.....	56
Table 2.3 Primers for Mammalian Two-Hybrid experiments.....	57
Table 3.1 N values of immunofluorescently labeled images of vascular smooth muscle cells and human embryonic kidney 293 cells in different stages of mitosis.....	74

List of Appendices

Appendix 1.....	135
-----------------	-----

List of Abbreviations

AAA	Abdominal aortic aneurism
AC	Adenylyl cyclase
ACD	Asymmetric cell division
ADP	Adenosine diphosphate
AGS	Activator of G protein signaling
ANOVA	Analysis of variance
aPKC	Atypical protein kinase c
BRET	Bioluminescence resonance energy transfer
CAIA	Collagen antibody-induced arthritis
cAMP	Cyclic adenosine monophosphate
CDK	Cyclin-dependent kinase
CHO	Chinese hamster ovary
CMV	Cytomegalovirus
DAG	Diacylglycerol
DMEM	Dulbecco's modified eagle medium
DMSO	Dimethyl sulfoxide
EYFP	Enhanced yellow fluorescent protein
FBS	Fetal bovine serum
FGFR3	Fibroblast growth factor receptor 3
FRET	Fluorescent resonance energy transfer
G protein	Guanine nucleotide-binding protein
GAP	GTPase-accelerating protein

GAPDH	Glyceraldehyde 3-phosphate dehydrogenase
GDI	Guanine nucleotide dissociation inhibitor
GDP	Guanosine diphosphate
GEF	Guanine nucleotide Exchange Factor
GIRK	G protein-coupled inwardly rectifying K ⁺ channel
GMC	Ganglion mother cell
GoLoco	Gai/o-Loco
GPCR	G protein-coupled receptor
GPR	G protein regulatory
GPSM	G protein signaling modulator
GRK	G protein-coupled receptor kinase
GTP	Guanosine triphosphate
GTPase	Guanosine triphosphate phosphohydrolase
GTPγS	Guanosine 5'-O-[gamma-thio] triphosphate
G$\alpha\beta\gamma$	Heterotrimeric G protein
HBS	Hepes-buffered saline
HDAC5	Histone deacetylase 5
HEK-293	Human embryonic kidney 293 cells
HSPA8	Heat shock A8 protein
Insc	Inscuteable
IP₃	Inositol triphosphate
MAP	Mitogen-activated protein
MDCK	Madin-Darby canine kidney cells

MTT	3-(4,5-dimethylthiazol-2-yl)-2,5-diphenyltetrazolium bromide
NEB	New England Biolabs
NIN	Ninein
NLRP3	NOD-like receptor family, pyrin domain containing 3 protein
NuMA	Nuclear mitotic apparatus protein
PAK	p21-activated kinase
PAR	Partitioning defective protein
PBS	Phosphate-buffered saline
Pins	Partner of Inscuteable
PKA	cAMP-dependent protein kinase
PKC	Protein kinase C
PLA2	Phospholipase A2
PLCβ	Phospholipase C β
PTX	Pertussis toxin
qPCR	Quantitative polymerase chain reaction
Rap1	Ras-related protein 1
Ras GRF	Ras protein-specific guanine nucleotide-releasing factor
RBD	Ras-binding domain
RGS	Regulator of G protein signaling
Ric-8	Resistance to inhibitors of cholinesterase 8
RNAi	RNA interference
RRR	Relative response ratio
RT	Reverse transcriptase

SELPLG	Selectin P ligand
SEM	Standard error of the mean
serum dep.	Serum deprivation/starvation
serum rep.	Serum replacement/addition
SHR	Spontaneously hypertensive rat
SNAP25	Synaptosomal-associated protein 25
SNP	Single nucleotide polymorphism
STRING	Search Tool for the Retrieval of Interacting Genes
SVIL	Supervillin
TBST	Tris-buffered saline with Tween 20
TPR	Tetratricopeptide repeat
VSMC	Vascular smooth muscle cell
WKY	Wistar-Kyoto rat
α2-AR	α 2 adrenergic receptor

1 INTRODUCTION

The functional role of G protein signaling modulator 3 (GPSM3) in mammalian cells remains poorly understood relative to other components of the G protein-mediated signaling machinery. I hypothesize that GPSM3, like other G protein-mediated signaling components, plays a role in the process of cell division, likely via an as yet undefined interaction with the mitotic spindle. The purpose of this study is to investigate this potential role in a vascular smooth muscle cell (VSMC) model system.

1.1 G PROTEIN SIGNALING

1.1.1 *G PROTEIN SIGNALING OVERVIEW*

Guanine nucleotide-binding protein (G protein)-mediated signaling is a preeminent mechanism used by cells to communicate with each other and sense environmental changes. Canonically, signaling occurs through three main protein components: a G protein-coupled receptor (GPCR), a heterotrimeric G protein ($G\alpha\beta\gamma$), and an effector (Neves et al. 2002; Ferguson 2001; Jacoby et al. 2006) (Figure 1.1). Briefly, when a GPCR is activated by its ligand, it promotes the exchange of guanosine diphosphate (GDP) for guanosine triphosphate (GTP) by the α subunit of the heterotrimeric G protein. This in turn is thought to promote the dissociation of the $G\alpha$ and $G\beta\gamma$ subunits, which are then free to independently shuttle to and interact with downstream effectors. Examples of effectors include adenylyl cyclase (AC), which plays a central role in the cyclic adenosine monophosphate (cAMP) signal pathway, and phospholipase C β (PLC β), which

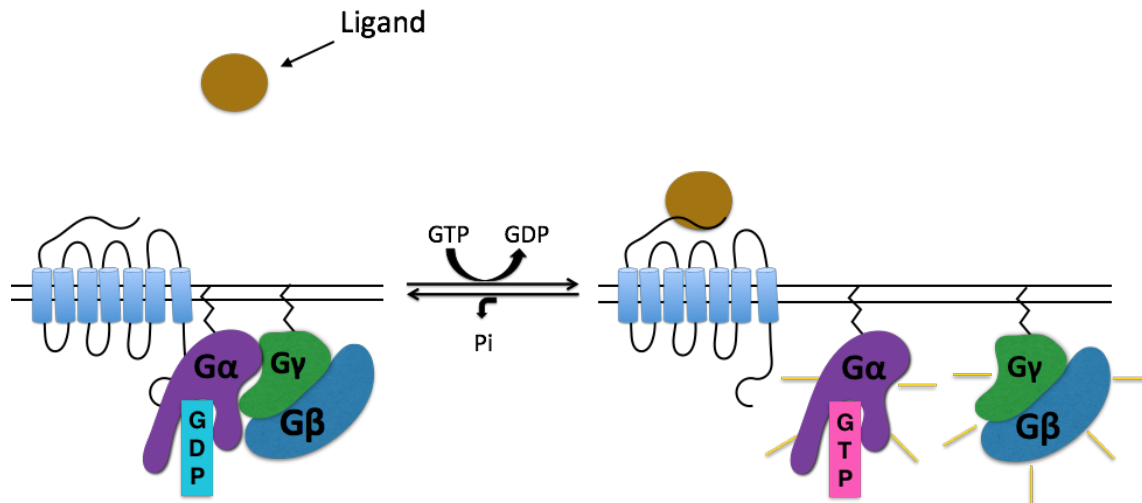


Figure 1.1. Receptor-mediated activation of heterotrimeric G proteins. The binding of the extracellular ligand to the receptor causes a conformational; change of the receptor, which leads to the activation of the $G\alpha$ subunit. This activation promotes the exchange of GDP for GTP and is thought to cause the dissociation of the $G\beta\gamma$ dimer from the complex. Both the GTP-bound $G\alpha$ and $G\beta\gamma$ subunit are capable of initiating signals by interacting with downstream effectors. The process is terminated by the GTPase activity of the $G\alpha$ subunit that can hydrolyze GTP to GDP, returning the $G\alpha$ subunit to its inactive form and promoting the reformation of the $G\alpha\beta\gamma$ heterotrimer complex.

triggers the phosphatidylinositol/diacylglycerol signal pathway (Neves et al. 2002; Smrcka 2008). Eventually, the intrinsic guanosine triphosphate phosphohydrolase (GTPase) activity of $G\alpha$ will hydrolyze the bound GTP molecule, which results in the reformation of the $G\alpha\beta\gamma$ complex and terminates GPCR signaling.

1.1.2 *G PROTEIN COUPLED RECEPTORS*

GPCRs are the largest superfamily of receptors in the human genome and approximately 30% of currently marketed prescription pharmaceuticals act on GPCRs, making them the most common and historically successful therapeutic target family (some reports place this number closer to 50%) (Jacoby et al. 2006; Overington et al. 2006; Kobilka 2007). These receptors transduce a wide variety of extracellular signals, including hormones, autocrine and paracrine factors, chemokines, and neurotransmitters, to the interior of the cell (Neves et al. 2002). GPCRs share a specific structural organization: seven membrane-spanning domains or transmembrane alpha helices connected by three intracellular loops and three extracellular loops, an N-terminal extracellular tail, and a C-terminal intracellular tail (Jastrzebska 2013). Many GPCRs also possess an eighth alpha helix attached by a linker to helix seven that runs parallel to the inside of the phospholipid bilayer which can influence G protein recognition (Kaye et al. 2011).

When a GPCR is activated by a ligand, typically via binding in a cavity formed between the transmembrane helices, conformational changes occur at its cytoplasmic surface that reveal residues in the intracellular loops and in the transmembrane helices that lead to G protein activation (Jastrzebska 2013; Trzaskowski et al. 2012). GPCRs activate G proteins by acting as

guanine nucleotide exchange factors (GEF), promoting the exchange of GDP for GTP on the $G\alpha$ subunit (Siderovski & Willard 2005). Activated GPCRs can be phosphorylated by G protein-coupled receptor kinases (GRKs), and that promotes their association with β -arrestins (Ferguson 2001; DeWire et al. 2007). These proteins block GPCR signaling through a steric mechanism and bring the receptors to clathrin-coated pits for internalization. Once internalized in endosomes, GPCRs can undergo degradation, continue signaling via G protein-independent mechanisms, or be recycled back to the plasma membrane. While this traditional view of GPCRs begins to outline their function, there are numerous additional facets to the story that illustrate the complexity of this process including the now widely accepted phenomenon of GPCR oligomerization and the evidence for receptor-G protein-effector complexes (Jastrzebska 2013; Chidiac 1998).

1.1.3 DIVERSITY OF $G\alpha$ PROTEINS AND SIGNALING

Up to the present time, 23 $G\alpha$ subunit isoforms have been identified (McIntire 2009; Preininger & Hamm 2004). $G\alpha$ subunits belong to a family of membrane-associated GTPases that function as molecular switches to control a wide array of cellular processes, and have been placed into four distinct subfamilies based on their sequence similarity and effector selectivity: Gs, Gi/o, Gq/11, and G12/13 (Neves et al. 2002; Zhao et al. 2013) (Table 1.1) (Figure 1.2). Gs subunits ($G_{\alpha s}$, $G_{\alpha olf}$) can stimulate AC activity, increasing cAMP production (Neves et al. 2002). This second messenger is capable of regulating proteins such as cAMP-dependent protein kinase (PKA), cAMP-dependent GEFs for calcium channels and a small GTPase known as Ras-related protein 1 (Rap1) (Weinstein et al. 2004; Neves et al. 2002). $G_{\alpha s}$ has also been found to interact

Table 1.1. Classes of G α subunits, their expression pattern, and their effectors.

Gα family	Gα subunit	Expression Profile	Effectors
G α_s	G α_s	Ubiquitous	Stimulation of adenylyl cyclase
	G α_{olf}	Olfactory neurons	Stimulation of adenylyl cyclase
G $\alpha_{i/o}$	G $\alpha_{i1/2/3}$	Ubiquitous	Inhibition of adenylyl cyclase, Ca ²⁺ channel closure
	G $\alpha_{oA/B}$	Brain	Inhibition of adenylyl cyclase, Ca ²⁺ channel closure
	G $\alpha_{t1/2}$	Retina	Stimulation of cGMP-phosphodiesterase
	G α_z	Brain/platelets	Inhibition of adenylyl cyclase, K ⁺ channel closure
G $\alpha_{q/11}$	G $\alpha_{q/11}$	Ubiquitous	Stimulation of PLC- β , Activate RhoGEFs*
	G $\alpha_{15/16}$	Hematopoietic cells	Stimulation of PLC- β , Activate RhoGEFs*
	G α_{14}	Lung, kidney, liver	Stimulation of PLC- β , Activate RhoGEFs*
G $\alpha_{12/13}$	G $\alpha_{12/13}$	Ubiquitous	Activate RhoGEFs*

* RhoGEFs activated by G $\alpha_{12/13}$ and G α_{14} are distinct.

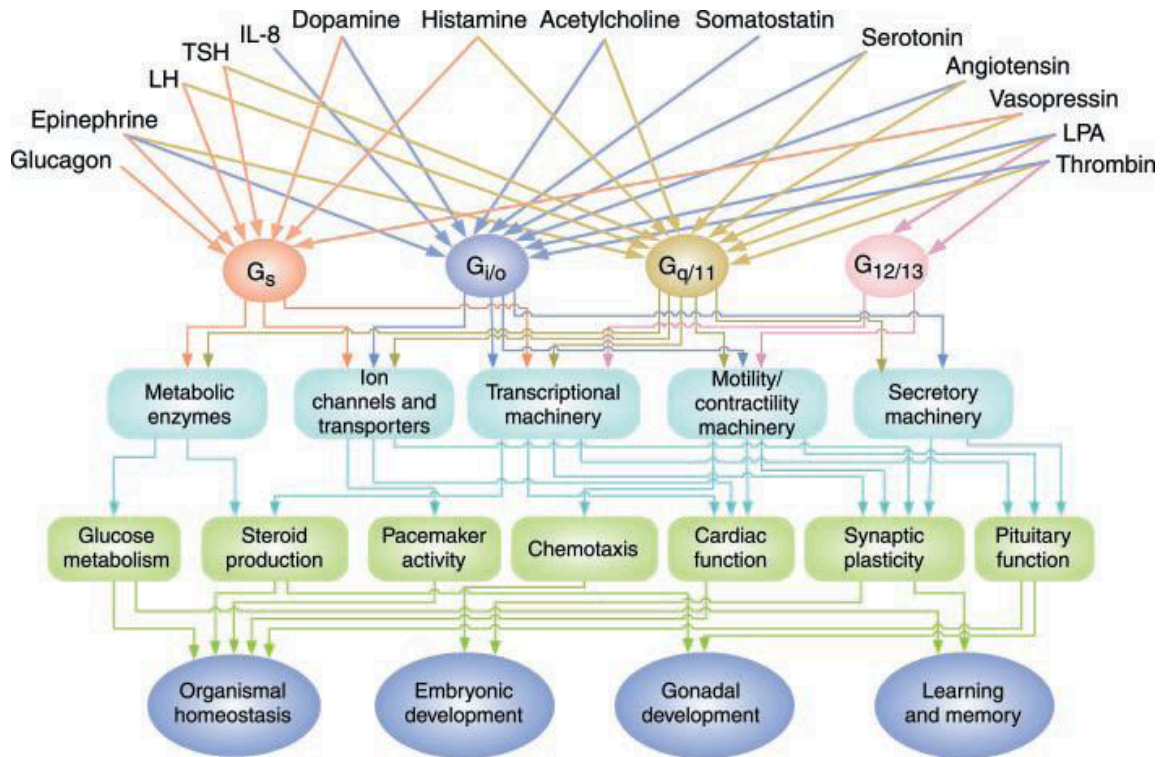


Figure 1.2. Regulation of systemic functions by signaling through G protein pathways. A schematic representation of how signaling through G protein pathways can regulate systemic functions. From Neves et al. 2002. Reprinted with permission from AAAS.

with tubulin in lipid rafts and can be internalized via lipid raft-derived vesicles (Dave et al. 2009). Members of the Gi/o subfamily (Gai1, Gai2, Gai3, Gao, Gaz, Gat) exhibit inhibitory effects on AC activity, thereby decreasing cAMP production (Neves et al. 2002). Gai/o subunits also play an important role in the process of cell division. The Gai and Gao subunits can be inhibited by pertussis toxin, which adenosine diphosphate (ADP)-ribosylates Gai/o subunits at their COOH-terminal region preventing them from interacting with a GPCR (Neves et al. 2002). Gq subunits (Gaq, Gα11, Gα14, Gα15, Gα16) primarily act on PLCβ leading to the production of two intracellular second messengers, inositol triphosphate (IP₃) and diacylglycerol (DAG), and via these the regulation of the release of intracellular calcium stores and the activity of protein kinase C (PKC), respectively (Neves et al. 2002; Rhee & Bae 1997). The effectors of G12/13 subunits (Gα12, Gα13) are not yet well understood, but have been shown to regulate Rho, a member of the Ras superfamily, and Rho-kinase activation via RhoGEFs (Neves et al. 2002).

1.1.4 *STRUCTURAL BASIS OF Gα PROTEIN ACTIVATION*

Gα protein subunits consist of a catalytic (Ras-like or GTPase) domain, a six-helix bundle domain (helical domain), and two flexible linker regions (linkers 1 and 2), connecting these two domains whose interface forms a deep cleft which functions as a GDP binding pocket (Figure 1.3) (Khafizov 2009; Lambright et al. 1994). The GTPase domain is made up of five helices (α1-α5) surrounding a six-stranded β sheet (β1-β6), while the helical domain is comprised entirely of α-helical secondary structures with one long central helix (αA) encompassed by five shorter helices (αB-αF) (Lambright et al. 1994). The three flexible loops (Switches I, II, and III) within

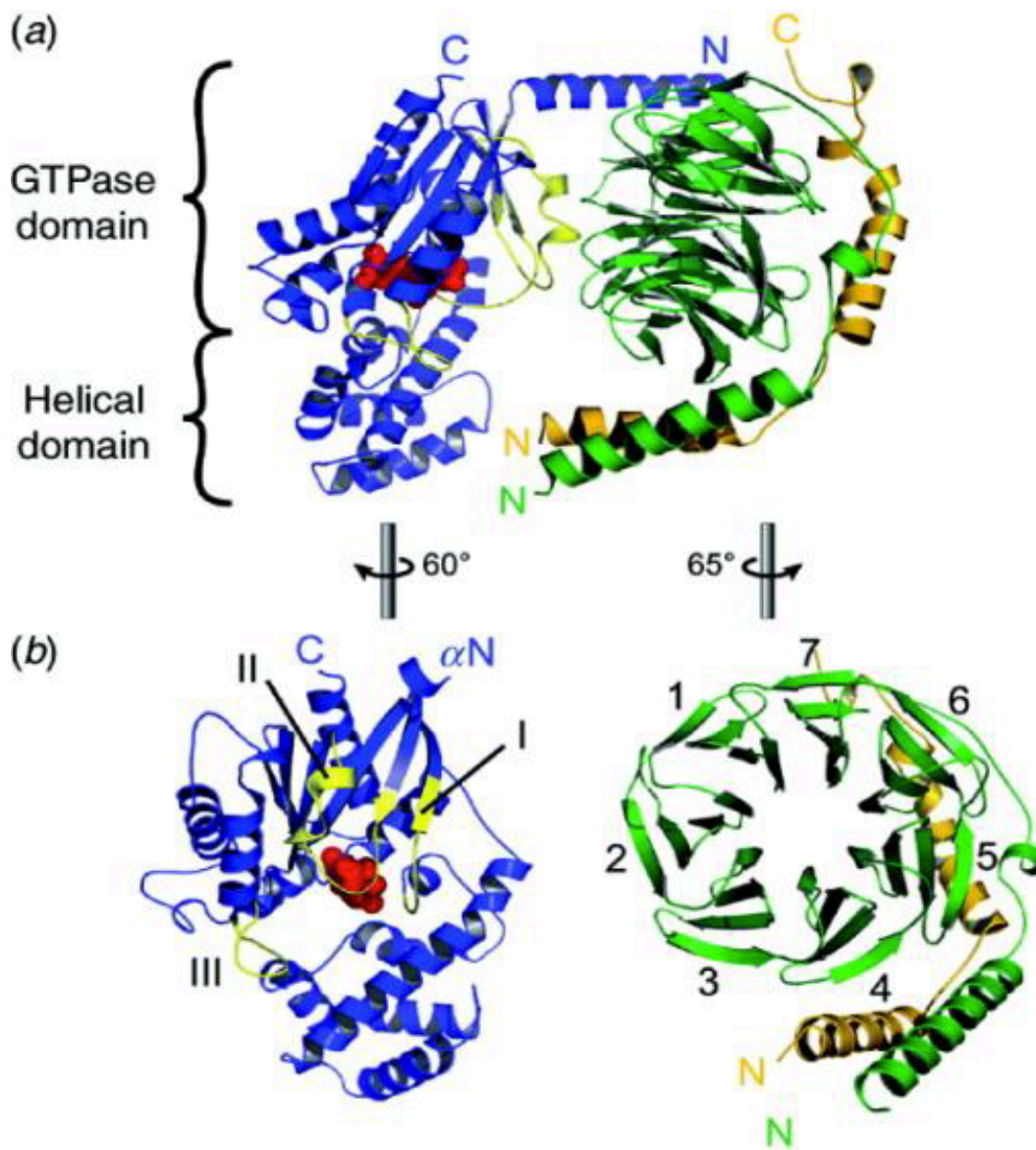


Figure 1.3. Structural features of heterotrimeric G proteins. (a) Ribbon model of Gai(GDP)β1γ1 heterotrimer. (b) The subunits have been rotated to show the intersubunit interface. From Oldham & Hamm 2006. Reprinted with permission from Cambridge University Press.

the GTPase domain undergo dramatic structural changes during the nucleotide exchange and hydrolysis cycle (Lambright et al. 1994; Mixon et al. 1995). The GTPase domain also contains binding sites for various receptors and effectors, as well as G $\beta\gamma$. An α -helical lid, part of the helical domain, is positioned over the nucleotide binding site, burying the bound nucleotide in the core of the protein (Lambright et al. 1994; Warner et al. 1998). The helical domain is the most divergent domain among the G α subunit families and therefore is thought to regulate binding of G α subunits to receptors and other regulators (Liu & Northup 1998).

Upon activation by a ligand, it has been suggested that the GPCR uses the N-terminal helix of G α to “pull” the G $\beta\gamma$ dimer and switch I and II regions away from the nucleotide binding pocket, resulting in GDP release (Iiri et al. 1998). Non-receptor GEFs such as resistance to inhibitors of cholinesterase 8 (Ric-8) work in a similar manner, promoting the pivoting of the helical and Ras-like domains away from each other and structural rearrangement of the switch I and II regions to allow for nucleotide exchange (Van Eps et al. 2015). The G α subunit most likely exists in a transient nucleotide-free state before binding of GTP, which exists at a much higher concentration in the cell relative to GDP (Smrcka 2008). The binding of GTP results in structural rearrangement of the heterotrimeric G protein that exposes the G α subunit’s effector binding site, thus leading to signal transduction. The duration of G protein signaling is determined by the length of time that the G α subunit is in its GTP-bound state (Ross & Wilkie 2000). The intrinsic GTP hydrolysis activity among the different G α protein subunits varies, although it is relatively slow in all cases compared to when it is stimulated by GTPase-accelerating proteins (GAP), which often occurs (Oldham & Hamm 2006). Structural studies have demonstrated the importance of the three switch regions in GTP hydrolysis, and inspection of the crystal structure

of fluoroaluminate-activated $G\alpha$ protein subunit reveals a functional role of conserved glutamine and arginine residues within the nucleotide-binding pocket (Coleman et al. 1994; Noel et al. 1993; Sondek et al. 1994).

1.1.5 DIVERSITY OF $G\beta\gamma$ SIGNALING

$G\beta$ and $G\gamma$ subunits, tethered to the membrane by fatty acyl modification of $G\gamma$, essentially function as dimers since the $G\beta\gamma$ complex is highly stable and only comes apart under denaturing conditions (Zhao et al. 2013; Neves et al. 2002). Up to the present time, 7 β subunit and 12 γ subunit isoforms have been identified (McIntire 2009). The first five β subunits are the most well studied, with the first four sharing greater than 80% amino acid sequence identity versus the fifth with 50% identity, and significantly lower identity amongst the γ subunits (Smrcka 2008). These different subunit isoforms can pair to form unique combinations; some combinations have been associated with specific receptors, but overall the significance of this diversity remains poorly understood (Kleuss et al. 1992; Kleuss et al. 1993).

Pertussis toxin (PTX)-dependent catalysis of adenosine diphosphate (ADP) ribosylation of Gai/o subunits prevents their interaction with and activation by GPCRs (Burns 1988). Many of the GPCR-dependent physiological processes that are inhibited by PTX are mediated by $G\beta\gamma$ subunits rather than $G\alpha$ subunits, and this accounts for the majority of known $G\beta\gamma$ -dependent signaling. Therefore it follows that the majority of $G\beta\gamma$ -dependent signaling appears to result from $G\beta\gamma$ dimers originally complexed with Gai/o protein subunits (Smrcka 2008).

G $\beta\gamma$ is required for receptor-stimulated activation since it stabilizes G α -receptor coupling, and has even been reported to bind to the receptor (Zhao et al. 2013; Smrcka 2008). G $\beta\gamma$ dimers also act as guanine nucleotide dissociation inhibitors (GDI), slowing down the intrinsic rate of GDP dissociation from the G α subunit by up fifty fold, as well as functioning to increase the rate of association of GDP (Gilman 1987). G $\beta\gamma$ targets a large number of effectors both directly and indirectly, including G protein-coupled inwardly rectifying K⁺ (GIRK) channels, PLC β , AC, and various kinases and calcium channels (Smrcka 2008; Rhee & Bae 1997) (Table 1.2). G $\beta\gamma$ specificity for receptors and effectors is poorly understood, but suggested mechanisms include tissue-specific expression, restricted subcellular localization, and precoupling of components (Smrcka 2008).

1.1.6 *STRUCTURAL BASIS OF G $\beta\gamma$ SIGNALING*

The G β subunit folds into a prototypical β -propeller made up of four-stranded β -sheets forming each of the seven blades of the propeller (Smrcka 2008) (Figure 1.3). An α -helical domain, comprised of the first 57-70 amino acids N-terminal to the β -propeller, forms a tight coiled-coil interaction with the G γ subunit (Smrcka 2008). The β -sheets of the propeller and the variable loops connecting the β strands are the most highly conserved regions of the protein (Smrcka 2008). G α subunits interact with G $\beta\gamma$ via two independent structural elements: the N-terminal α -helix of the G α subunit interacts with the first blade of the β -propeller at its side and the G α switch II region interacts with the top of the β -propeller (Smrcka 2008). Upon GTP binding, the switch II region undergoes conformational changes, but little difference in structure is seen in G $\beta\gamma$ upon release from G α (Smrcka 2008). This supports a theory that rather than dissociate, the

$G\alpha\beta\gamma$ heterotrimer simply undergoes a rearrangement during G protein activation. However, the more generally accepted theory of complete dissociation asserts that during activation both interfaces between $G\alpha$ and $G\beta\gamma$ are broken. In either case, traditionally it is taken that when bound to $G\alpha(\text{GDP})$, $G\beta\gamma$ cannot activate downstream effectors and thus $G\beta\gamma$ -mediated signaling relies on nucleotide exchange on the $G\alpha$ subunit (Scott et al. 2001). In a sense, $G\alpha(\text{GDP})$ and $G\beta\gamma$ are locked in a mutually inhibitory embrace with one another. However, an apparent second $G\beta\gamma$ binding site on $G_{ai/o}$ subunits, which is distant from the primary site and does not compete with the principal effector binding site, suggests that a $G_{ai/o}(\text{GDP})-(G\beta\gamma)_2$ complex could associate with effectors (Wang et al. 2009).

The absence of a catalytic site on $G\beta\gamma$ means that it acts as a modulator through regulated protein-protein interactions (Smrcka 2008). It has been suggested that the majority of these interactions occur at a single interaction “hot spot”, which through the use of key energetic residues mediates multiple types of chemical interactions (hydrophobic, ionic, etc.) without strict geometric requirements for binding, thus accommodating multiple structural and chemical motifs (Scott et al. 2001; Smrcka 2008).

1.1.7 KINETIC REGULATION OF G PROTEIN ACTIVITY

The kinetics of the G protein activation and deactivation reactions play a major role in G protein-mediated signaling. G proteins are normally found in the GDP-bound state and thus the first step in the cycle of nucleotide exchange at the $G\alpha$ subunit is GDP dissociation. The relatively high concentration of GTP in cells (both absolute concentration and relative concentration compared

to GDP) ensures a rapid association of the nucleotide-free G protein with GTP (Smrcka 2008). This means that GDP dissociation is the rate-limiting step of nucleotide exchange. GTP is typically hydrolyzed before it dissociates, thus beginning the cycle again. Three classes of regulators collaborate to tightly control the kinetics of G protein signaling: GAPs, GEFs, and GDIs (Figure 1.4).

GAPs such as the regulator of G protein signaling (RGS) proteins can increase GTP hydrolysis rates by up to 2000 fold (Mukhopadhyay & Ross 1999). Consequently, GAP proteins negatively regulate the G protein cycle by dampening signal output and by rapidly terminating G protein activation following the removal of the stimulus. It is also suspected that GAP proteins, namely RGS proteins, are able to potentiate receptor-mediated activation via a proposed kinetic scaffolding mechanism whereby they reduce depletion of $G\alpha(\text{GDP})$ levels in order to ensure rapid recoupling to the receptor and sustained G protein activation (Biddlecome et al. 1996; Zhong et al. 2003). They could potentially even directly or indirectly interact with GPCRs during nucleotide exchange (Lambert et al. 2010; Popov et al. 2000).

GEFs such as GPCRS dramatically increase the rate of GDP dissociation, leading to an increase in GTP association and G protein activation. Non-receptor GEFs such as Ric-8 share similar mechanisms with that of the receptor, promoting the dissociation of both GDP and GTP (Chan et al. 2011). At high GTP concentrations, such as those found intracellularly ($\sim 150 \mu\text{M}$), GTP association is greater than dissociation and $G\alpha(\text{GTP})$ predominates (Chan et al. 2011).

Interestingly, Ric-8B has also been reported to seemingly stabilize G proteins in their nucleotide-

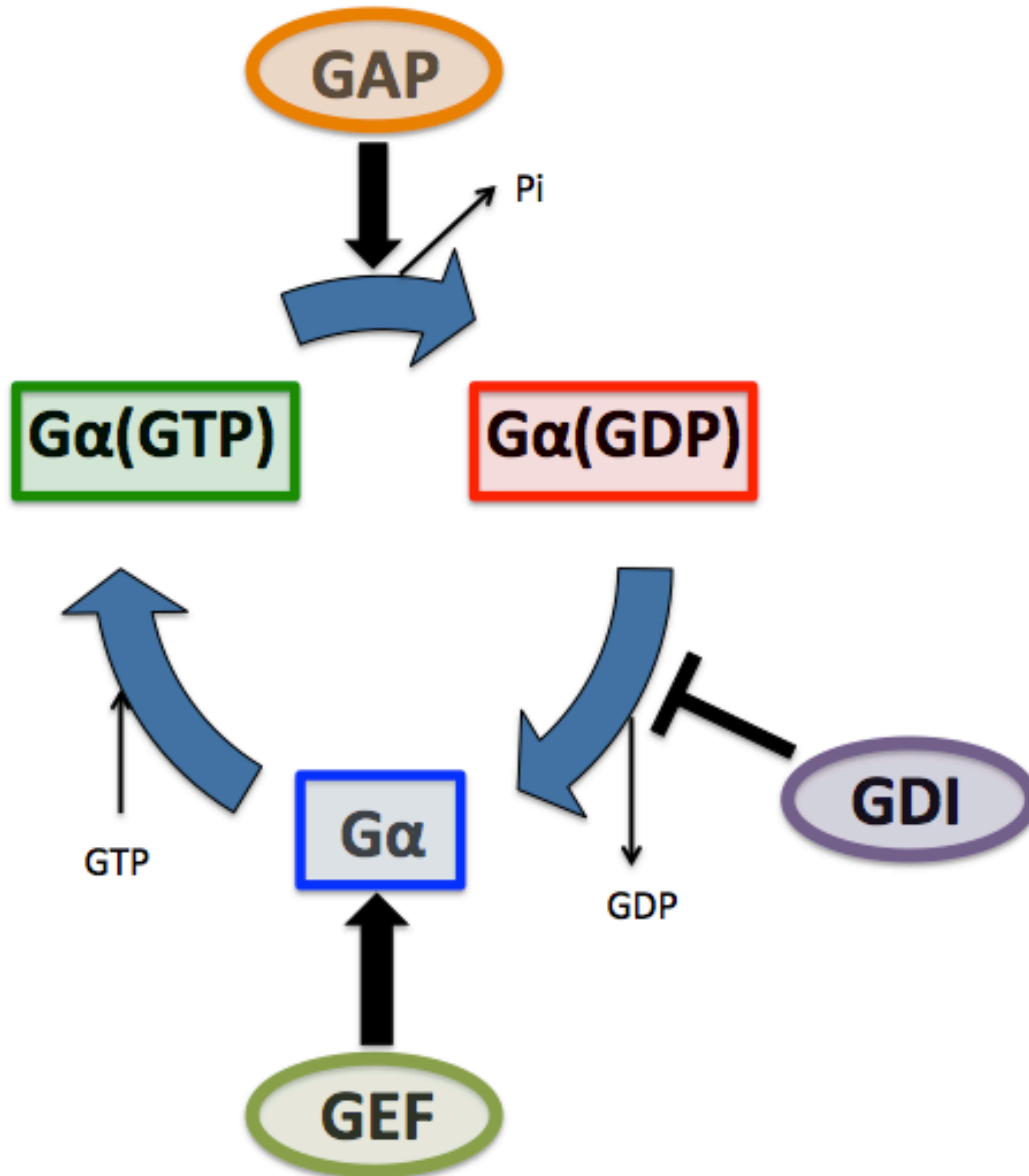


Figure 1.4. Regulation of G protein cycle. The rate of nucleotide exchange can be altered by guanine nucleotide exchange factors (GEFs) and guanine nucleotide dissociation inhibitors (GDIs). GTP hydrolysis can be regulated by GTPase accelerating proteins (GAPs).

free conformation, preventing them from denaturing and thereby increasing cellular G protein levels (Tall 2013).

Finally, GDIs such as G $\beta\gamma$ retard the already relatively slow rate of GDP dissociation from G α (Zhao et al. 2013). Proteins containing the G protein signaling modulator (GPSM) motif, also known as a G protein regulatory (GPR) motif or a GoLoco (Gai/o-Loco) motif, are the best studied group of proteins with GDI activity (Grandrath et al. 1999; Siderovski et al. 1999; Zhao et al. 2013). It has been reported that the rate of guanosine 5'-O-[gamma-thio] triphosphate (GTP γ S, a GTP analog which dissociates slowly and cannot be hydrolyzed to GDP) binding is decreased up to 80% in the presence of GPSM proteins (including GPSM3) or peptides derived from the GPSM motifs of RGS12 and RGS14 (Zhao et al. 2010; Windh & Manning 2002). They accomplish this by directly interacting with and stabilizing G α (GDP). These three groups of accessory proteins fine-tune G protein signaling, and as discussed below they have a wide range of other functions in the cell as well.

1.2 GPSM MOTIF-CONTAINING PROTEINS

1.2.1 IDENTIFICATION AND CHARACTERIZATION OF GPSM MOTIF-CONTAINING PROTEINS

The first GPSM motif identified is in *loco*, a RGS12 homologue found in *Drosophila melanogaster* and associated with impaired locomotor capabilities (Grandrath et al. 1999). C-terminal to its RGS domain the researchers identified a G protein interaction site, and this observation led to the discovery of several other proteins that shared this highly conserved 19

amino acid motif (Granderath et al. 1999; Siderovski et al. 1999). This motif was also quickly demonstrated to be a receptor-independent activator of $G\beta\gamma$ signaling. A yeast-based functional screen was used to take advantage of this, which tested a mammalian library for cDNAs encoding proteins that activate the pheromone response pathway in the absence of a GPCR. This led to the discovery of the AGS proteins, many of which contain at least one GPSM motif (Takesono et al. 1999; Cao et al. 2004).

The GPSM motif has a relatively high affinity for GDP-bound $G\alpha$ compared to nucleotide-free or GTP-bound $G\alpha$, stabilizing this form and slowing down spontaneous nucleotide exchange (Kimple, Willard, et al. 2002; Kimple, Kimple, et al. 2002; Siderovski & Willard 2005). A significant conformational change of the switch region of the $G\alpha$ subunit is induced upon binding of a GPSM domain, making $G\alpha(\text{GDP})\text{-}G\beta\gamma$ and $G\alpha(\text{GDP})\text{-GPSM}$ complexes mutually exclusive (Bernard et al. 2001; Siderovski & Willard 2005). A GPSM motif consensus peptide that was derived from GPSM1, also known as activator of G protein signaling (AGS) 3, inhibits $G\alpha(\text{GDP})$ from binding to $G\beta\gamma$ ten times more effectively than the $G\beta\gamma$ hot spot-binding peptide (SIGK, which also interferes with the binding between $G\beta\gamma$ and $G\alpha$) (Ghosh et al. 2003). Additionally, this peptide was shown to cause rapid dissociation between $G\beta\gamma$ subunits and $G\alpha$ subunits at a rate 13-fold higher than the intrinsic rate of $G\alpha$ (Ghosh et al. 2003). Full-length RGS14 failed to disrupt G protein heterotrimers *in vitro* or in cells, but a peptide derived from the RGS14 GPSM motif prevented the reformation of $G\alpha\beta\gamma$ heterotrimers (Mittal & Linder 2006; Webb et al. 2005). While the GPSM motif seems to consistently prevent reassociation of subunits, its ability to promote dissociation appears to depend on the cellular or experimental context and the GPSM motif-containing protein in question.

1.2.2 DIVERSITY OF GPSM MOTIF-CONTAINING PROTEINS

The diverse collection of GPSM-motif containing proteins is currently divided into four distinct families: 1) the RGS and Ras-binding domain (RBD) proteins RGS12, RGS14, and *Drosophila* Loco, each of which contains a single GPSM motif, 2) the multiple tetratricopeptide repeat (TPR) motif proteins GPSM1/AGS3, GPSM2/LGN, *Drosophila* Partner of Inscuteable (Pins), and *Caenorhabditis elegans* GPR-1 and GPR-2, which contain one to four GPSM motifs, 3) the relatively small proteins GPSM3/G18/AGS4 and GPSM4/Pcp-2, which contain three and two GPSM motifs, respectively, and 4) Rap1GAP, which contains a single GPSM motif at its N-terminus (Figure 1.5).

The majority of the GPSM motifs interact mainly with G α i and G α o with varying affinities, however some also interact with other G proteins (Zhao et al. 2010; Mittal & Linder 2006; Willard et al. 2006; Willard et al. 2007). GPSM1, for example, interacts with G α t and blocks rhodopsin-induced dissociation of GDP (Natochin & Artemyev 2000). Therefore, the GPSM motif can be said to interact with G proteins from the G α i/o subunit family. As many of these proteins contain multiple GPSM motifs, they are capable of binding multiple G α subunits at one time (Bernard et al. 2001; Adhikari & Sprang 2003; Kimple et al. 2004; Jia et al. 2012). It appears that in GPSM1, cooperative binding of G α subunits among its GPSM motifs occurs (Adhikari & Sprang 2003). Conversely, competitive binding among the GPSM motifs in Pins has been demonstrated and is thought to contribute to ultrasensitivity in regulatory pathways (Smith & Prehoda 2011).

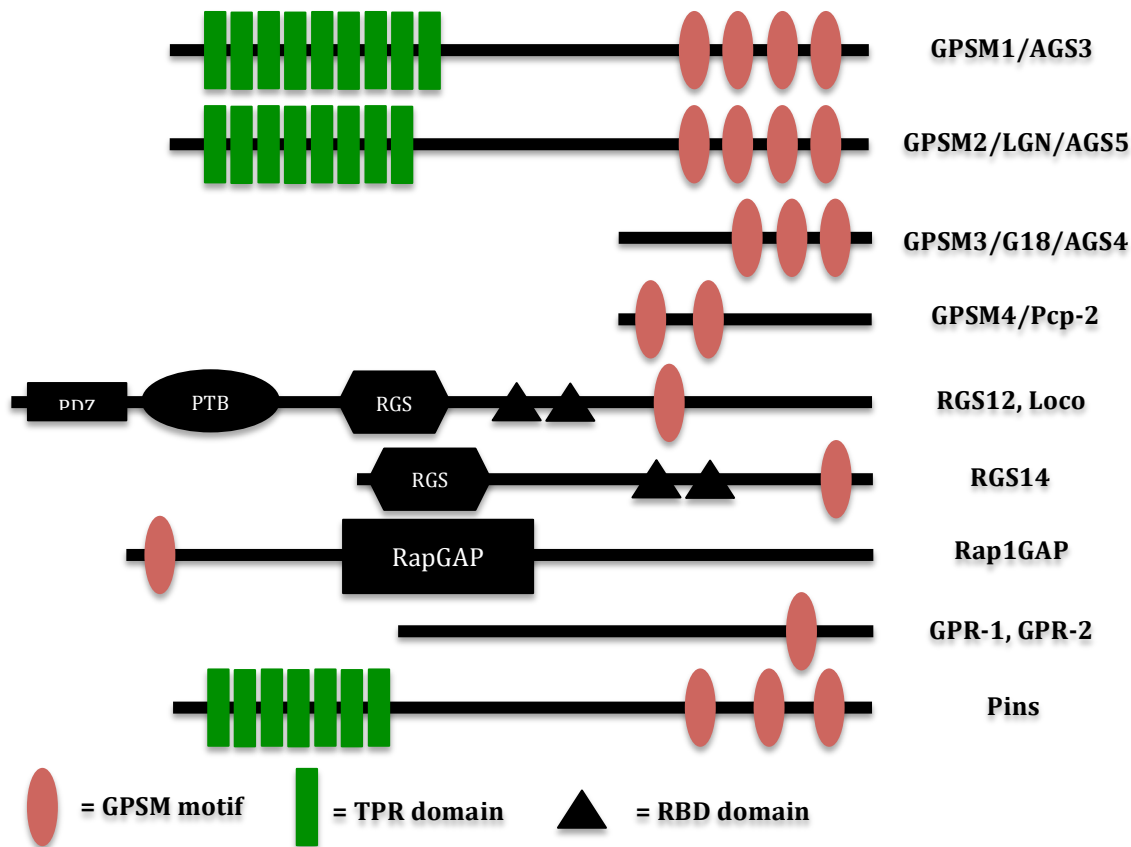


Figure 1.5. Diversity of GPSM motif-containing proteins. The GPSM motif, also known as the GPR motif or GoLoco motif, is found singly or in tandem arrays in a number of different proteins. Domain abbreviations are G protein signaling modulator, GPSM; PSD-95/Discs large/ZO-1 homology domain, PDZ; phosphotyrosine-binding domain, PTB; regulator of G protein signaling domain, RGS; Ras-binding domain, RBD; Rap-specific GTPase-activating protein domain, RapGAP; tetratricopeptide repeat, TPR. Asterisk denotes N-terminal variation of GPSM motif sequence between isoforms I and II of Rap1GAP.

1.2.3 MOLECULAR BASIS FOR THE GDI ACTIVITY OF GPSM MOTIF- CONTAINING PROTEINS

The crystal structure of the GPSM motif in RGS14 associated with Gαi1 demonstrates the significance of both the Asp/Glu-Gln-Arg triad (or acidic-glutamine-arginine triad) of the GPSM motif and the switch II region of the Gα subunit (Kimple, Kimple, et al. 2002) (Figure 1.6). The N-terminal α-helix of the GPSM peptide inserts between the switch II and α3 helix regions of the Gα subunit, displacing these two regions away from each other and in the process deforming the normal site of Gβγ association. The side chain of the arginine finger within the acidic-glutamine-arginine triad, which defines the final residues of the conserved 19 amino acid GPSM motif signature, reaches into the nucleotide binding pocket of Gα and makes direct contact with the α and β phosphate of the bound GDP via its basic δ-guanididium group (Kimple, Kimple, et al. 2002; Siderovski & Willard 2005; Thomas et al. 2008). It has also been shown that the binding of the GPSM motif displaces an arginine within the switch I region of Gα, and instead of contacting the α and β phosphate groups it contacts the 3' hydroxyl group of the GDP ribose sugar moiety (Willard et al. 2004). This newly formed interaction is believed to underlie the GDI activity of the GPSM motif.

Mutation of the arginine in the acidic-glutamine-arginine triad to phenylalanine results in the complete loss of GDI activity and the ability to bind Gαi/o subunits, while mutation to less bulky alanine or leucine residues causes a significant decrease in GDI activity but no change in binding affinity

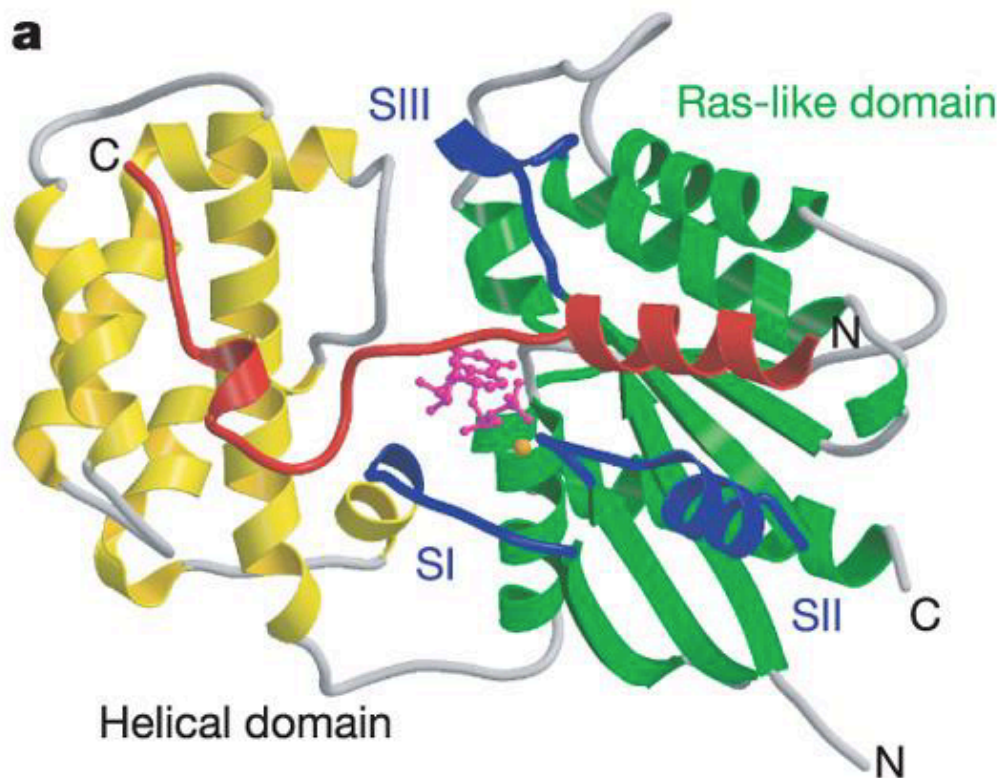


Figure 1.6. The GPSM motif of RGS14 interacts with Gai1. Ribbon drawing of R14GL peptide (red) in contact with the Ras-like (green) and all-helical (yellow) domains of Gai1. Also shown are the three switch regions of Gai1 (blue), GDP (magenta), and Mg²⁺ (orange). From Kimple, Kimple, et al. 2002. Reprinted with permission from Nature Publishing Group.

(Kimple, Kimple, et al. 2002; Peterson et al. 2000; Takesono et al. 1999; Peterson et al. 2002; Bernard et al. 2001). This means that the arginine of the acidic-glutamine-arginine triad is a significant, but not an absolute, determinant of guanine nucleotide dissociation inhibitor activity (Willard et al. 2004). The glutamine residue preceding it is also a crucial determinant of GDI activity, forming extensive backbone interactions with the $G\alpha$ subunit which kinks the GPSM motif peptide backbone allowing the arginine side chain to fully extend into the nucleotide-binding pocket (Kimple, Kimple, et al. 2002; Willard et al. 2004). Mutating this residue to alanine eliminates GDI activity and $G\alpha$ binding (Peterson et al. 2002). Finally, the acidic residue preceding glutamine is important for structurally anchoring glutamine via a side chain hydrogen bond (Willard et al. 2004).

The selectivity of the various GPSM motifs for G proteins is determined principally by the all-helical domain of the $G\alpha$ subunit and residues C-terminal to the conserved 19 amino acid core GPSM motif. A $G_{\alpha o}$ -insensitive GPSM motif peptide derived from RGS14 and GPSM1 exhibited GDI activity on a chimeric $G_{\alpha o}$ subunit containing the all-helical domain of $G_{\alpha i 1}$ (Kimple, Kimple, et al. 2002). Alternatively, replacing the C-terminal domain of RGS14 with the corresponding region from Pcp-2, a GPSM motif-containing protein that is sensitive to $G_{\alpha o}$, leads to a gain of function similar to wild-type Pcp-2 (Kimple, Kimple, et al. 2002).

1.2.4 REGULATION OF GPSM MOTIF FUNCTION

Although the regulation of GPSM motif function remains poorly studied, a few forms of regulation have been identified. Most GPSM motif-containing proteins contain at least one phosphorylation site located within or N-terminal to the core GPSM motif, which theoretically could affect their function. Phosphorylation of the PKA substrate Thr-494 just N-terminal to the GPSM motif of RGS14 results in increased GDI activity by up to three fold (Hollinger et al. 2003). Phosphorylation of the GPSM motifs in GPSM1 by LKB1, on the other hand, reduces its ability to interact with G proteins (Blumer et al. 2003). Phosphorylation of the Thr-450 site N-terminal to the first GPSM motif in GPSM2 by PBK/TOPK leads to enhanced cell growth (Fukukawa et al. 2010a). Whether this effect is related to G protein signaling or the $G\alpha$ -GPSM2-NuMA ternary complex is unclear. It therefore appears that phosphorylation is a commonly used means to regulate GPSM motif-containing proteins (Blumer et al. 2007).

Expression of some GPSM motif-containing proteins appears to be developmentally regulated. GPSM1 mRNA levels in the heart change during the course of development, and expression has been shown to decline in the aging rat brain (Pizzinat et al. 2001; Blumer et al. 2002). GPSM1 is also upregulated in the brain of a rat model of craving following cocaine exposure (Bowers et al. 2004). GPSM2 expression has been reported to change with the cell cycle (Whitfield et al. 2002; Du & Macara 2004).

Regulation via the activation of GPCRs has also been demonstrated. Activation of the $\alpha 2$ adrenergic receptor ($\alpha 2$ -AR) or the μ -opioid receptor greatly diminishes the bioluminescence

resonance energy transfer (BRET) signal observed between GPSM1 and G α i. Interestingly, co-expression of RGS4 in this overexpression system inhibits this effect, suggesting that both nucleotide exchange and hydrolysis play a role in this regulatory effect (Oner, An, et al. 2010). Coupling between GPSM3 and G α i is also reported to be reduced upon activation of the α 2-AR (Oner, Maher, et al. 2010). Recently, evidence has been found that this regulation may be the result of direct coupling of a GPSM-G α (GDP) complex with a GPCR, suggesting this could represent a unique signaling triad that parallels the well-defined heptahelical receptor-G $\alpha\beta\gamma$ -effector system (Robichaux et al. 2015). This study used a version of G α i2 that was mutated to be pertussis toxin-insensitive and tethered to α 2-AR. Pertussis toxin was used to ensure that only the tethered G α subunits were being tested. When bound by either GPSM3 or GPSM1, agonist activation was shown to reduce BRET signals between both of these proteins and G α i2 by up to 40%. This is an intriguing result as many GPSM-motif containing proteins have more than one GPSM motif, and could therefore bind multiple G α subunits and could conceivably act to scaffold associated receptors. It has also been reported that GPSM-G α (GDP) complexes can be regulated by non-receptor GEFs such as Ric-8A, catalyzing the separation of GPSM motifs from G α (GDP) in both GPSM1 and GPSM2, with an apparent preference for myristoylated G α subunits (Thomas et al. 2008; Tall & Gilman 2005). It should be noted that while Ric-8A does bind to GPSM1, it has not always been shown to facilitate G α i-induced suppression of adenylyl cyclase and thus may not always act as a GEF in a cellular environment (Tse et al. 2015). RGS7 appears to oppose this process, promoting the reassociation of G α (GDP) with GPSM-motif containing proteins (Tall & Gilman 2005).

Regulation of GPSM motif function can also occur via the action of other GPSM motifs within the same protein. These additional motifs can create an ultrasensitivity by acting as competitive decoys, competing against the activation of the functionally relevant GPSM motif (Lu et al. 2012; Smith & Prehoda 2011). High-affinity decoy sites add a threshold to the response, while low-affinity decoy sites contribute the ultrasensitive component by ensuring a sigmoidal response.

1.2.5 CELLULAR FUNCTIONS OF GPSM MOTIF-CONTAINING PROTEINS

Functional studies of GPSM motif-containing proteins indicate their involvement in a wide range of physiological roles, including cell division, neuronal outgrowth, craving and addiction, autophagy, and ion channel regulation (Blumer et al. 2007). GPSM1 is upregulated in the prefrontal cortex of rats during late withdrawal following repeated cocaine exposure (Bowers et al. 2004). It has therefore been suggested that GPSM1 regulates cocaine-induced behavioral plasticity via G protein signaling in the prefrontal cortex. GPSM1 has also been linked to early events in the autophagic pathway in human intestinal HT-29 cells, likely prior to autophagosome formation (Pattingre et al. 2003). The influence of GPSM motif-containing proteins on G protein-regulated ion channels has been investigated in both HEK293 cells and *X. laevis* oocytes expressing GIRK channels. Full-length GPSM2 and peptides derived from its GPSM motifs activate basal G $\beta\gamma$ -dependent K⁺ currents, while siRNA knockdown of GPSM2 decreased basal K⁺ currents in primary neuronal cultures (Wiser et al. 2006). Pcp-2 modulated receptor regulation of Cav2.1 calcium channels expressed in *X. laevis* oocytes, but had no effect on the basal current (Kinoshita-Kawada et al. 2004). Complexes between G α_i (GDP) and the GPSM

regions of GPSM1, Pins, and GPSM2 have been found to regulate both *Drosophila* and mammalian asymmetric cell division (ACD). This will be discussed in greater later.

GPSM motif-containing proteins may also play a role in hypertension. Altered Gai/o mediated cell signaling has been linked to hypertension; in fact, an increased level of Gai is one of the earliest events in animal models of hypertension (Sato & Ishikawa 2010; Anand-Srivastava 1996). In the aorta of 6 week old spontaneously hypertensive (SHR) rats, expression of Gai was increased by 40% compared to that in normotensive Wistar-Kyoto (WKY) rats (Anand-Srivastava 1992). Uncoupling of GPCRs and Gai via treatment with pertussis toxin normalizes the expression of Gai in SHR rats and results in the reduction of blood pressure to normotensive levels, delaying the onset of hypertension (Li & Anand-Srivastava 2002; Kost et al. 1999). GPSM1 null mice exhibit altered blood pressure control mechanisms, including increased baroreceptor reflex sensitivity and an inability to restore arterial pressure following treatment with the vasodilating agent sodium nitroprusside (Blumer et al. 2008).

1.3 ASYMMETRIC CELL DIVISION

1.3.1 *ASYMMETRIC CELL DIVISION OVERVIEW*

Mitotic cell division can be divided into two basic categories: symmetric cell division and asymmetric cell division. Conventional cell division produces two identical daughter cells, whereas ACD results in daughter cells with differing fates (Figure 1.7). In ACD, the mother cell establishes an axis of polarity followed by unequal distribution of cell fate determinants, as well as unequal orientation of the mitotic spindle along the axis. This involves shifting their division

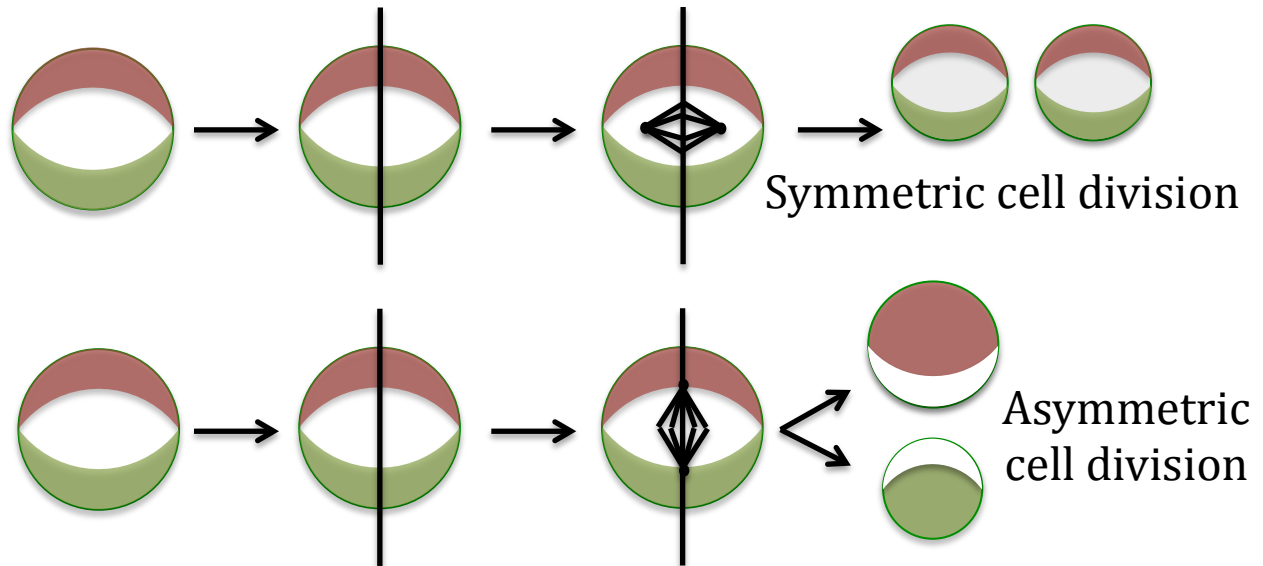


Figure 1.7. Symmetric versus asymmetric cell division. Symmetric divisions produce two identical daughter cells. Asymmetric cell division produces daughter cells with differing cell fates as a result of unequal distribution of fate determinants and resources. Red and green crescents represent different fate determinants (proteins and RNAs) that can be equally or unequally partitioned into daughter cells and may differentially influence the developmental potential of those cells. Adapted from Mapelli & Gonzalez 2012.

machinery toward a specific region of the cell cortex (Goldstein 2003). Finally, the cell will asymmetrically divide into two daughter cells (Gönczy 2008). ACD is used by many species to maintain stem cell populations, as well as during development to generate cellular diversity. ACD has been well studied in *Drosophila melanogaster* neuroblasts and *Caenorhabditis elegans* embryos, however ACD in mammalian systems remains poorly understood (Willard et al. 2004).

Virtually all of the proteins involved in the process of ACD in lower metazoan models are evolutionary conserved in mammals (Johnston et al. 2009). *D. melanogaster* neuroblasts undergo asymmetric cell divisions to produce a large apical neuroblast and a smaller ganglion mother cell (GMC) (Willard et al. 2004). The apical determinants Bazooka (partitioning defective protein 3, PAR-3, in mammals), PAR-6, and aPKC form a protein complex that recruits the Inscuteable (Insc) protein to the apical cell cortex, directs spindle orientation, and helps segregate the basal determinants Numb, Miranda, and Prospero. Partner of Inscuteable (Pins, GPSM1 and GPSM2 in mammals) is recruited by Insc to the apical cell cortex, where it then binds Gai and Mud (nuclear mitotic apparatus protein, NuMA, in mammals) to form a ternary complex that directs spindle positioning and contributes to the generation of pulling forces on astral microtubules via the direct interaction between Mud and the minus-end-directed microtubule motor Dynein/Dynactin (Mapelli & Gonzalez 2012) (Figure 1.8).

1.3.2 G PROTEINS AND THEIR ACCESSORY PROTEINS IN ASYMMETRIC CELL DIVISION

G proteins are best known for their role in signal transduction downstream of seven transmembrane receptors, but they also play an essential role in the process of cell division. Gai2

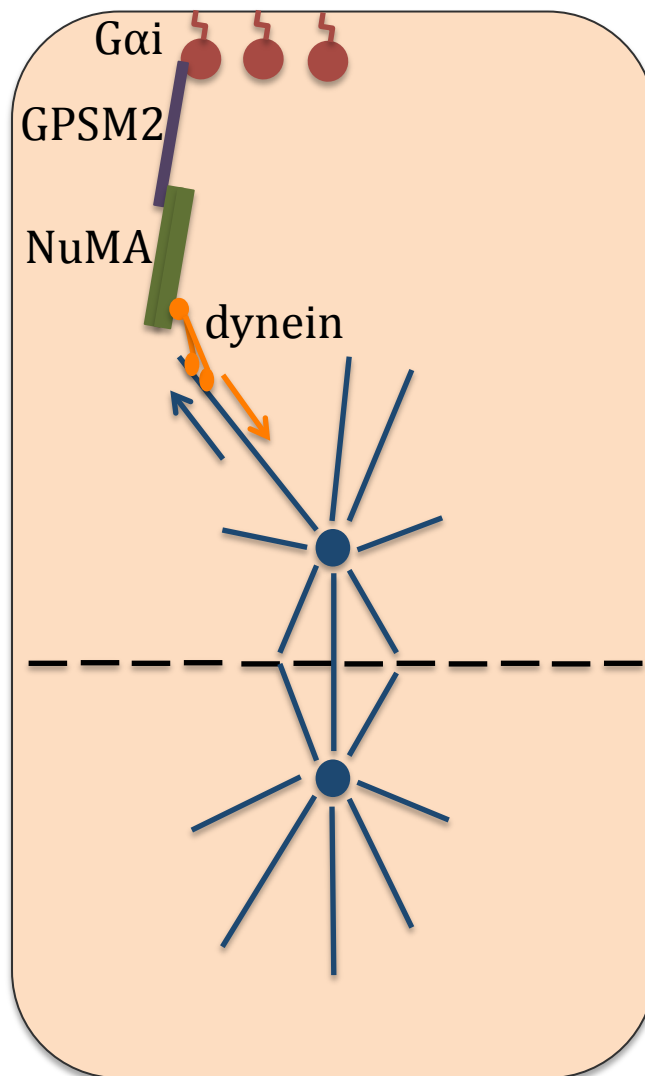


Figure 1.8. Positioning of the mitotic spindle by GPSM2. The ternary complex ($G\alpha i$ -GPSM2-NuMA), along with dynein/dynactin, positions the mitotic spindle poles in asymmetric cell division.

has been reported to bind to the kinetochores of chromatin during mitosis in 3T3 cells (Crouch & Simson 1997; Crouch et al. 2000). G α localizes to the mitotic spindle in a human carcinoma cell line and multiple animal cell lines, where it co-localizes with β -tubulin (Wu & Lin 1994). Furthermore, in bovine brain cells, G β subunits are incorporated into the mitotic spindle and interact with the mitotic spindle (Wu et al. 1998).

In *gpb-1* (the G β homologue) mutant *C. elegans* embryos, cell division axes are randomly orientated and centrosome positions are abnormal (Zwaal et al. 1996). Similar results were seen in neural progenitor cells in the developing mouse neocortex. When the carboxy-terminal region of β -adrenergic receptor kinase, which is known to sequester free G $\beta\gamma$ without affecting G α signaling, was overexpressed, it led to a shift in spindle orientation. When GPSM1 was knocked down in neural progenitor cells via RNA interference (RNAi), alterations in spindle orientation similar to that seen with G β mutants or knockdowns was observed (Sanada & Tsai 2005). G β and GPSM1 appear to participate in the same processes.

G α subunits and GPSM2/GPSM1 also appear to participate in similar cell division-related roles. In *C. elegans* embryos with RNAi directed against GOA-1 or GPA-16 (G α homologues), centrosomes fail to separate properly and incorrect spindle orientations occur as a result of a lack of centrosome rotation, abnormal centrosome starting positions, and incorrect paths of centrosome migration (Gotta & Ahringer 2001; Miller & Rand 2000). Simultaneous inactivation of these G α subunits results in the almost complete loss of spindle pulling forces from both the anterior and posterior poles of the dividing cell (Hampoelz & Knoblich 2004). It also results in the mitotic spindle being centrally instead of asymmetrically located, leading to an equal first

cleavage rather than the cleavage plane being asymmetrically displaced toward the posterior. RNAi targeted to GPR-1 and GPR-2, which replace the function of GPSM1 and GPSM2 in *C. elegans*, produced similar results (Schneider & Bowerman 2003a; Srinivasan et al. 2003). When GPB-1 is also inactivated, the result is the same, implying that this is due to the loss of $G\alpha$ subunit function and not constitutive activation of $G\beta\gamma$ (Gotta & Ahringer 2001). Overexpression of *Gai1* in Madin-Darby canine kidney (MDCK) cells, but not *Gas*, causes pronounced oscillations and rotations of the mitotic spindle indicative of strong pulling forces exerted on its astral microtubules. An identical phenotype is observed with the overexpression of GPSM2 (Du & Macara 2004).

Numerous studies have implied that the coupling between GPSM motif-containing proteins and G proteins is important for the proper functioning of the latter during cell division. *Gai* proteins and GPSM motif-containing proteins share similar subcellular localization during mitosis, and the interaction between GPSM domains and G proteins influences the subcellular localization of GPSM motif-containing proteins during both interphase and mitosis (Cho & Kehrl 2007; Shu et al. 2007). Blocking this interaction leads to abnormal exaggerated mitotic spindle rocking in kidney epithelial cells and cytokinesis defects (Willard et al. 2008; Cho & Kehrl 2007).

The most thoroughly studied GPSM motif-containing protein in the context of cell division is GPSM2. The expression levels of GPSM2 have been observed to increase during metaphase in mammalian cell division. Furthermore, subcellular localization studies indicate that GPSM2 is important for the cortical positioning of the spindle pole, which likely reflects stronger pulling or pushing forces on the spindle pole (Blumer et al. 2006). Immunocytochemical staining shows

GPSM2 at the spindle in cells at metaphase, and at the midzone and midbody in cytokinetic cells (Fukukawa et al. 2010a). A similar pattern of upregulation during mitosis and localization to the midbody of cytokinetic cells has been reported for Ric-8A (Boullaran et al. 2014). GPSM2 transcript levels are upregulated in a large proportion of breast cancers, and treatment of those cells with siRNA targeting GPSM2 resulted in incomplete cell division and significant growth suppression in breast cancer cells (Fukukawa et al. 2010a).

In its inactive form, the N-terminus and C-terminus of GPSM2 interact with one another, precluding the GPSM motifs from interacting with Gai. However, fluorescent resonance energy transfer (FRET) studies demonstrate that when it binds the nuclear mitotic apparatus protein (NuMA), the intramolecular association between the two termini is released and GPSM2 can bind Gai (Du & Macara 2004). This anchors the complex to the cell cortex, and the association between NuMA and the dynein/dynactin structure accounts for this complex's ability to interact with microtubules. The motor activity of dynein/dynactin pulls the mitotic spindle to the cell cortex, thus forming the spindle poles (Merdes et al. 2000) (Figure 1.8).

Precise mitotic spindle orientation is thought to be achieved through cycles of astral microtubule stabilization and destabilization (Dave et al. 2009). Gai acts not only as a membrane tether but also as a switch, allowing ratcheting of pulling forces by rapid cycling of nucleotide exchange which causes temporary release between components of the Gai-GPSM2-NuMA complex (Tall & Gilman 2005). This rapid cycling is accomplished by GAP and GEF activity of accessory proteins. In *C. elegans*, RGS7 and Ric-8A fulfill these roles, respectively (Dave et al. 2009). RGS14, which contains both a GPSM motif and an RGS domain, could in theory act as a GAP in

addition to binding G α i making it as attractive candidate for participation in mitotic spindle orientation (Shu et al. 2007; Cho et al. 2005). GPSM3, which displays GEF activity and an ability to act as a GDI and bind G α i, is another attractive prospect for a role in cell division.

1.4 G PROTEIN SIGNALING MODULATOR 3 (GPSM3)

1.4.1 IDENTIFICATION AND CHARACTERIZATION OF GPSM3

GPSM3 is a 160 amino acid protein encoded by a gene within the major histocompatibility complex class III region of chromosome 6 (Cao et al. 2004; Zhao et al. 2010) (Figure 1.9). GPSM3 was first discovered in a yeast-based functional screen for activators of the pheromone response pathway in the absence of a GPCR. The yeast-based system was used to screen a human prostate leiomyosarcoma cDNA library, and one of the cDNAs isolated in the screen was GPSM3 (Cao et al. 2004). It contains three GPSM motifs at its C-terminus (conflicting reports exist regarding the activity of the second GPSM motif), while its short N-terminus contains multiple proline residues (14 out of 60 amino acids in total) (Kimple et al. 2004; Oner, Maher, et al. 2010; Zhao et al. 2010). Two different protein isoforms of GPSM3, with different N-terminal polypeptide sequences, have been predicted in the human genomic sequence database curated by Ensembl (Billard et al. 2014). The consensus among a number of studies is that GPSM3 is localized to the cytoplasm in cells, with it sometimes being seen in the nucleus and other times enriched at the plasma membrane (Cao et al. 2004; Giguère, Laroche, Oestreich, Duncan, et al. 2012; Giguère, Laroche, Oestreich & Siderovski 2012; Zhao & Chidiac 2015). Studies show that GPSM3 mRNA is detectable in a variety of tissues such as the heart, placenta, lung, liver, brain, and spleen (Cao et al. 2004; Zhao et al. 2010). However, the public GeneAtlas database of the

```
1  MEAERPQEEEDGEQGPPQDEEGWPPPNSTTRPWRSA  
37  PPSPPP GTRHTALGPRSASLLSLQTELLDLVAEAQSR  
76  RLEEQRATFYTPQNPSSLAPAPLRPLEDREQLYSTILSH  
116 QCQRMEAQRSEPPLPPGGQELLELLRVQGGGRMEE  
153 QRSRPPHTHC
```

Figure 1.9. Amino acid sequence of GPSM3. The three GPSM motifs are highlighted in green. The proline-rich N-terminal region is highlighted in red.

human transcriptome shows that expression is restricted to hematopoietic cells with the highest signal strength in whole blood and CD14⁺ monocytes (Giguère et al. 2013). GPSM3 expression is also seen in rat epithelial cells and vascular smooth muscle cells (Zhao & Chidiac 2015).

The list of protein-protein interactions that GPSM3 participates in has grown steadily in the literature over the past few years, with many partners being associated with G protein signaling (Table 1.2). GPSM3 has been shown to bind members of the Gai/o family, coupling with Gao and all three isoforms of Gai (Cao et al. 2004). It shows a strong preference for Gai over Gao. GPSM3 does not interact with Gas, Gaq, or Gα16. A study has shown that GPSM3 also associates with the first four isoforms of Gβ, however it apparently does not interact with Gβγ (Giguère, Laroche, Oestreich & Siderovski 2012; Cao et al. 2004). RGS5 has been identified as an interaction partner of GPSM3 (Zhao & Chidiac 2015), and BRET signals between GPSM3 and the α2 adrenergic receptor have been observed as well (Oner, Maher, et al. 2010). GPSM3 appears to form a complex with NOD-like receptor family, pyrin domain containing 3 protein (NLRP3) and the heat shock A8 protein (HSPA8) (Giguère et al. 2014). The 14-3-3 family of proteins stabilize GPSM3, and up to 25 potentially regulatory phosphorylation sites have been identified in GPSM3 (Giguère, Laroche, Oestreich, Duncan, et al. 2012; Bian et al. 2014).

1.4.2 *FUNCTIONAL ROLES OF GPSM3*

GPSM3 was discovered in a yeast-based screen that required Gβγ activation to single out activating proteins, and the GPSM motif is capable of promoting the dissociation of heterotrimer subunits (Cao et al. 2004; Ghosh et al. 2003). This would be expected to lead to the activation of

Table 1.2. GPSM3 protein-protein interaction partners.

Protein	Reference
Confirmed via interaction study	
Gαi1-3	(Cao et al. 2004; Zhao et al. 2010)
Gαo	(Cao et al. 2004; Zhao et al. 2010)
Gβ1-4	(Giguère, Laroche, Oestreich & Siderovski 2012)
14-3-3 family members	(Giguère, Laroche, Oestreich, Duncan, et al. 2012)
NOD-like receptor family, pyrin domain containing 3 protein (NLRP3)	(Giguère et al. 2014)
Heat shock protein A8 (HSPA8)	(Giguère et al. 2014)
α2 adrenergic receptor	(Oner, Maher, et al. 2010)
RGS5	(Zhao & Chidiac 2015)
Experimental evidence	
Fibroblast growth factor 3 (FGFR3)	(Lehner et al. 2004)
Supervillin (SVIL)	(Nebl et al. 2002)

PLC β , however one study showed that overexpression of GPSM3 fails to appreciably increase inositol phosphate levels and another showed that it in fact resulted in a decrease in inositol phosphate levels by greater than 50% (Cao et al. 2004; Giguère, Laroche, Oestreich & Siderovski 2012). This suggests that GPSM3 does not promote G $\beta\gamma$ -mediated cell signaling via the promotion of heterotrimer dissociation. When expressed in the presence of membrane-tethered or GPCR-tethered G α i1/2, GPSM3 is apparently redistributed to the plasma membrane (Willard et al. 2008; Robichaux et al. 2015; Oner, Maher, et al. 2010). G α i/o mutants incapable of binding to GPSM motifs did not exhibit this effect (Willard et al. 2008). Agonist activation of the α 2A adrenergic receptor leads to decreased BRET signals between G α i2 and GPSM3. This suggests that seven transmembrane receptors can bind G α i-GPSM3 complexes and that receptor activation leads to reversible dissociation between GPSM3 and G α i in a cycle analogous to that seen with receptor and G $\alpha\beta\gamma$ (Robichaux et al. 2015). GPSM3 also appears to be regulated by the non-receptor GEFs, with the interaction between GPSM3 and G α i1 being regulated in a biphasic manner by Ric-8A depending on its level of expression. However, the increasing BRET signal at high Ric-8A concentrations is likely due to the observation that Ric-8A increases G α i1 expression levels (Oner et al. 2013).

As expected, GPSM3 demonstrates G protein regulatory effects on G α subunits. The three GPSM motifs in its C-terminal region display GDI activity for G α i/o subunits (Cao et al. 2004; Zhao et al. 2010; Oner, Maher, et al. 2010). Whether all three of these GPSM motifs can bind G α i/o subunits at the same time remains to be seen, however reports on GPSM motifs suggest that additional motifs may act as competitive decoys in order to create one ultrasensitive functional motif (Lu et al. 2012; Smith & Prehoda 2011). The proline-rich N-terminal domain of

GPSM3 exhibits the unique ability to differentially affect the nucleotide state of different G α subunits, which is not surprising since repetitive proline-rich sequences are often found to be docking sites for signaling modules (Zhao et al. 2010; Cao et al. 2004). The N-terminal region of GPSM3 displays weak GDI effects on G α _o, but interestingly it exhibits GEF activity on G α _{i1} (Zhao et al. 2010). It has also been shown that GPSM3 enhances the GAP activity of RGS5 by binding to it, and that this binding in turn impedes the inhibitory effect of GPSM3 on GTP turnover (Zhao & Chidiac 2015). GPSM3 may also regulate the stability of G β subunits before they become complexed with G γ (Giguère, Laroche, Oestreich & Siderovski 2012).

1.4.3 *GPSM3 DISEASE ASSOCIATION*

GPSM3 has been linked to a large number and variety of diseases. Significant increases in the expression of GPSM3 are observed in a rat model for polycystic kidney disease compared to the non-cystic controls (Lenarczyk et al. 2015). In prostate cancer models which mimic angiogenesis, GPSM3 expression increases by greater than two-fold relative to controls, and it has been identified as a gene required for the proliferation of p53 human cancer cell lines (Lapan et al. 2009; Xie et al. 2012). Expression changes in GPSM3 have also been connected to cell culture adaptation (Tompkins et al. 2012). GPSM3 polymorphisms are associated with childhood obesity in Hispanic populations and atopic dermatitis (Comuzzie et al. 2012; Chang et al. 2012). The connection between GPSM3 and autoimmune disease has been well established, with links to ulcerative colitis, systemic lupus, rheumatoid arthritis, and ankylosing spondylitis (Pathan et al. 2009; Barcellos et al. 2009; Giguère et al. 2013).

The first connection between GPSM3 and arthritis was discovered when polymorphisms within the human GPSM3 gene locus were identified as being significantly less prevalent in multiple autoimmune diseases (Sirota et al. 2009; Corona et al. 2010). These protective genetic variants have been found to result in a decrease in GPSM3 transcript abundance in individuals homozygous for the single nucleotide polymorphisms (Gall, Wilson, et al. 2016). The effects of GPSM3 on myeloid-dependent autoimmune disease have been studied in a GPSM3^{-/-} mouse model in which collagen antibody-induced arthritis (CAIA) was induced (Giguère et al. 2013). Mice lacking GPSM3 were protected from CAIA, showing significant decreases in paw swelling and clinical disease scores, as well as a reduction in inflammation and cartilage erosion compared to controls. Furthermore, monocyte-representative pro-inflammatory cytokines and chemokine receptors were decreased in GPSM3^{-/-} mouse paws, and GPSM3-deficient myeloid cells had reduced migration.

GPSM3 mRNA and protein levels are both seen to decrease when the monocytic THP-1 cell line is differentiated into macrophage-like cells, suggesting a role in both differentiation and migration of monocytes. Knockdown of GPSM3 in this cell line disrupts *ex vivo* migration towards certain chemokines (Gall, Wilson, et al. 2016). In the human promyelocytic leukemia NB4 cell line, GPSM3 transcript and protein levels increase in response to retinoic acid-induced differentiation into a model of neutrophil physiology (NB4*). Reducing GPSM3 expression in NB4* cells using siRNA disrupts chemotaxis towards chemoattractants involved in neutrophil recruitment to the arthritic joint (Gall, Schroer, et al. 2016). Interleukin-1 β , triggered by NLRP3-dependent inflammasome activators, is negatively regulated by GPSM3 (Giguère et al. 2014). GPSM3-null mice have enhanced serum and peritoneal interleukin-1 β production following

intraperitoneal aluminum hydroxide injection, and bone marrow-derived macrophages lacking GPSM3 expression show a significant increase in NLRP3-dependent IL-1 β secretion (Giguère et al. 2014).

1.4.4 *GPSM3 IN VASCULAR SMOOTH MUSCLE CELLS*

Vascular smooth muscle cells (VSMCs) typically have a contractile phenotype that allows the smooth muscle comprised of them to expand and contract, thereby controlling the diameter of the vasculature. However, the transition of VSMCs from a contractile to a migratory, proliferative phenotype is known to underlie cardiovascular disease and also occurs in response to isolation and culturing (Sandison et al. 2016; Dzau et al. 2002; Fingerle et al. 1989). Other GPSM motif-containing proteins such as GPSM2 and GPSM1 have been implicated in both cell migration (Taymans et al. 2006; Kamakura et al. 2013) and proliferation, while GPSM3 has previously been linked with cell migration (Giguère et al. 2013; Gall et al. 2016). Therefore, vascular smooth muscle cells, which are known to express GPSM3, are an excellent model to study a potential role for GPSM3 in cell division (Zhao & Chidiac 2015). In this study, VSMCs, in addition to other tissues, were obtained from Wistar-Kyoto rats (WKY) and spontaneously hypertensive rats (SHR). SHR rats display significantly higher blood pressure than their WKY counterparts (approximately 193 mmHg compared to approximately 133 mmHg) (Leung et al. 2016). In addition to elevated blood pressure, these rats have many other differences with normotensive WKY rats including increased Gai-mediated pathway activity likely contributing to hypertension, increased innervation in the spleen and thymus, and increased inflammation of the liver, heart, kidney, and brain (Kost et al. 1999; Purcell & Gattone 1992; Sun et al. 2006).

SHR vascular smooth muscle cells have been shown to divide at a rate 1.75 times that of WKY VSMCs (Hadrava et al. 1991). This increased proliferation rate could be linked to the hypertensive phenotype in SHR rats as division of VSMCs could increase blood vessel wall thickness and in the process decrease the diameter of the vessel. Additionally, a difference in GPSM3 protein expression in VSMCs was seen in our lab, with VSMCs derived from SHR rats exhibiting greater expression than WKY-derived VSMCs (Zhao 2011). Elevated expression of GPSM3 could be linked to the increased rate of proliferation in VSMCs and the hypertensive phenotype of SHR rats.

1.5 RESEARCH PURPOSE AND AIMS

The fundamental participants of GPCR-mediated cell signaling were originally recognized to be the receptors, heterotrimeric G proteins, and effectors. However, over time, studies have begun to reveal that signaling processes are not as simple as once imagined. Accessory proteins such as GPSM3 fine-tune signals by influencing the nucleotide-state of the $G\alpha$ subunit, and may participate in non-canonical G protein signaling via alternative complexes. They also perform other cellular functions, such as their role in asymmetric cell division. However, GPSM3 has not been linked to cell division in the literature at this time. The purpose of this study is to investigate whether or not GPSM3 plays such a role. I hypothesize that G protein signaling modulator 3 plays a role in cell division of mammalian cells, likely via an interaction with the mitotic spindle. This role in mammalian cells is investigated in a vascular smooth muscle cell model system. The specific aims of this study are:

- 1. To investigate the difference in GPSM3 transcript and protein levels between normotensive Wistar-Kyoto rats and spontaneously hypertensive rats.**
- 2. To investigate whether GPSM3 expression is linked to the rate of cell division.**
- 3. To investigate potential mechanisms of action for GPSM3 in the process of cell division via its interaction with other proteins and its localization during mitosis.**

2 METHODS

2.1 TISSUE SAMPLE COLLECTION

Dr. Robert Gross performed all tissue sample collection. All animal work was carried out in accordance with official guidelines. Four male Wistar-Kyoto (WKY) and four male spontaneously hypertensive (SHR) rats (Harlan Laboratories, Indianapolis, IL) were sacrificed at 10 weeks of age, after the onset of hypertension in the SHR rats. Rats were anaesthetized with 3% isoflurane gas, then sacrificed by cardiac puncture and whole blood was collected. Tissue samples from the aorta, heart, liver, lung, and spleen were collected. Leukocytes were isolated from heparin-treated whole blood using a ficoll-hypaque solution and differential centrifugation according to the method of Böyum 1968. All samples were stored at -80°C .

2.2 AORTIC VASCULAR SMOOTH MUSCLE CELL ISOLATION

Vascular smooth muscle cells (VSMCs) were kindly provided by Dr. Robert Gros. All animal work was carried out in accordance with official guidelines. A modified version of the protocol from Cornwell & Lincoln 1989 was used to isolate the VSMCs. Male WKY and SHR rats at 10 weeks of age were used, after the onset of hypertension in the SHR rats. Rat aortas were cleaned and cut longitudinally. Adipose tissue was removed via enzymatic digestion by placing aortas in 1 ml of Ham's F12 medium (ThermoFisher Scientific, Waltham, MA, with 1% gentamycin and 10% fetal bovine serum, FBS) and 1 mg of collagenase per aorta and incubating for 20 minutes at 37°C . Medium was removed. 1 ml of Ham's F12 medium and 1 mg of collagenase per aorta were added and sample was incubated for 30 minutes at 37°C , followed by removal of the medium and a further, identical incubation in fresh medium supplemented with collagenase.

Samples were centrifuged for 5 minutes at 200 x g at room temperature. The supernatant was then discarded. The pellet was resuspended in 1 ml of Ham's F12 medium, and 1 mg collagenase, and 0.5 mg elastase per aorta and incubated for 90 minutes at 37°C. Sample was collected by pipette and filtered using a Nitex 100 µm cell strainer to dissociate clumps into a uniform single-cell suspension. 10 ml Dulbecco's Modified Eagle Medium (DMEM, Gibco Life Technologies, Carlsbad, CA) (with 10% FBS) was then added to the filtrate. The cell suspension was then centrifuged for 5 minutes at 200 x g at room temperature. Supernatant was collected and discarded. Cells were resuspended in 10 ml DMEM (with 10% FBS and 10% fungizone/gentamicin), and then plated in a 10 cm cell culture dish.

2.3 SERUM STARVATION AND REPLACEMENT

2.3.1 *SERUM STARVATION AND REPLACEMENT PRIOR TO RNA AND PROTEIN EXTRACTION*

WKY and SHR vascular smooth muscle cells were grown in DMEM (with 10% FBS) at 37°C. When cells were 60% confluent, medium was removed and cells were washed in 1X sterile phosphate-buffered saline (PBS, Fisher Scientific) (137 mM NaCl, 2.7 mM KCl, 10 mM Na₂HPO₄, pH 7.4). DMEM (with 0% FBS) was then added and cells were incubated for 48 hours at 37°C. Medium was then removed, cells were washed in sterile PBS again, and DMEM (with 10% FBS) was added. Cells were grown for an additional 48 hours at 37°C. Cells were collected and processed for either RNA extraction or protein extraction at 24 hour intervals during the course of the experiment.

2.3.2 SERUM STARVATION AND REPLACEMENT PRIOR TO IMMUNOFLUORESCENT LABELING

WKY and SHR vascular smooth muscle cells were grown in DMEM (with 10% FBS) at 37°C. When cells were 40% confluent, medium was removed and cells were washed in sterile phosphate buffered saline (PBS). DMEM (with 0% FBS) was then added and cells were incubated for 24 hours at 37°C. Medium was then removed, cells were washed in sterile PBS again, and DMEM (with 10% FBS) was added. SHR VSMCS were grown for an additional 12 hours at 37°C while WKY VSMCs were grown for an additional 20 hours at 37°C. Cells were then prepared for immunofluorescent labeling and imaging.

2.4 RNA EXTRACTION

Total RNA was extracted from both cell culture and homogenized tissue samples using TRIzol reagent (Invitrogen, Carlsbad, CA). Samples were incubated in TRIzol reagent at room temperature for 5 minutes. 200 µl of chloroform per 1 ml of TRIzol reagent was added and samples were vortexed for 15 seconds. Samples were incubated at room temperature for 3 min, following which they were centrifuged at 4°C for 15 minutes at 5300 x g. The aqueous phase was extracted, and 500 µl of isopropanol per 1 ml TRIzol reagent used was added to precipitate RNA. Samples were incubated at room temperature for 10 minutes, and then centrifuged at 4°C at 5300 x g for 20 minutes. Supernatant was removed and pellets were superficially washed with 1 ml 75% ethanol per 1 ml TRIzol reagent used. Samples were centrifuged at 4°C at 5300 x g for 10 minutes. The supernatant was removed, and pellets allowed to air dry. Dry pellets were stored at

-80°C, and later suspended in DEPC water (Life Technologies) and diluted to 0.05 µg/µl. RNA purity and concentrations were quantified through spectrophotometry (NanoDrop Lite, Thermo Scientific). RNA samples with an absorbance ratio ($A_{260\text{ nm}} / A_{280\text{ nm}}$) of 1.8-2.2 were determined to be sufficiently pure for use in PCR applications.

2.5 REVERSE TRANSCRIPTION (RT-PCR) AND QUANTITATIVE POLYMERASE CHAIN REACTION (QPCR)

RNA samples (2 µg) were reverse transcribed (RT-PCR) to generate first strand cDNA using a High Capacity cDNA Reverse Transcription Kit (Applied Biosystems) on a T100 Thermo Cycler (BioRad). Primer sets directed against target genes of interest were designed using the National Centre for Biotechnology Information Nucleotide sequences database (www.ncbi.nlm.gov/nucore) and Invitrogen's OligoPerfect Designer primer designing tool (www.thermofisher.com/oligoperfect/). Primers were custom manufactured by and purchased from Sigma-Aldrich (St. Louis, MO) Custom DNA Oligos (Table 2.1). mRNA expression levels of GPSM3 were determined through qPCR carried out in 384 well plates using fluorescent nucleic acid dye SensiFAST SYBR Green No-ROX kit (Bioline) based assays, following the manufacturer's protocol. Reactions were carried out on CFX384 Real Time PCR Detection System and analyzed using a CFX Manager 3.0 program (BioRad). The cycle threshold was set so that exponential increases in amplification were approximately level between all samples at the linear phase of the amplification curves. Relative mRNA levels of rGPSM3 were generated from five-fold serial dilutions of pooled cDNA samples, and then normalized to a reference gene (GAPDH in tissue samples and β 2-microglobulin in VSMC primary culture samples). Reference

Table 2.1. Primers for qPCR

Target gene	Forward Primer	Reverse Primer
GPSM3	5'-CCTTCTCTCTGGGACTCAAA-3'	5'- AGCCCTCACAACCTGTTTAG-3'
GAPDH	5'-AACTTTGTGAAGCTCATTTCCT-3'	5'-ATTGATGGTATTCGAGAGAAGG-3'
B2M (β 2-microglobulin)	5'- ACGTTTGTCTTGGTGATGTG-3'	5'-CAGTAGTCCCTGATGCTCCT-3'

genes were stable across all samples and conditions to allow comparative assessments on the relative change in the expression of GPSM3.

2.6 PROTEIN ISOLATION

Cell lysates were prepared by washing twice with ice-cold 1X phosphate-buffered saline (PBS, Fisher Scientific) (137 mM NaCl, 2.7 mM KCl, 10 mM Na₂HPO₄, pH 7.4) and scraped into 150 μ l of ice-cold lysis buffer (250 mM NaCl, 50 mM Tris pH 8, 5 mM EDTA, 0.5% Triton X-100 (IGEPAL), phenylmethylsulfonyl fluoride protease inhibitor tablet (Roche, 04693116001), 20 mM Na₄P₂O₇, 10 mM NaF, and 20 mM Na₃VO₄). Cell lysates were homogenized by vigorous pipetting and underwent three consecutive freeze-thaw cycles via flash freezing with liquid nitrogen. Pellets were sedimented by centrifugation at 11,000 x g for 15 minutes at 4°C. Supernatants were collected and protein concentrations were determined using a Bicinchoninic Acid Protein Assay Kit (Sigma, BCA1) and a VICTOR3V Microplate Reader (PerkinElmer, 1420-251).

2.7 IMMUNOBLOTTING

Protein samples were prepared in 5X Laemmli loading (sample) buffer (60 mM Tris-HCl pH 6.8, 2% SDS, 10% glycerol, 5% β -mercaptoethanol, 0.02% bromophenol blue) and balanced with 1X sample buffer for equal protein concentration. Samples were heated at 99°C for 5 minutes prior to gel loading and gel electrophoresis in order to denature the proteins. Equal amounts of protein (30 μ g) were separated by 15% SDS-PAGE and wet transferred onto nitrocellulose membrane

(Whatman Protran). Membranes were incubated for 1 hour in blocking buffer (Tris-buffered saline, 0.1% Tween 20, 5% skim milk) and rocked at room temperature before overnight incubation at 4°C, rocking with either: anti-GPSM3 (1:500, GeneScript custom ordered, described in Zhao & Chidiac 2015) or anti- β tubulin for protein loading control (1:1000, Pierce PA5-16863). Following overnight incubation, membranes were washed 4 times for 5 min with TBST (Tris-buffered saline, 0.1% Tween 20) and incubated for 1 h at room temperature with horseradish peroxidase-conjugated secondary antibodies: anti-rabbit IgG (1:4000, Pierce 31463). Immunoblots were then washed 4 times for 5 min with TBST. Immunoblots were visualized with SuperSignal West Pico chemiluminescent substrate (ThermoFisher Scientific, 34080) and digitally imaged using Bio-Rad VersaDoc camera and Quantity One program (Bio-Rad, model GS-700). Relative protein expression levels from immunoblots were quantified and analyzed using densitometry software (Quantity One, Bio-Rad). Relative densitometric signal of protein bands were determined with subtraction of background signal of immunoblots, and GPSM3 protein bands were then normalized to corresponding β -tubulin bands.

2.8 TRANSFECTION

All transfections were performed using the Human Embryonic Kidney 293 (HEK-293) cell line under standard conditions of 37°C and 5% CO₂, in DMEM with 10% FBS. HEK-293 cells are commonly used for *in vitro* experiments due to their ease of transient transfection (Li et al. 2013).

2.8.1 TRANSFECTION FOR MTT ASSAY AND CELL COUNTING

Plasmid constructs encoding EYFP (enhanced yellow fluorescent protein)-tagged GPSM3 were generously donated by Dr. Joe Blumer from the Medical University of South Carolina and are described in Oner et al. 2010. To summarize the protocol, cells were seeded and grown to 70-85% confluence in a 100 mm dish before transfection. Once 70-85% confluent, 400 ng of EYFP or EYFP-GPSM3 DNA plasmid was diluted in 450 μ l of sterilized water in a sterile tube. 50 μ l of 2.5 M CaCl_2 was added to the diluted DNA, followed by 500 μ l of 2x HEPES-buffered saline (HBS) solution (0.28 M NaCl, 0.05 M HEPES, 1.5 mM Na_2HPO_4 , pH 7.0) that was slowly dripped over the DNA/ CaCl_2 solution and then mixed immediately. The mixture was then slowly dripped over the cells which were incubated for ~18 hours with the transfection reagents.

Following incubation, cells were washed with 1x PBS three times and fresh DMEM with 10% FBS was added. Cells were allowed to recover from transfection for 3-6 hours and then diluted 1 in 12.5 in addition fresh DMEM with 10% FBS. Cells were then reseeded in 24-well plates with 500 μ l per well.

2.8.2 TRANSFECTION FOR MAMMALIAN TWO-HYBRID ASSAY

Transfections were performed using Lipofectamine 2000 (Life Technologies, 11668-019) according to the manufacturer's protocol. To summarize the protocol, cells were seeded and grown to 70% confluence before transfection. Once 70% confluent, 10 μ l of Lipofectamine 2000 reagent was diluted into 250 μ l of Opti-MEM[®] I Reduced Serum Medium (Life Technologies, 31985-070) in an Eppendorf tube. In a separate eppendorf tube, 1 μ g of each plasmid DNA to be

transfected was diluted in 250 μ l of Opti-MEM® I Reduced Serum Medium and both eppendorf tubes were incubated at room temperature for 5 minutes. The contents of the eppendorf tubes were thoroughly mixed together and were incubated at room temperature for 20 minutes. The combined mixture was added to the cells and the cells were plated in a 96-well clear bottom white assay plate. The mixture was allowed to incorporate into the cells for 24 hours.

2.9 MTT ASSAY

An MTT assay measures time-related changes in the metabolic activity of cells via their ability to reduce MTT reagent (tetrazolium salts) into formazan crystals. The purple formazan crystals can then be solubilized in DMSO and quantified by spectrophotometry. This can be used as a proxy for measuring the proliferation rate of cells. Transfected cells were subjected to an MTT assay on each of the five days of the experiment in order to assess changes in cell population, with the first day being marked as day 0. Separate wells were used for each day as MTT reagent is cytotoxic and the cells can be damaged and even killed during the course of the MTT assay (Riss 2006). A nonlinear regression was performed on both data sets using an exponential plateau model with the equation $Y = Y_0 + (Y_{\max} - Y_0) * (1 - e^{(-k * x)})$, where Y_0 is the Y-intercept, Y_{\max} is the plateau value, e is Euler's number, k is the growth rate constant measured in reciprocal units to those x is measured in (days^{-1}), x is time in days, and Y is the absorbance value representing cell population size. Doubling time (DT) can then be calculated as $DT = \ln 2 / k$.

50 μ l of 2.5 mg/ml 3-(4,5-dimethylthiazol-2-yl)-2,5-diphenyltetrazolium bromide (MTT reagent, Sigma M2128) was added to each well in a 24-well plate and incubated at 37°C for 2 hours.

Following incubation, medium was slowly aspirated so as to not disrupt the formazan crystals. 500 μ l of working grade dimethyl sulfoxide (DMSO) was added to each well and the plate was covered in aluminum foil. Plates were rocked for 2 hours and then absorbance was measured using a wavelength of 595 nm on a Thermo Multiskan Spectrum 1500 spectrophotometer (ThermoFisher Scientific, 51118750). Three control wells per plate containing only 500 μ l of DMSO are also measured and the average value of these was subtracted from the experimental values.

2.10 CELL COUNT ASSAY

To ensure that the MTT data was indicative of an increased rate of proliferation and not increased cell size resulting in increased metabolism, cell counts were performed on cells expressing EYFP or EYFP-GPSM3. Five locations chosen at random within each well were imaged using an Olympus IX71 fluorescent microscope (Olympus Canada) and the number of cells expressing EYFP or EYFP-GPSM3 was analyzed using ImageJ software.

2.11 IMMUNOFLUORESCENT LABELING

Adherent cells were washed once in 1 ml 37°C PBS. Cells are then fixed by incubation in 1 ml 4% formaldehyde for 10 minutes at room temperature and then washed five times with 1 ml room temperature PBS. Cells were then incubated in 1 ml 0.25% triton X-100 (in PBS) for 5 minutes at room temperature and then washed five times with 1 ml room temperature PBS. Cells were incubated in 1 ml room temperature PBS containing 10% FBS for 1 hour. Next, cells were

incubated in 1 ml anti-GPSM3 primary antibody and anti- β -tubulin primary antibody (diluted 1:500 in PBS) overnight at 4°C. Cells were then washed five times with 1 ml room temperature PBS and then incubated in 1 ml AlexaFluor 488 goat anti-rabbit and AlexaFluor 568 goat anti-mouse secondary antibodies (diluted 1:500 in PBS) for 1 hour at room temperature in the dark. Cells were then washed five times in 1 ml room temperature PBS. Cells are next incubated in 250 μ l DAPI (ThermoFisher Scientific, 62248) (diluted 1:1000 in PBS) for 5 minutes at room temperature and then washed three times with 1 ml room temperature PBS. Finally, cells are immunomounted by applying a small drop of medium to a glass slide and placing the cell-coated coverslip face down onto the droplet. The slide is stored in the dark for at least 2 hours until dry. Cells are then visualized on an Olympus FV1000 confocal microscope at the Robarts Research Institute's Confocal Microscopy Core Facility. 10 μ g/ μ l anti-GPSM3 primary antibody blocking peptide (GenScript) was added to the 1 ml PBS containing anti-GPSM3 primary antibody and anti- β -tubulin primary antibody (diluted 1:500) and incubated overnight at 4°C for the blocking peptide experiments. The blocking peptide sequence, EAERPQEEEDGEQC, corresponds to the first fourteen amino acids of GPSM3 following the initial methionine.

2.12 MAMMALIAN TWO-HYBRID SYSTEM

The CheckmateTM Mammalian Two-Hybrid System (Promega, E2440) enables *in vivo* detection of protein-protein interactions. This is accomplished using three vectors: pACT, pBIND, and pG5luc (Figure 2.1). Both the pACT and pBIND vectors utilize a human cytomegalovirus (CMV) immediate early promoter to drive expression. In addition, the pBIND vector expresses the *Renilla reniformis* luciferase under the control of the SV40 promoter, which allows for

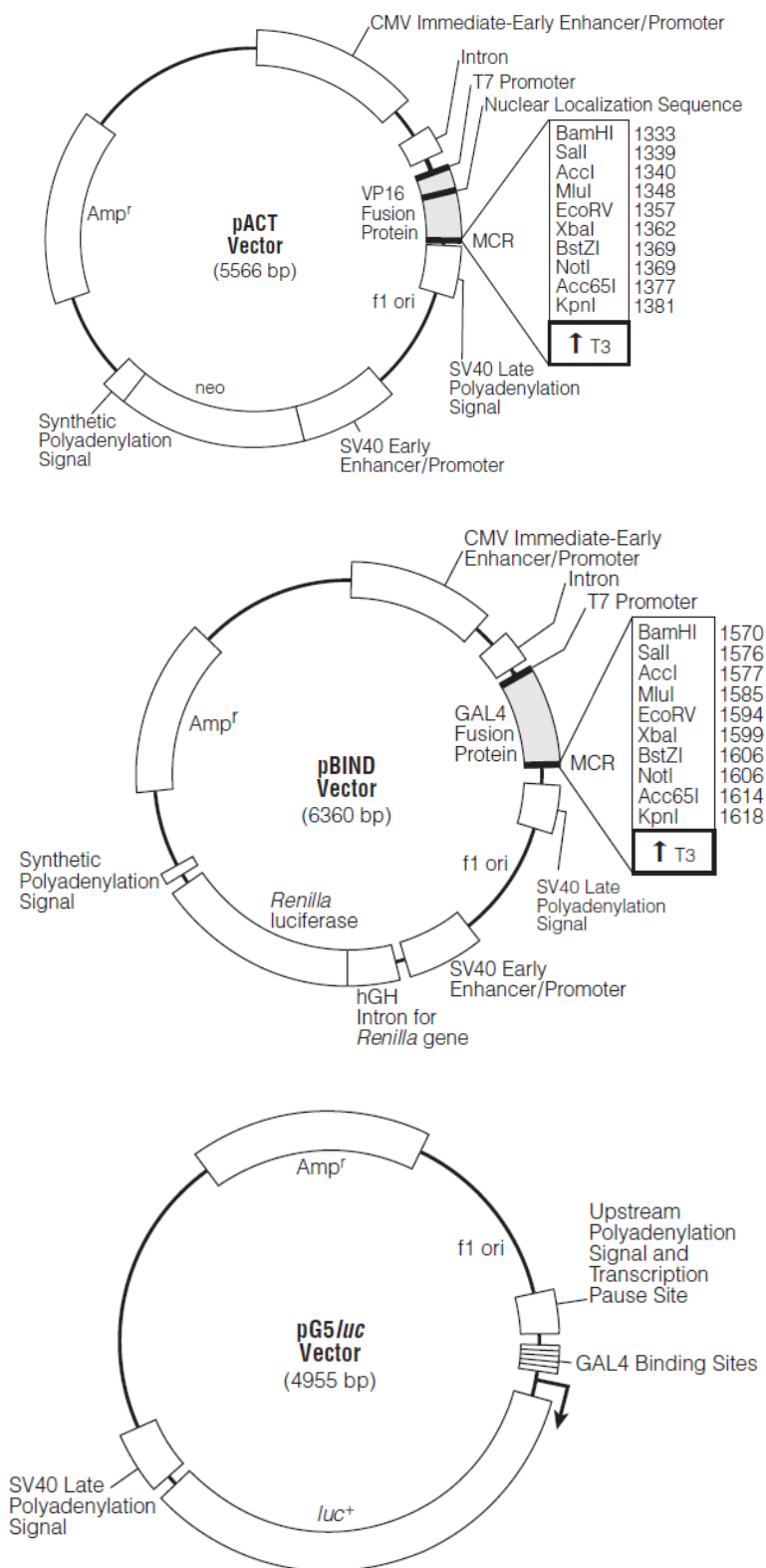


Figure 2.1. Checkmate™ Mammalian Two-Hybrid System vectors.

normalization of differences in transfection efficiency. The pG5*luc* vector contains five GAL4 binding sites upstream of a minimal TATA box, which in turn is upstream of the firefly luciferase gene. Subcloning a target gene into the pACT vector and subsequent expression results in the protein of interest with a C-terminally attached transcriptional activation domain. Subcloning a target gene into the pBIND vector and subsequent expression results in the protein of interest with a C-terminally attached DNA-binding domain. When a gene of interest with an attached transcriptional activation domain interacts with a second gene of interest with an attached DNA-binding domain, these two attached domains become closely associated. This results in the promotion of the assembly of RNA polymerase II complexes at the TATA box of the pG5*luc* vector, which increases transcription of the firefly luciferase reporter gene. Each gene of interest is subcloned into both the pACT and pBIND vectors. This is done to overcome the phenomenon of vector directionality, which is the apparent difference in strength of observed interactions depending on the vector context of each insert. Therefore, each protein-protein interaction is tested with both possible fusion protein interactions. The kit also provides positive control vectors: pACT-MyoD and pBIND-Id. A negative control consists of pACT and pBIND without inserts. See Table 2.2 for a list of genes of interest.

2.13 DNA CONSTRUCTS

Plasmids encoding the genes of interest were subjected to PCR using Platinum[®] Pfx DNA polymerase (ThermoFisher Scientific, 11708021) as per the manufacturer's instructions and primers (Table 2.3) designed to introduce highly specific nucleotide sequences (restriction sites) on either side of the gene. PCR products were run on a 1% agarose gel (0.011 g/ml UltraPure[™]

Agarose (Invitrogen), 40 mM Tris-acetate, 1 mM EDTA, 0.02 µl/ml ethidium bromide, pH 8.3) for 45-120 minutes at 100-150 V. DNA bands were viewed on gel under UV light, excised, and then purified using a Gel/PCR DNA Extraction Kit (FroggaBio, Toronto, ON, DF100) as per the manufacturer's instructions. Genes of interest that were considered too long for the PCR method to be reliable were altered using gBlocksTM designed by Dr. Alexey Pereverzev to have the necessary restriction sites (synthesized using the Gibson AssemblyTM method based on the technique described by Gibson et al. 2009). Plasmids encoding both the genes of interest as well as the parent vectors were then digested with the appropriate restriction enzymes (Table 2.2) as per the manufacturer's instructions. The digested fragments of DNA were separated on 1% agarose gel (0.011 g/ml UltraPureTM Agarose (Invitrogen), 40 mM Tris-acetate, 1 mM EDTA, 0.02 µl/ml ethidium bromide, pH 8.3) for 45-120 minutes at 100-150 V. DNA bands were viewed on gel under UV light, excised, and then purified using a GenepHlowTM Gel/PCR Kit (FroggaBio, DFH100) as per the manufacturer's instructions. Each digested gene of interest was then ligated into both parent vectors using T4 DNA Ligase (Promega, M1801). The products of these ligations were then transformed into Subcloning EfficiencyTM DH5αTM Competent Cells (ThermoFisher Scientific, 18265017) as per manufacturer's instructions and plated on an agar plate containing 100 µg/ml ampicillin and incubated overnight at 37°C. Bacterial colonies were chosen and grown in selective medium overnight at 37°C and at 225 RPM. Plasmid was then purified using PrestoTM Mini Plasmid Kit (FroggaBio, PDH300) as per manufacturer's instructions. The Robarts Research Institute DNA Sequencing Facility (London, ON) confirmed all DNA sequences via fluorescent DNA sequencing.

Table 2.2. Genes of interest and the restriction enzymes used for subcloning.

Gene	Company (plasmid)	Restriction enzymes
GPSM3	Kindly provided by Dr. David P. Siderovski, Department of Physiology and Pharmacology, West Virginia University School of Medicine, Morgantown, WV, USA	SalI (Invitrogen, 15217-029), XbaI (Fermentas, FD0684)
GPSM3-mGL		SalI (Invitrogen, 15217-029), XbaI (Fermentas, FD0684)
GNAI1 (G α i1)	cDNA Resource Center, GNAI10EI00	SalI (Invitrogen, 15217-029), XbaI (Fermentas, FD0684)
GNAI2 (G α i2)	cDNA Resource Center, GNAI20EI00	SalI (Invitrogen, 15217-029), XbaI (Fermentas, FD0684)
GNAS (G α s)	cDNA Resource Center, GNA0SSEI00	SalI (Invitrogen, 15217-029), XbaI (Fermentas, FD0684)
GNAO (G α o)	cDNA Resource Center, GNA00AEI00	SalI (Invitrogen, 15217-029), XbaI (Fermentas, FD0684)
GNAO (G α o-Q205L)	cDNA Resource Center, GNA00A00C0	SalI (Invitrogen, 15217-029), XbaI (Fermentas, FD0684)
GNB1 (G β 1)	cDNA Resource Center, GNB0100000	SalI (Invitrogen, 15217-029), XbaI (Fermentas, FD0684)
FGFR3	DNASU Plasmid Repository, HsCD00294949	SalI (Invitrogen, 15217-029), XbaI (Fermentas, FD0684)
SELPLG	DNASU Plasmid Repository, HsCD00041063	SalI (Invitrogen, 15217-029), XbaI (Fermentas, FD0684)
NUMA1 (NuMA)	Addgene, Plasmid #28238	SalI (Invitrogen, 15217-029), MluI (Roche, 10663721) KflI (ThermoFisher Scientific, FD2164), SpeI (NEB, R0133S), SalI (Invitrogen, 15217-029), NotI (NEB, R0189S)
NIN (Ninein)	DNASU Plasmid Repository, HsCD00516498	
SVIL (Supervillin)	Addgene, Plasmid #13040	SalI (Invitrogen, 15217-029), MluI (Roche, 10663721)

Table 2.3. Primers for Mammalian Two-Hybrid experiments.

Target	Forward Primer	Reverse Primer
GPSM3, GPSM3-mGL	5'-ACGCGTCGACCCATGGAGGCT GAGAGACCCAGGAAGAAGAG-3'	5'- GCTCTAGATCAGCAGGTGT GTGTGGGGGGCCGGGACCT-3'
GNAI1/2 (<i>Gai1</i> , <i>Gai2</i>)	5'-ACGCGTCGACCCATGGGCTGC ACGCTGAGCGCCGAGGACAAG-3'	5'-CGAGGCTGATCAGCGGGTTTA AACGGGCCCTCTAGACTCGAG-3'
GNAS (<i>Gas</i>)	5'- ACGCGTCGACCCATGGGCTGC CTCGGGAACAGTAAGACCGAG-3'	5'-CGAGGCTGATCAGCGGGTTTA AACGGGCCCTCTAGACTCGAG-3'
GNAO (<i>Gαo</i> , <i>Gαo</i> - Q205L)	5'-ACGCGTCGACCCATGGGATGT ACTCTGAGCGCAGAGGAGAGA-3'	5'-GCTCTAGATCAGTACAAG CCGCAGCCCCGGAGGTTGTT-3'
GNB1 (<i>Gβ1</i>)	5'-ACGCGTCGACCCATGAGTGA GCTTGACCAGTTACGGCAGGAG-3'	5'-GCTCTAGATTAGTTCCAG ATCTTGAGGAAGCTATCCCA-3'
FGFR3	5'-ACGCGTCGACCCATGGGCGCC CCTGCCTGCGCCCTCGCGCTC-3'	5'-GCTCTAGACTACGTCCGC GAGCCCCACTGCTGGGTGG-3'
SELPLG	5'-ACGCGTCGACCCATGCCTCT GCAACTCCTCCTGTTGCTGATC-3'	5'-GCTCTAGACTAAGGGAGG AAGCTGTGCAGGGTGAGGTC-3'

2.14 LUCIFERASE ASSAY SYSTEM

The Dual-Glo[®] Luciferase Assay System (Promega, E2920) was utilized to quantify luciferase reporter gene expression as a measure of the strength of tested protein-protein interactions, as per manufacturer's instructions. Briefly, a volume of Dual-Glo[®] Reagent equal to the volume of culture medium in the well was added to each well, mixed, and allowed to sit for 10 minutes while cell lysis occurred. Firefly luciferase luminescence was then measured using a VICTOR3V Microplate Reader (PerkinElmer, 1420-251). To quench this reaction, a volume of Dual-Glo[®] Stop & Glo[®] Reagent equal to the original culture medium volume was then added to each well, mixed, and allowed to incubate for 10 minutes at room temperature. *Renilla* luminescence was then measured. Wells were measured in the same order on each plate when measuring Firefly and *Renilla* luminescence. Nontransfected cells were used to assess background luminescence (for both Firefly and *Renilla* luciferase) and this background was subtracted from all luminescence readings. Firefly luciferase luminescence was then normalized to *Renilla* luminescence to account for differences in transfection efficiency. Finally, a relative response ratio (RRR) is then calculated in order to evaluate the results in the context of the positive and negative controls, using the following equation:

$$\text{RRR} = \frac{(\text{experimental sample ratio}) - (\text{negative control ratio})}{(\text{positive control ratio}) - (\text{negative control ratio})}$$

2.15 STATISTICAL ANALYSES

Data are presented as means \pm SEM. Statistical analyses were performed using GraphPad Prism[®] 5.0 and p-values of <0.05 were considered statistically significant. mRNA levels in VSMC primary cultures from WKY and SHR rats were analyzed by a two-tailed t-test. Serum starvation mRNA and protein data, as well as mammalian two-hybrid data, were analyzed by one-way analysis of variance (ANOVA) with Tukey's Multiple Comparison test. Tissue mRNA levels, MTT assay data, and cell count data were analyzed by two-way ANOVA followed by Bonferroni posttests. MTT assay data were also subjected to nonlinear regression and analyzed by F test.

3 RESULTS

3.1 DIFFERENTIAL EXPRESSION OF GPSM3 IN WKY AND SHR RATS

RNA was extracted from WKY-derived and SHR-derived VSMCs, reverse transcribed, and subjected to qPCR. GPSM3 mRNA levels were assessed relative to β 2-microglobulin mRNA levels. GPSM3 transcript levels were significantly increased in SHR-derived VSMCs relative to WKY-derived VSMCs by approximately two-fold ($p < 0.05$) (Figure 3.1). GPSM3 transcript levels were also assessed in various tissues from WKY and SHR rats to ascertain whether or not this model of hypertension resulted in changes to GPSM3 levels as is seen in vascular smooth muscle cells. The investigated tissues included heart, aorta, liver, lung, spleen, and leukocytes. RNA was extracted from these tissues, reverse transcribed, and subjected to qPCR. GPSM3 mRNA levels were assessed relative to glyceraldehyde 3-phosphate dehydrogenase (GAPDH) mRNA levels. The GPSM3 expression profile obtained from these tissues is comparable to that seen in previous studies (Cao et al. 2004; Zhao et al. 2010). GPSM3 transcript levels in the heart and liver were low relative to the spleen, leukocytes, and lungs (Figure 3.2). Furthermore, GPSM3 transcript levels were shown to be relatively high in aortic tissue for the first time. GPSM3 levels were significantly increased in the spleen of SHR rats relative to WKY rat spleen, with a p value less than 0.01. No significant differences were observed in the other tissues.

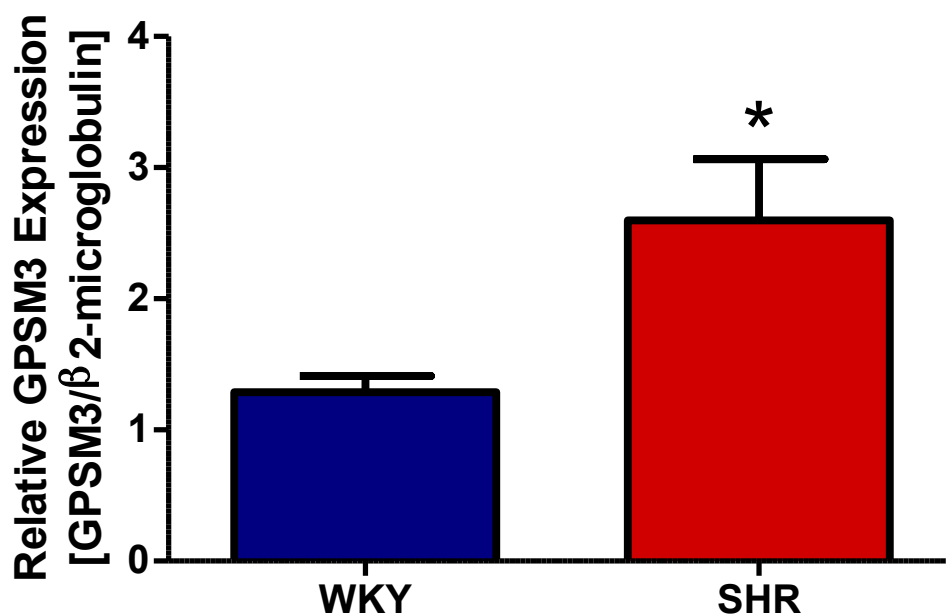


Figure 3.1. GPSM3 mRNA levels in WKY-derived and SHR-derived VSMCs. GPSM3 mRNA levels were assessed relative to β2-microglobulin mRNA levels. Data are presented as means ± SEM of seven independent experiments (N=7) performed in triplicate. Statistical analysis was done using an unpaired t-test. *P<0.05.

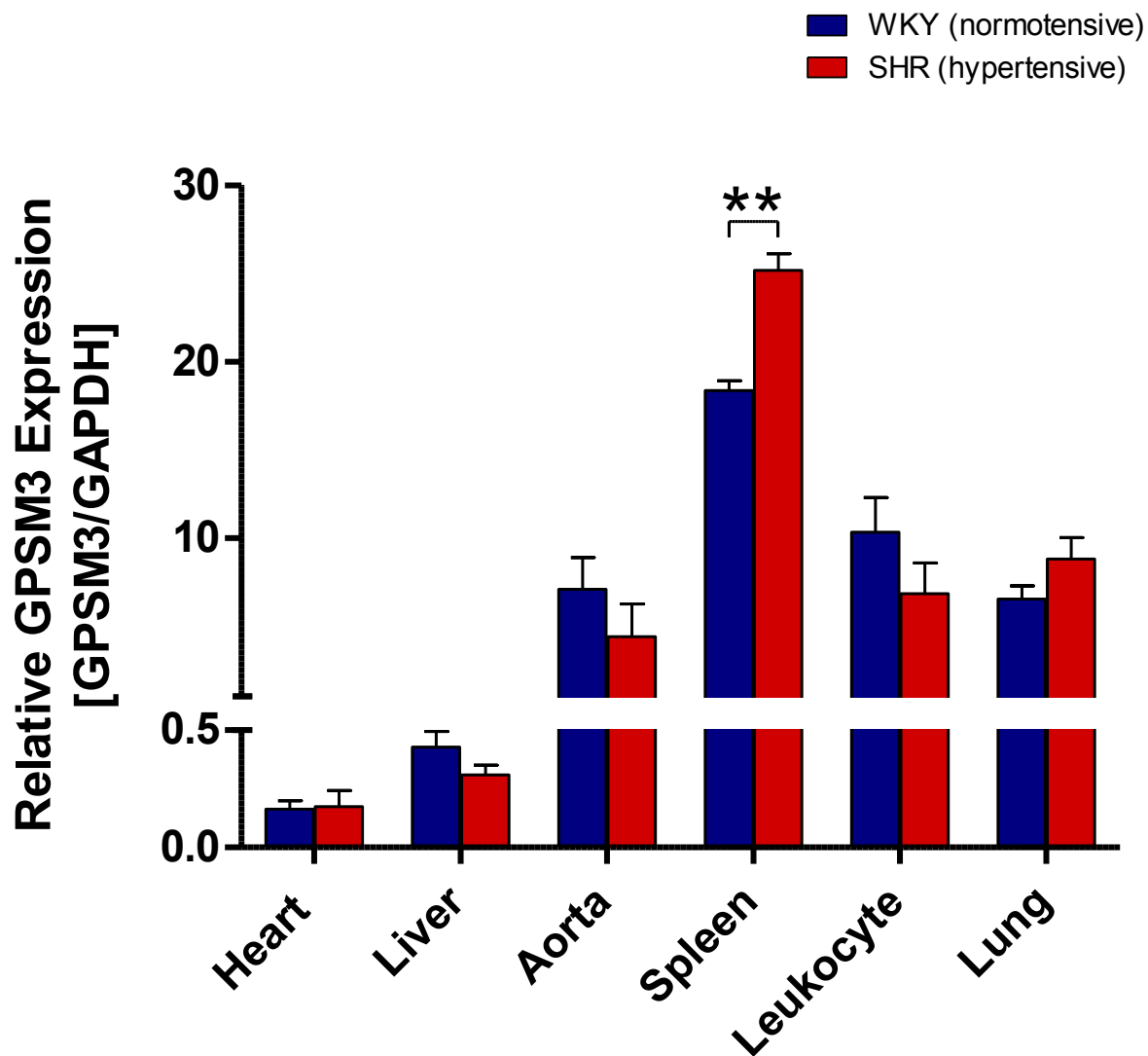


Figure 3.2. GPSM3 mRNA levels in different WKY and SHR rat tissue types. GPSM3 mRNA levels were assessed relative to GAPDH mRNA levels. Data are presented as means \pm SEM of three to four independent experiments ($N \geq 3$) performed in triplicate. Statistical analyses were done using two-way ANOVA followed by Bonferroni posttests. ****** $P < 0.01$.

3.2 GPSM3 EXPRESSION AND RATE OF CELL DIVISION

VSMCs were serum starved by using serum-free medium to induce reversible cell cycle arrest (Chen et al. 2012). This was followed by the reintroduction of serum-containing medium to induce synchronized progression through the G2 and M phases of the cell cycle, simulating an increased rate of proliferation (Chen et al. 2012). Actively proliferating cells not subjected to this protocol were used as a control. Overall RNA and protein synthesis is relatively unaffected by the protocol (Zetterberg & Sköld 1969). Therefore, changes in gene expression can be indicative of that gene playing a role in the rate of cell division.

Protein and mRNA levels were measured in both WKY- and SHR-derived VSMCs. GPSM3 mRNA levels in WKY-derived VSMCs showed no changes in response to serum starvation and serum replacement (Figure 3.3). GPSM3 mRNA levels in SHR-derived VSMCs, however, showed a significant decrease in response to serum starvation (p value less than 0.05), and levels returned to control levels following serum replacement (Figure 3.4). GPSM3 mRNA levels were assessed relative to β 2-microglobulin mRNA levels. GPSM3 protein could not be detected by immunoblot in cell lysates from WKY-derived VSMCs (Figure 3.5). The same trend observed with mRNA in SHR-derived VSMCs was found with GPSM3 protein levels (Figure 3.6). GPSM3 protein levels decreased in response to serum starvation, and returned to levels comparable to control levels following serum replacement.

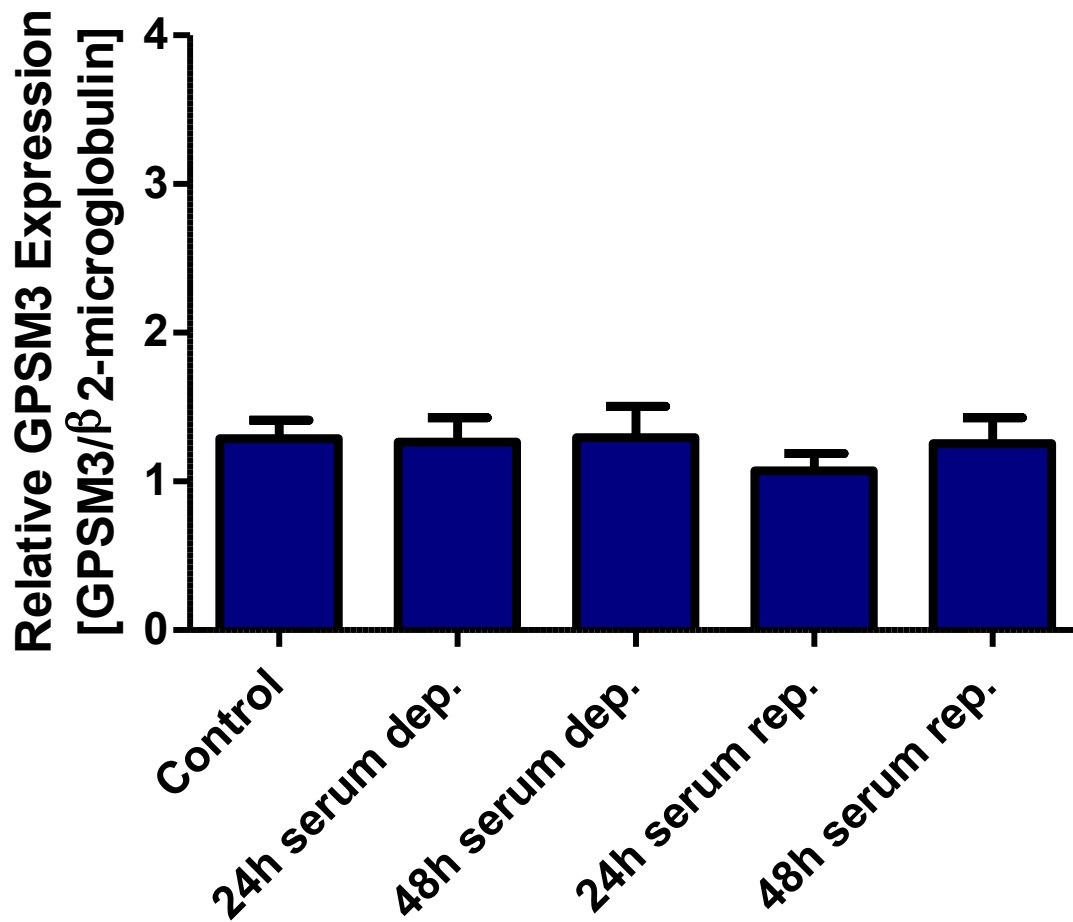


Figure 3.3. Effect of serum deprivation and serum replacement on GPSM3 mRNA levels in WKY-derived VSMCs. Cells were treated for 48 hours with serum-free medium (serum dep.), followed by 48 hours of medium with 10% FBS (serum rep.). Actively proliferating cells were used as a control. GPSM3 mRNA levels were assessed relative to β2-microglobulin mRNA levels. Data are presented as mean ± SEM of three to five independent experiments ($N \geq 3$) performed in triplicate. Statistical analyses were done using one-way ANOVA followed by Tukey's Multiple Comparison test.

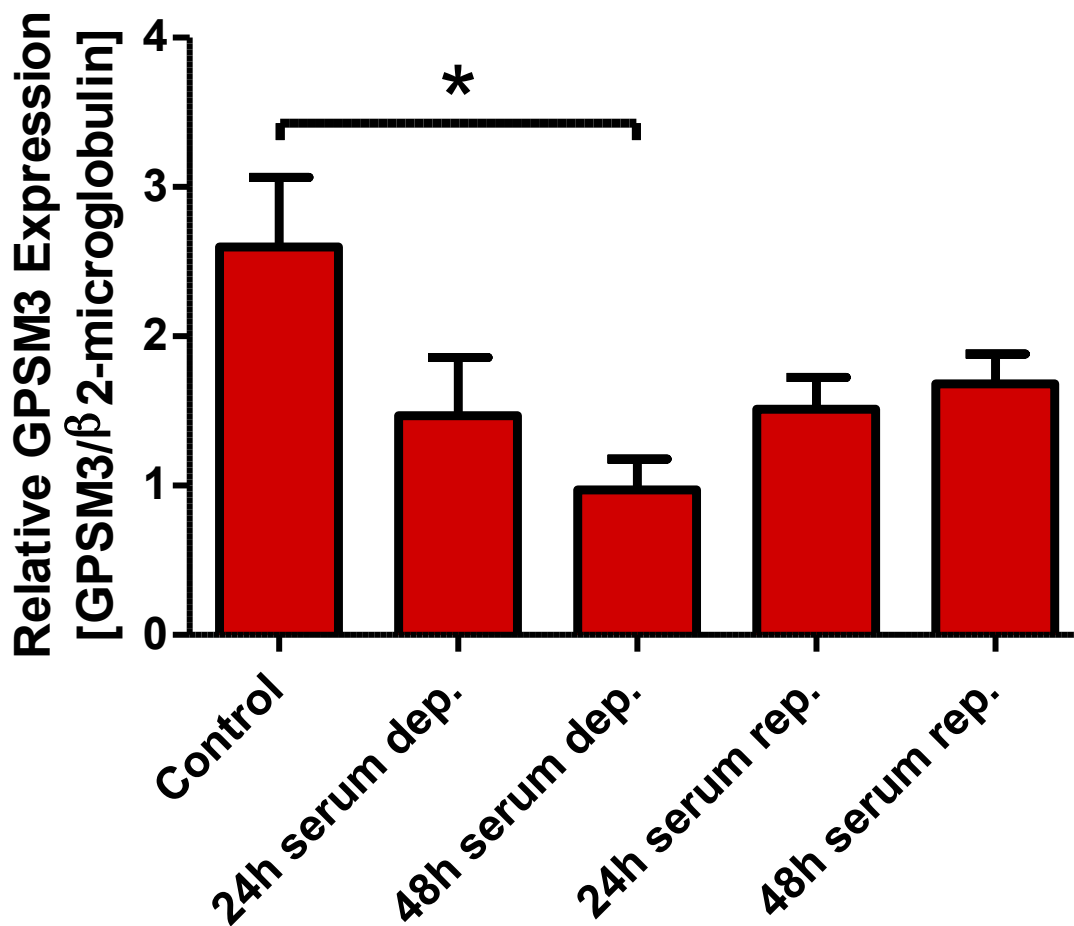


Figure 3.4. Effect of serum deprivation and serum replacement on GPSM3 mRNA levels in SHR-derived VSMCs. Cells were treated for 48 hours with serum-free medium (serum dep.), followed by 48 hours of medium with 10% FBS (serum rep.). Actively proliferating cells were used as a control. GPSM3 mRNA levels were assessed relative to β 2-microglobulin mRNA levels. Data are presented as mean \pm SEM of five to eight independent experiments ($N \geq 5$) performed in triplicate. Statistical analyses were done using one-way ANOVA followed by Tukey's Multiple Comparison test. * $P < 0.05$.

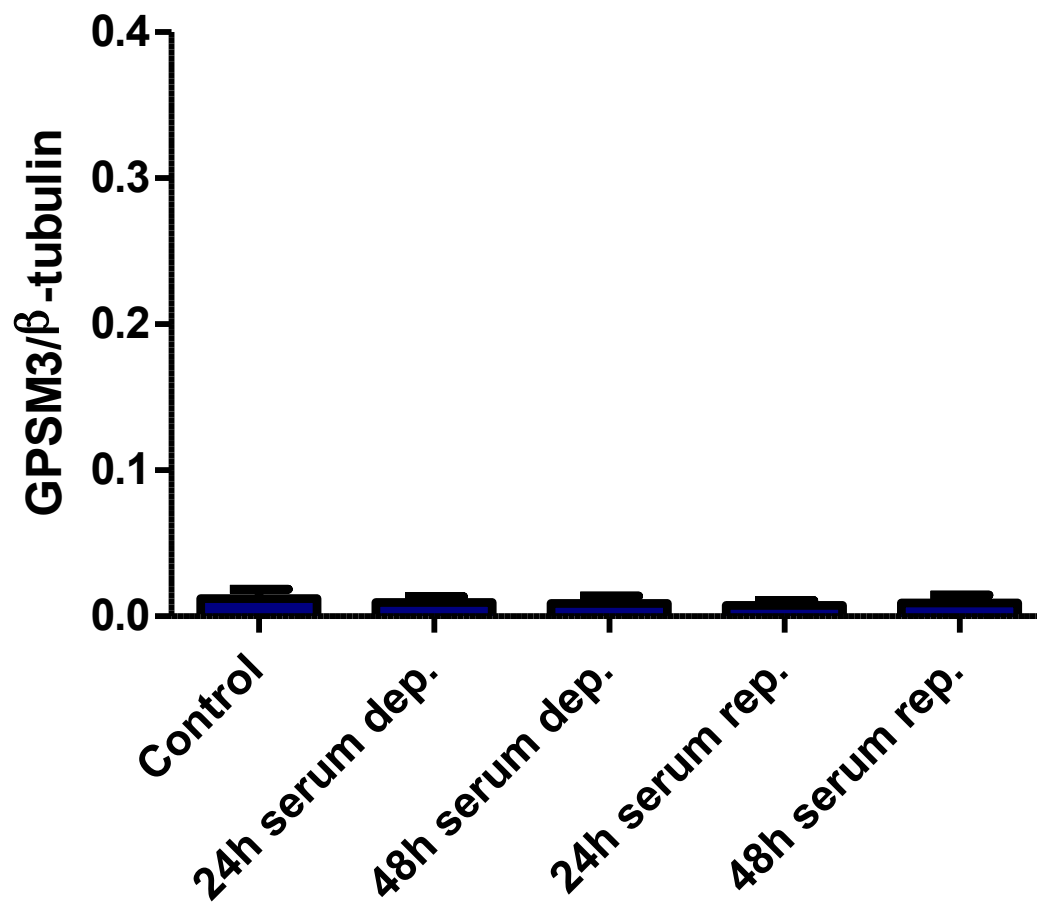
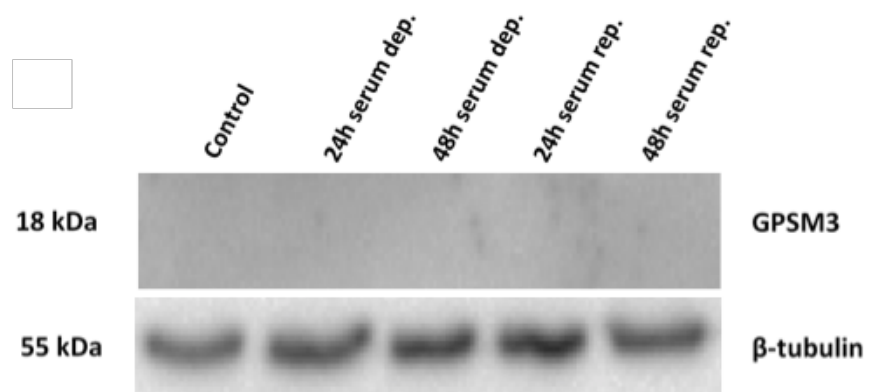
A**B**

Figure 3.5.

Figure 3.5 (previous page). Effect of serum deprivation and serum replacement on GPSM3 protein levels in WKY-derived VSMCs. (A) Cells were treated for 48 hours with serum-free medium (serum dep.), followed by 48 hours of medium with 10% FBS (serum rep.). Actively proliferating cells were used as a control. GPSM3 protein levels were assessed relative to β -tubulin protein levels. Data are presented as mean \pm SEM of three independent experiments (N=3). Statistical analyses were done using one-way ANOVA followed by Tukey's Multiple Comparison test. (B) Representative immunoblot of serum deprivation and replacement experiment. The upper immunoblot was probed for GPSM3 protein. The lower immunoblot was probed for β -tubulin protein.

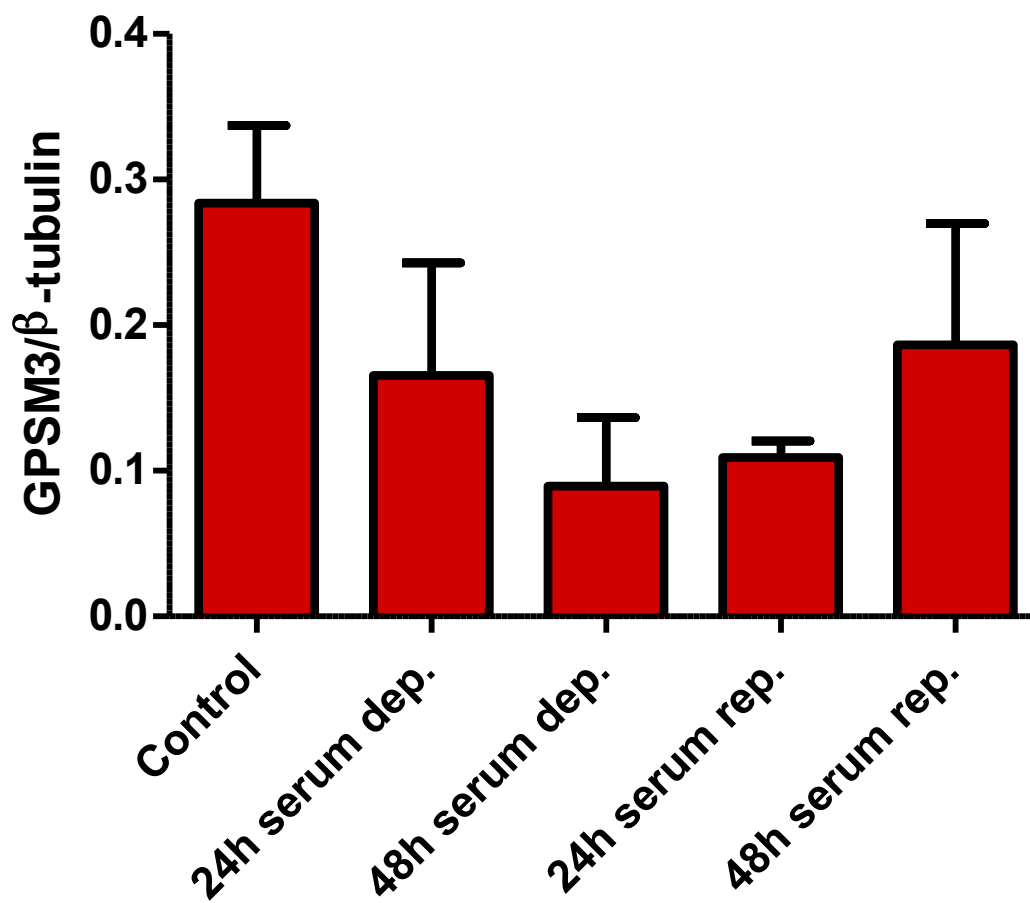
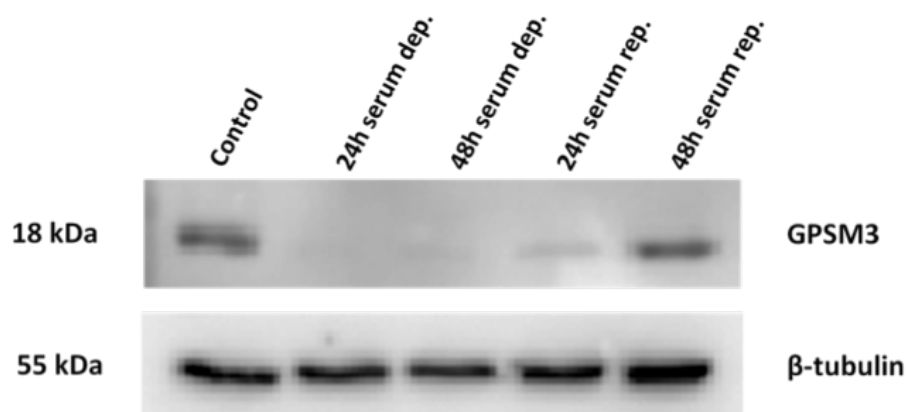
A**B**

Figure 3.6.

Figure 3.6 (previous page). Effect of serum deprivation and serum replacement on GPSM3 protein levels in SHR-derived VSMCs. (A) Cells were treated for 48 hours with serum-free medium (serum dep.), followed by 48 hours of medium with 10% FBS (serum rep.). Actively proliferating cells were used as a control. GPSM3 protein levels were assessed relative to β -tubulin protein levels. Data are presented as mean \pm SEM of five independent experiments (N=5). Statistical analyses were done using one-way ANOVA followed by Tukey's Multiple Comparison test. (B) Representative immunoblot of serum deprivation and replacement experiment. The upper immunoblot was probed for GPSM3 protein. The lower immunoblot was probed for β -tubulin protein.

HEK-293 cells were transfected with 400 ng of either EYFP or EYFP-GPSM3 DNA plasmid and plated at approximately 8% confluency. Transfection of cells with EYFP-GPSM3 resulted in greater absorbance readings on day 1 and day 2 relative to the cells transfected with EYFP with p values less than 0.01 and 0.05, respectively (Figure 3.7). Cell populations transfected with EYFP-GPSM3 appeared to reach confluence one day earlier, or 33% faster, compared to the control cell populations. To further analyze the data, nonlinear regression was performed using an exponential plateau equation to compare the growth rates of the two groups of cells. The growth rate plus or minus standard error of cells transfected with EYFP-GPSM3 plasmid was $0.7228 \pm 0.1076 \text{ days}^{-1}$ with a doubling time of 0.96 ± 0.14 days. The growth rate of cells transfected with EYFP plasmid was $0.3935 \pm 0.0962 \text{ days}^{-1}$ with a doubling time of 1.76 ± 0.43 days. An F test was conducted, where both data sets were fit simultaneously with common minimum and maximum values and independent values of the growth rate k (either independent between data sets or forced to be common between the two data sets). Holding the parameter common for the two data sets caused a significant decrease in the goodness of the fit (as indicated by an increase in the sum of the squares), thus indicating that they are significantly different with a p value less than 0.05. Therefore, the growth rate of the cells transfected with EYFP-GPSM3 was found to be significantly higher than the control group.

The results of counting cells expressing EYFP-GPSM3 or EYFP were similar to those obtained by the MTT assay. Cells transfected with EYFP-GPSM3 had a significantly higher cell population size on day 2 compared to those transfected with EYFP (Figure 3.8). Thus, higher rates of cell division are correlated with higher levels of GPSM3, and increasing the expression of GPSM3 appears to be sufficient to increase the rate of proliferation of cells.

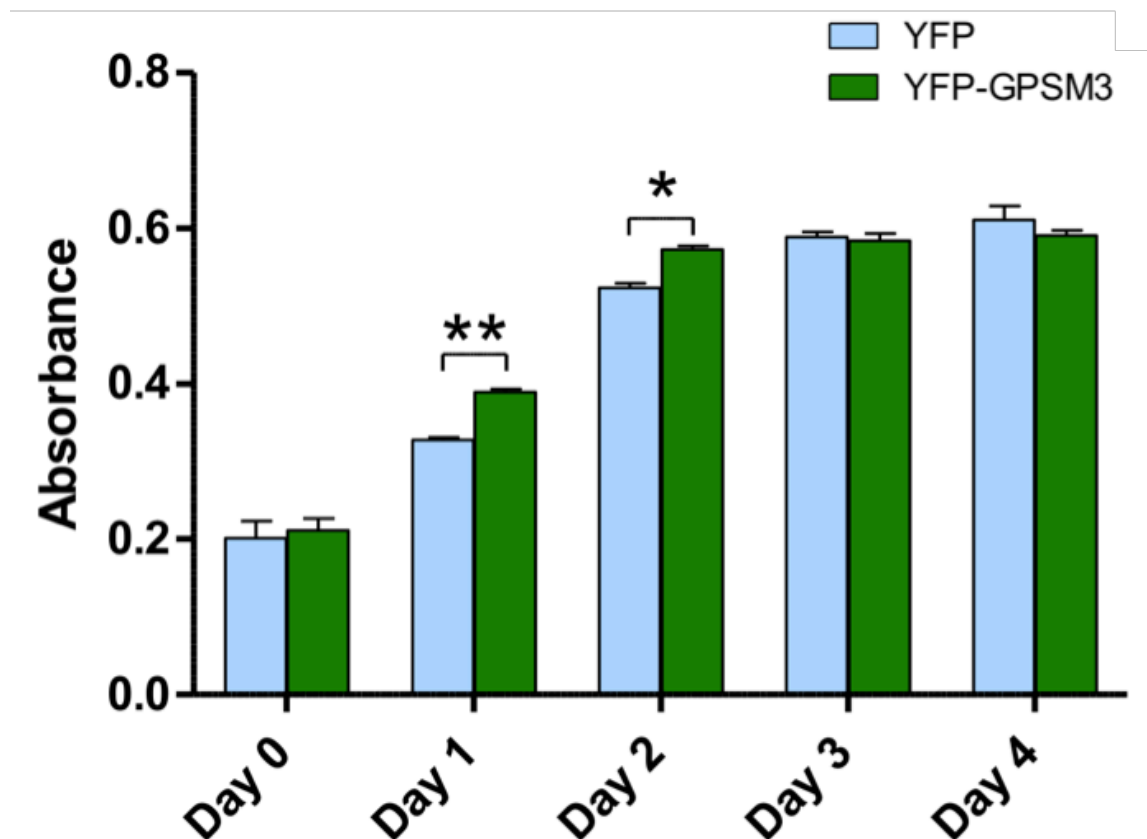


Figure 3.7. Effect of EYFP-tagged GPSM3 transfection on cell proliferation in HEK-293 cells as measured by MTT assay. HEK-293 cells were transfected with either EYFP-GPSM3- or EYFP-encoding DNA plasmid and seeded in a 24-well plate. Cells were treated with MTT reagent for 2 hours and then formazan crystals were recovered and solubilized in DMSO. Absorbance was measured at 595 nm. Data are presented as mean \pm SEM of five independent experiments (N=5) performed in triplicate. Statistical analyses were done using two-way ANOVA followed by Bonferroni posttests. * $P < 0.05$. ** $P < 0.01$.

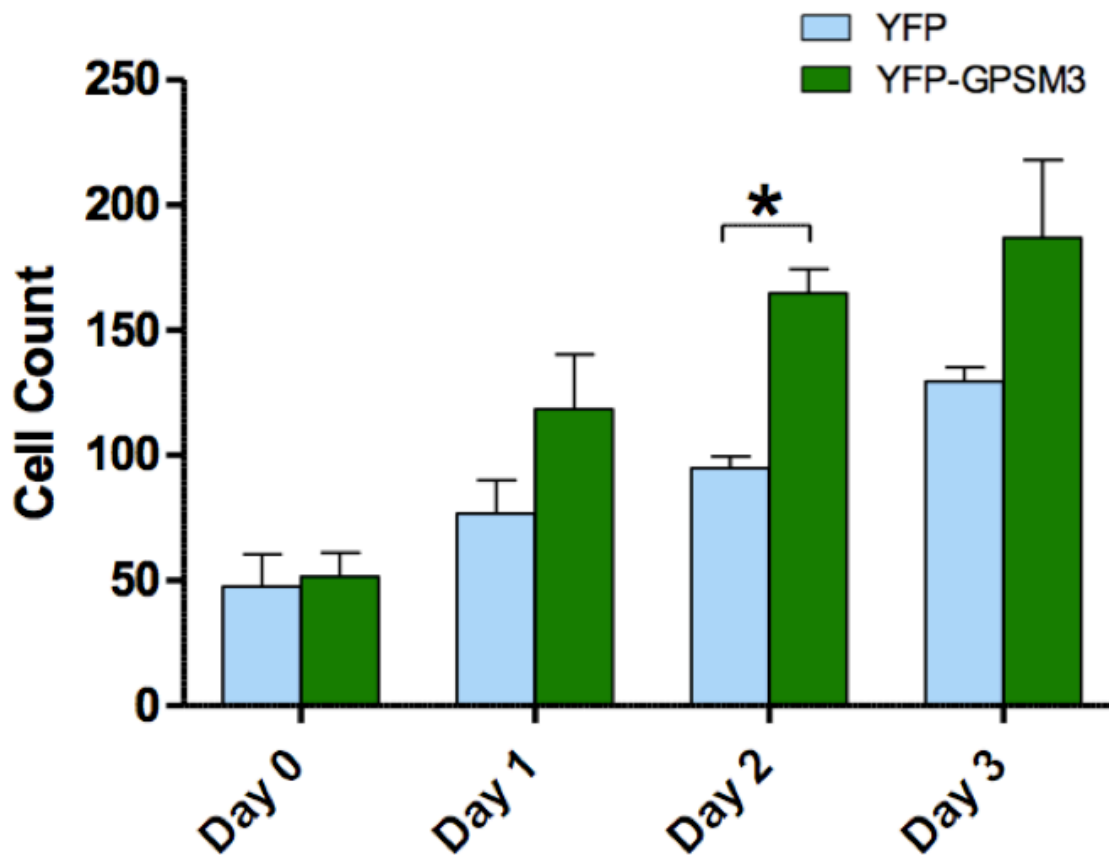


Figure 3.8. Effect of EYFP-tagged GPSM3 transfection on cell proliferation in HEK-293 cells as measured by cell counting. HEK-293 cells were transfected with either EYFP-GPSM3- or EYFP-containing plasmid and seeded in a 24-well plate. Cell counts were performed using ImageJ software. Data are presented as mean \pm SEM of three independent experiments (N=3) performed in triplicate. Statistical analyses were done using two-way ANOVA followed by Bonferroni posttests. *P<0.05.

3.3 GPSM3 LOCALIZATION DURING MITOSIS IN VASCULAR SMOOTH MUSCLE CELLS

N values for images of each cell type during each stage of mitosis can be found in Table 3.1. In interphase, GPSM3 localized to the nucleus with limited expression in the cytosol in both WKY and SHR vascular smooth muscle cells (Figure 3.9). Little to no co-localization between GPSM3 and β -tubulin was observed during interphase. Cells in metaphase showed clear co-localization between GPSM3 and β -tubulin, presumably along the mitotic spindle fibers that attach to chromatin lined up at the metaphase plate (Figure 3.10A). The same co-localization of GPSM3 and β -tubulin was seen during anaphase as the chromatin were pulled to opposite ends of the dividing cells (Figure 3.11A). Finally, co-localization was observed between GPSM3 and β -tubulin during telophase at the midbody (Figure 3.12A).

As a control, primary antibodies were incubated overnight at 4 °C with 10 μ g/ml anti-GPSM3 primary antibody blocking peptide before use in order to confirm that the anti-GPSM3 primary antibody was in fact binding specifically to GPSM3 protein. After incubation, immunofluorescent labeling was carried out as described previously. Co-localization between GPSM3 and β -tubulin was no longer seen during metaphase (Figure 3.10B), anaphase (Figure 3.11B), or telophase (Figure 3.12B). Any remaining fluorescence seen with the anti-GPSM3 primary antibody and the AlexaFluor 468 goat anti-rabbit secondary antibody can be attributed to non-specific binding by the anti-GPSM3 primary antibody. To further confirm the validity of this antibody for immunofluorescent labeling, HEK-293 cells were subjected to a protocol identical to that for WKY VSMCs. No co-localization was observed between GPSM3 and β -

Table 3.1. N values of immunofluorescently labeled images of vascular smooth muscle cells and human embryonic kidney 293 cells in different stages of mitosis.

Stage of Mitosis	VSMC		VSMC (with blocking peptide)		HEK-293
	WKY	SHR	WKY	SHR	
Interphase	8	8	0	0	0
Metaphase	13	3	3	3	5
Anaphase	4	3	3	3	3
Telophase	11	3	0	3	0

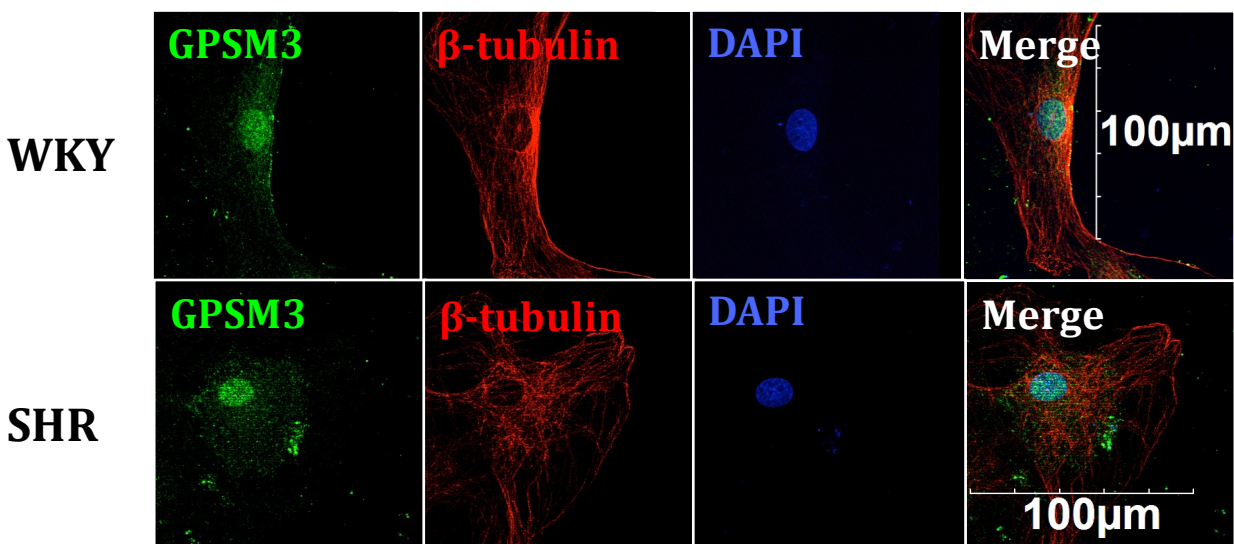
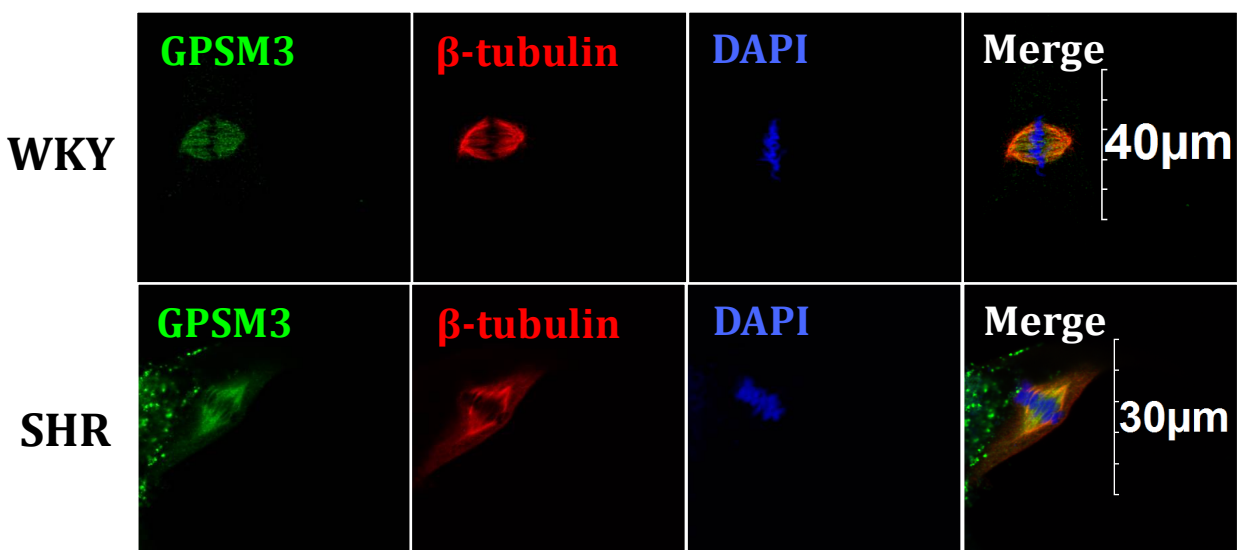


Figure 3.9. Localization of GPSM3 and β -tubulin during interphase in WKY and SHR vascular smooth muscle cells. Primary vascular smooth muscle cells were serum starved for 24 hours, and following serum replacement (20 hours for WKY cells, 12 hours for SHR cells) cells were fixed and subjected to immunofluorescent labeling. Cells were probed with anti-GPSM3 primary antibody (1:500) and anti- β -tubulin primary antibody (1:500), followed by AlexaFluor 488 goat anti-rabbit secondary antibody (1:500) and AlexaFluor 568 goat anti-mouse secondary antibody (1:500). Nuclei were stained using DAPI. Panels labeled in top left corners. Cell type indicated by label to left of panels. Cells imaged are representative of the majority of cells imaged.

A



B

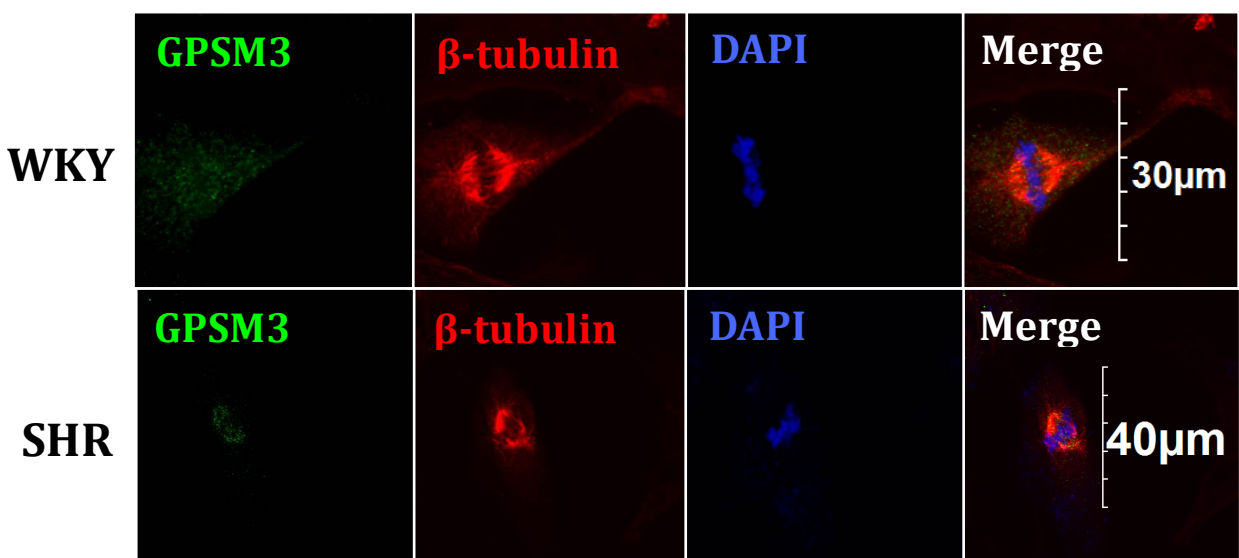
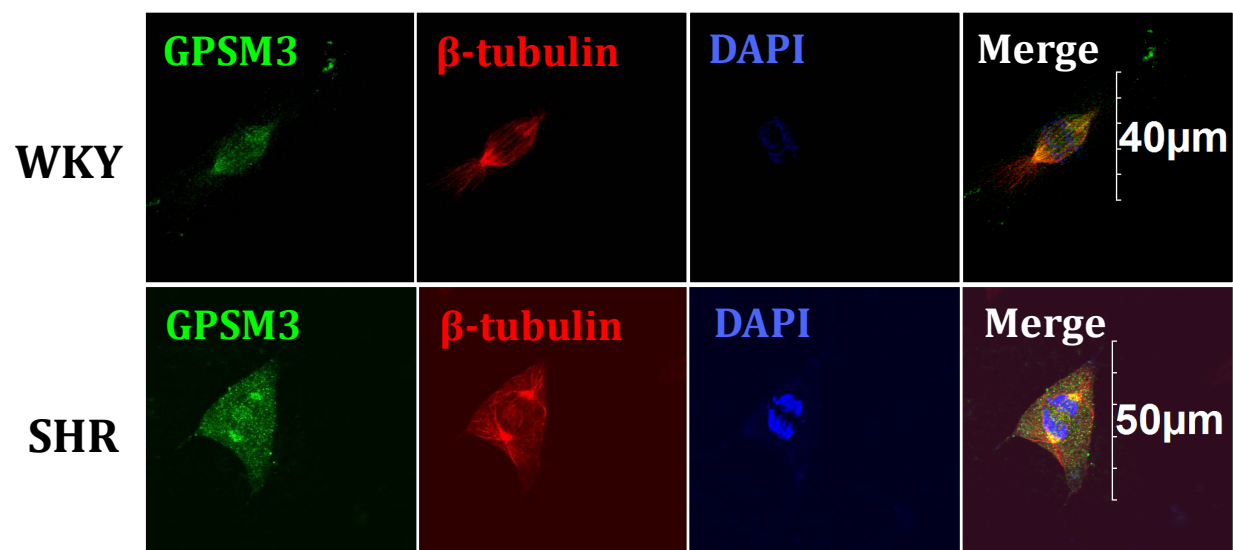


Figure 3.10.

Figure 3.10 (previous page). Co-localization of GPSM3 and β -tubulin during metaphase in WKY and SHR vascular smooth muscle cells. (A) Primary vascular smooth muscle cells were serum starved for 24 hours, and following serum replacement (20 hours for WKY cells, 12 hours for SHR cells) cells were fixed and subjected to immunofluorescent labeling. Cells were probed with anti-GPSM3 primary antibody (1:500) and anti- β -tubulin primary antibody (1:500), followed by AlexaFluor 488 goat anti-rabbit secondary antibody (1:500) and AlexaFluor 568 goat anti-mouse secondary antibody (1:500). Nuclei were stained using DAPI. Panels labeled in top left corners. Cell type indicated by label to left of panels. (B) Anti-GPSM3 primary antibody (1:500) and anti- β -tubulin primary antibody (1:500) were incubated overnight at 4 °C with 10 μ g/ml anti-GPSM3 primary antibody blocking peptide before use (as in panel A). Cells imaged are representative of the majority of cells imaged.

A



B

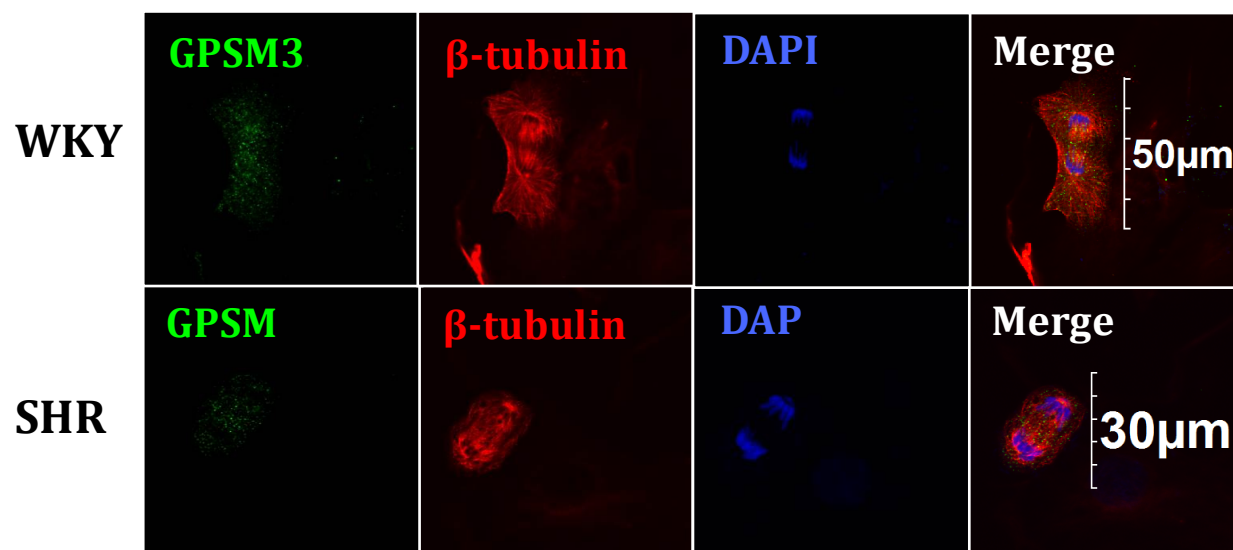
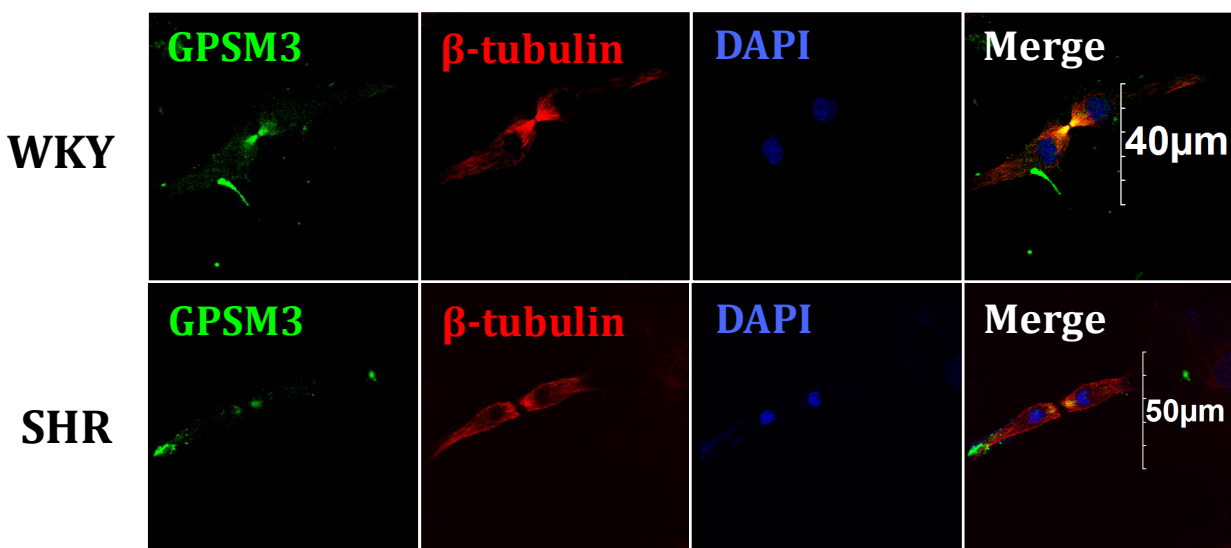


Figure 3.11.

Figure 3.11 (previous page). Co-localization of GPSM3 and β -tubulin during anaphase in WKY and SHR vascular smooth muscle cells. (A) Primary vascular smooth muscle cells were serum starved for 24 hours, and following serum replacement (20 hours for WKY cells, 12 hours for SHR cells) cells were fixed and subjected to immunofluorescent labeling. Cells were probed with anti-GPSM3 primary antibody (1:500) and anti- β -tubulin primary antibody (1:500), followed by AlexaFluor 488 goat anti-rabbit secondary antibody (1:500) and AlexaFluor 568 goat anti-mouse secondary antibody (1:500). Nuclei were stained using DAPI. Panels labeled in top left corners. Cell type indicated by label to left of panels. (B) Anti-GPSM3 primary antibody (1:500) and anti- β -tubulin primary antibody (1:500) were incubated overnight at 4 °C with 10 μ g/ml anti-GPSM3 primary antibody blocking peptide before use (as in panel A). Cells imaged are representative of the majority of cells imaged.

A



B

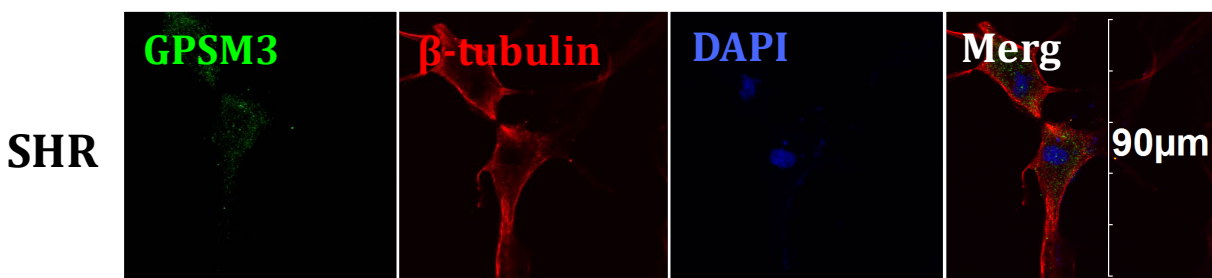


Figure 3.12.

Figure 3.12 (previous page). Co-localization of GPSM3 and β -tubulin during telophase in WKY and SHR vascular smooth muscle cells. (A) Primary vascular smooth muscle cells were serum starved for 24 hours, and following serum replacement (20 hours for WKY cells, 12 hours for SHR cells) cells were fixed and subjected to immunofluorescent labeling. Cells were probed with anti-GPSM3 primary antibody (1:500) and anti- β -tubulin primary antibody (1:500), followed by AlexaFluor 488 goat anti-rabbit secondary antibody (1:500) and AlexaFluor 568 goat anti-mouse secondary antibody (1:500). Nuclei were stained using DAPI. Panels labeled in top left corners. Cell type indicated by label to left of panels. (B) Anti-GPSM3 primary antibody (1:500) and anti- β -tubulin primary antibody (1:500) were incubated overnight at 4 °C with 10 μ g/ml anti-GPSM3 primary antibody blocking peptide before use (as in panel A). Cells imaged are representative of the majority of cells imaged.

tubulin antibody signals in HEK-293 cells (Figure 3.13). Similar to the observation of non-specific binding in vascular smooth muscle cells when anti-GPSM3 primary antibody blocking peptide was used, diffuse and non-specific staining was seen in HEK-293 cells as well.

Additional controls were also used to confirm the validity of these antibodies for immunofluorescent labeling. GPSM3 and β -tubulin were labeled independently from one another to ensure neither antibody was influencing the localization of the other (Figures 3.14 and 3.15). Immunofluorescent labeling with only the secondary antibodies was performed to demonstrate that these antibodies were not responsible for the observed localization of patterns (Figure 3.16).

3.4 MAMMALIAN TWO-HYBRID ASSAY FOR GPSM3 PROTEIN INTERACTORS

The heterotrimeric G protein subunits tested were as follows: *Gai1*, *Gai2*, *Gao*, *GaoQ205L*, *Gas*, and *G β 1* (Figure 3.17). As expected, the assay showed an interaction between GPSM3 and both *Gai1* and *Gai2*. Both interactions gave strong positive signals that were statistically significant relative to the negative control (p value less than 0.001). *Gas* and *Gao* did not produce a detectable signal. *Gao-Q205L*, a form of the *Gao* subunit containing a mutation that renders it constitutively active, failed to produce a signal significantly greater than that of the negative control. No interaction was detected between GPSM3 and *G β 1* either. As expected, all negative vector controls failed to produce detectable signals (Figure 3.18).

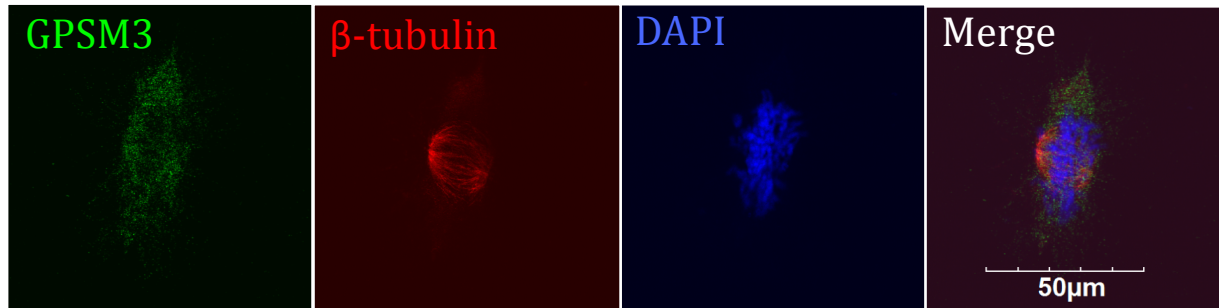


Figure 3.13. Localization of GPSM3 and β -tubulin during metaphase in HEK-293 cells.

HEK-293 cells were serum starved for 24 hours, and 20 hours after serum replacement cells were fixed and subjected to immunofluorescent labeling. Cells were probed with anti-GPSM3 primary antibody (1:500) and anti- β -tubulin primary antibody (1:500), followed by AlexaFluor 488 goat anti-rabbit secondary antibody (1:500) and AlexaFluor 568 goat anti-mouse secondary antibody (1:500). Nuclei were stained using DAPI. Panels labeled in top left corners. Cell type indicated by label to left of panels. Cells imaged are representative of the majority of cells imaged.

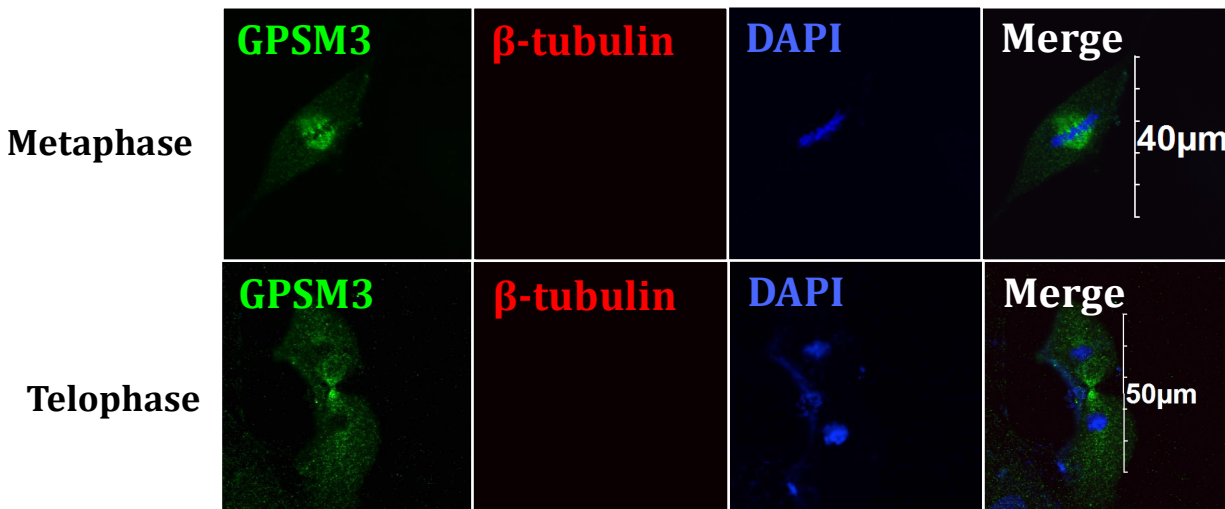


Figure 3.14. Localization of GPSM3 during metaphase and telophase in WKY vascular smooth muscle cells. Primary vascular smooth muscle cells were serum starved for 24 hours, and 20 hours following serum replacement cells were fixed and subjected to immunofluorescent labeling. Cells were probed with anti-GPSM3 primary antibody (1:500), followed by AlexaFluor 488 goat anti-rabbit secondary antibody (1:500). Nuclei were stained using DAPI. Panels labeled in top left corners. Cell cycle stage indicated by label to left of panels. Cells imaged are representative of the majority of cells imaged. N=3.

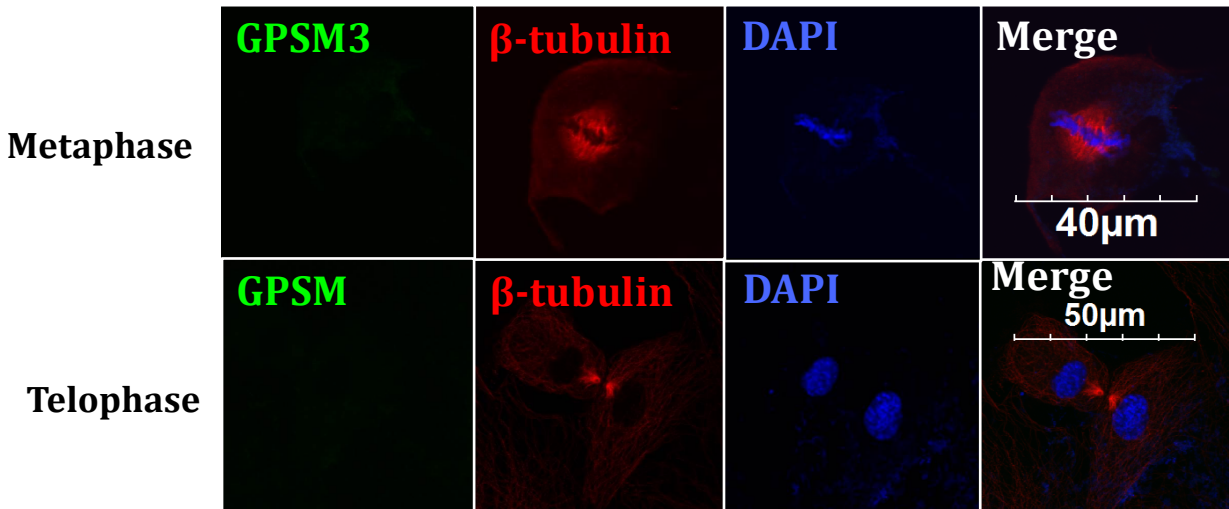


Figure 3.15. Localization of β -tubulin during metaphase and telophase in WKY vascular smooth muscle cells. Primary vascular smooth muscle cells were serum starved for 24 hours, and 20 hours following serum replacement cells were fixed and subjected to immunofluorescent labeling. Cells were probed with anti- β -tubulin primary antibody (1:500), followed by AlexaFluor 568 goat anti-mouse secondary antibody (1:500). Nuclei were stained using DAPI. Panels labeled in top left corners. Cell cycle stage indicated by label to left of panels. Cells imaged are representative of the majority of cells imaged. N=3.

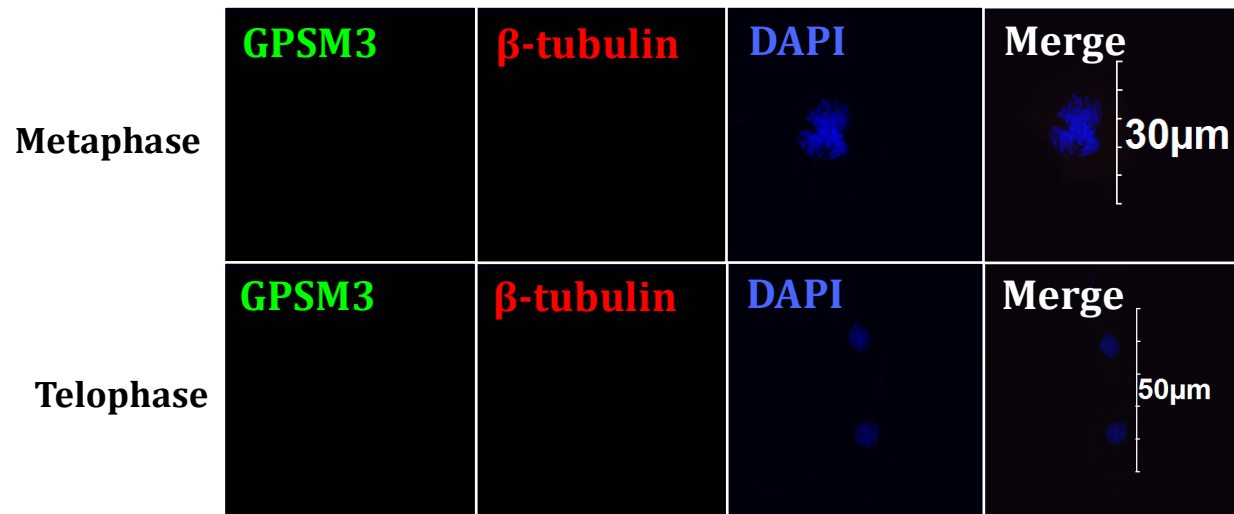


Figure 3.16. Localization of secondary antibodies during metaphase and telophase in WKY vascular smooth muscle cells. Primary vascular smooth muscle cells were serum starved for 24 hours, and 20 hours following serum replacement cells were fixed and subjected to immunofluorescent labeling. Cells were probed with AlexaFluor 488 goat anti-rabbit secondary antibody (1:500) and AlexaFluor 568 goat anti-mouse secondary antibody (1:500). Nuclei were stained using DAPI. Panels labeled in top left corners. Cell cycle stage indicated by label to left of panels. Cells imaged are representative of the majority of cells imaged. N=3.

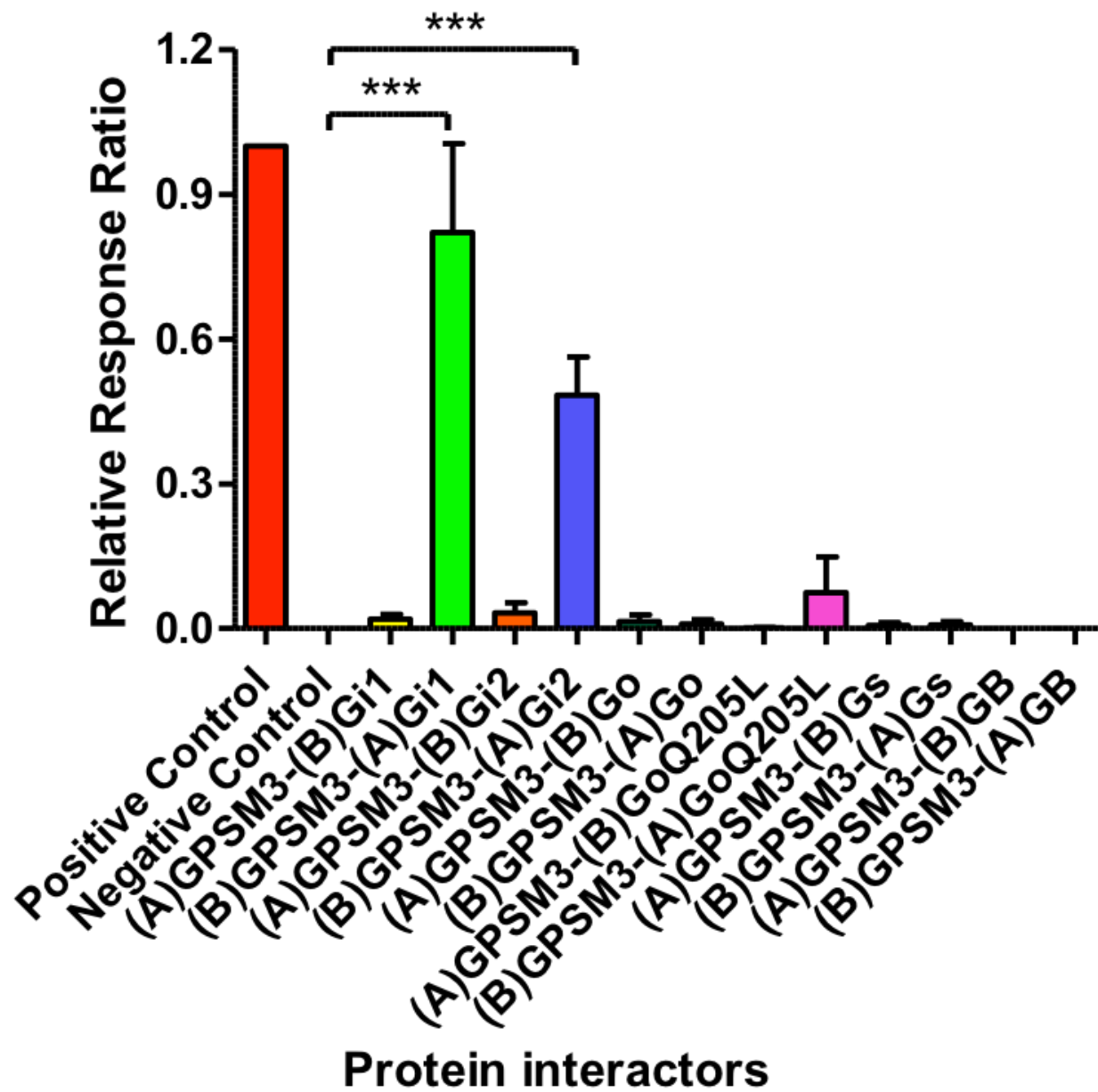


Figure 3.17.

Figure 3.17 (previous page). Mammalian Two-Hybrid luciferase assay results between GPSM3 and heterotrimeric G proteins. DNA plasmids were made by subcloning genes of interest into the pACT and pBIND vectors. Both vectors, as well as the pG5luc vector, were then transiently transfected into HEK-293 cells and luminescence was measured to detect protein-protein interactions. (A) indicates that the protein's corresponding gene has been subcloned into the pACT vector. (B) indicates that the protein's corresponding gene has been subcloned into the pBIND vector. All data are presented as luciferase/Renilla output, which has been normalized to the positive and negative control values to produce a relative response ratio (RRR). Data are presented as mean \pm SEM of three to eight independent experiments ($N \geq 3$) performed in triplicate. Statistical analyses were done using one-way ANOVA followed by Tukey's Multiple Comparison test. *** $P < 0.001$.

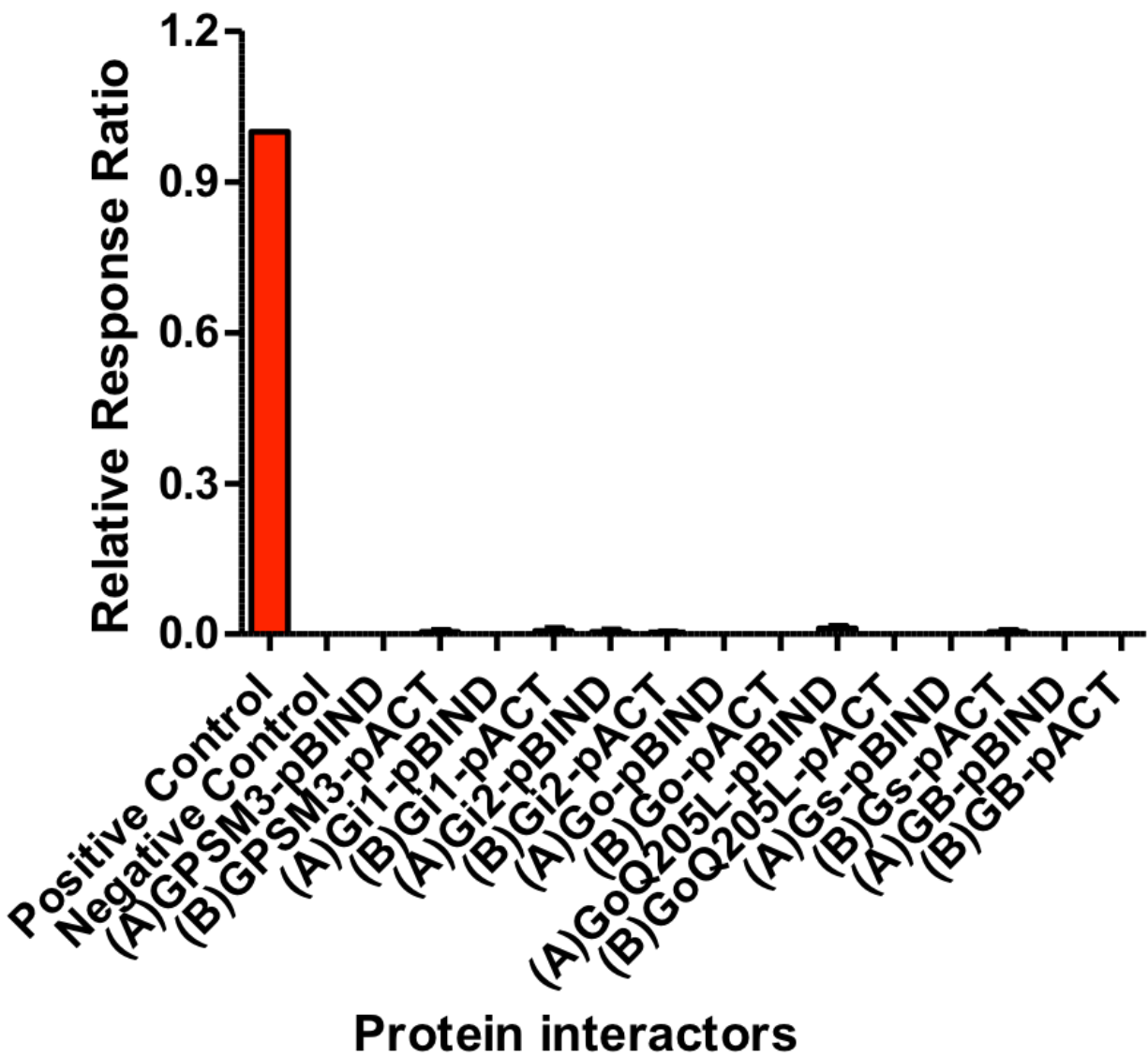


Figure 3.18.

Figure 3.18 (previous page). Mammalian Two-Hybrid luciferase assay results of heterotrimeric G protein vector controls. DNA plasmids were made by subcloning genes of interest into the pACT and pBIND vectors. Both vectors, as well as the pG5luc vector, were then transiently transfected into HEK-293 cells and luminescence was measured to detect protein-protein interactions. (A) indicates that a gene has been subcloned into the pACT vector. (B) indicates that a gene has been subcloned into the pBIND vector. All data are presented as luciferase/Renilla output, which has been normalized to the positive and negative control values to produce a relative response ratio (RRR). Data are presented as mean \pm SEM of three independent experiments (N=3) performed in triplicate. Statistical analyses were done using one-way ANOVA followed by Tukey's Multiple Comparison test.

Proteins associated with cell division are the second class of proteins tested for interaction with GPSM3 (Figure 3.19). NuMA and ninein both failed to produce a statistically significant signal. GPSM3 also failed to interact with itself. As expected, all negative vector controls failed to produce detectable signals (Figure 3.20).

The third and final class of proteins consists of those predicted to interact with GPSM3 by online databases (Figure 3.21). SELPLG failed to produce a detectable signal. FGFR3 and supervillin both produced positive signals above that of the negative control, however neither of these signals were statistically significant as assessed using ANOVA followed by Tukey's Multiple Comparison test. As expected, all negative vector controls failed to produce detectable signals (Figure 3.22).

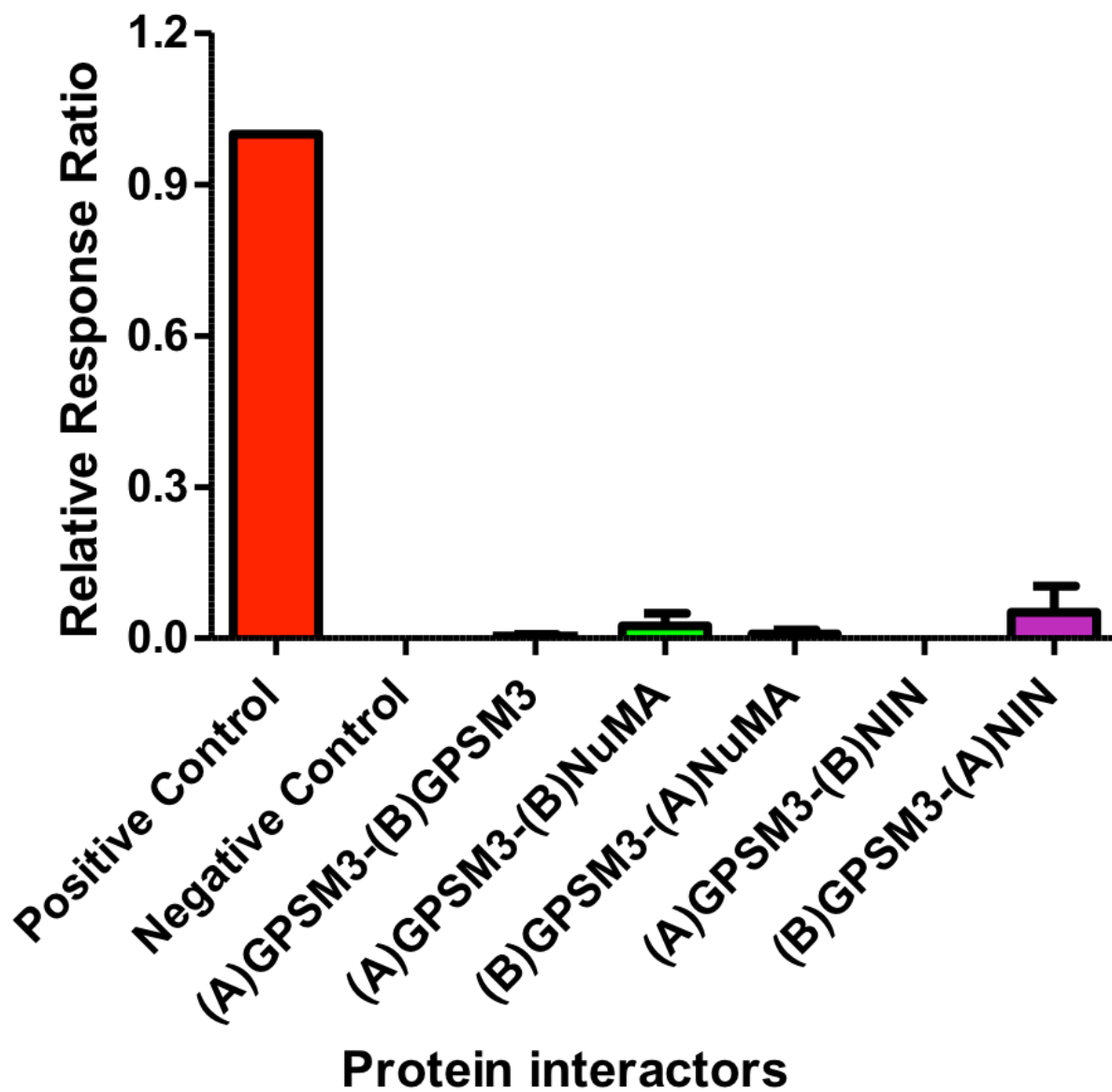


Figure 3.19.

Figure 3.19 (previous page). Mammalian Two-Hybrid luciferase assay results between GPSM3 and mitosis-related proteins of interest. DNA plasmids were made by subcloning genes of interest into the pACT and pBIND vectors. Both vectors, as well as the pG5luc vector, were then transiently transfected into HEK-293 cells and luminescence was measured to detect protein-protein interactions. (A) indicates that a gene has been subcloned into the pACT vector. (B) indicates that a gene has been subcloned into the pBIND vector. All data are presented as luciferase/Renilla output, which has been normalized to the positive and negative control values to produce a relative response ratio (RRR). Data are presented as mean \pm SEM of three independent experiments (N=3) performed in triplicate. Statistical analyses were done using one-way ANOVA followed by Tukey's Multiple Comparison test.

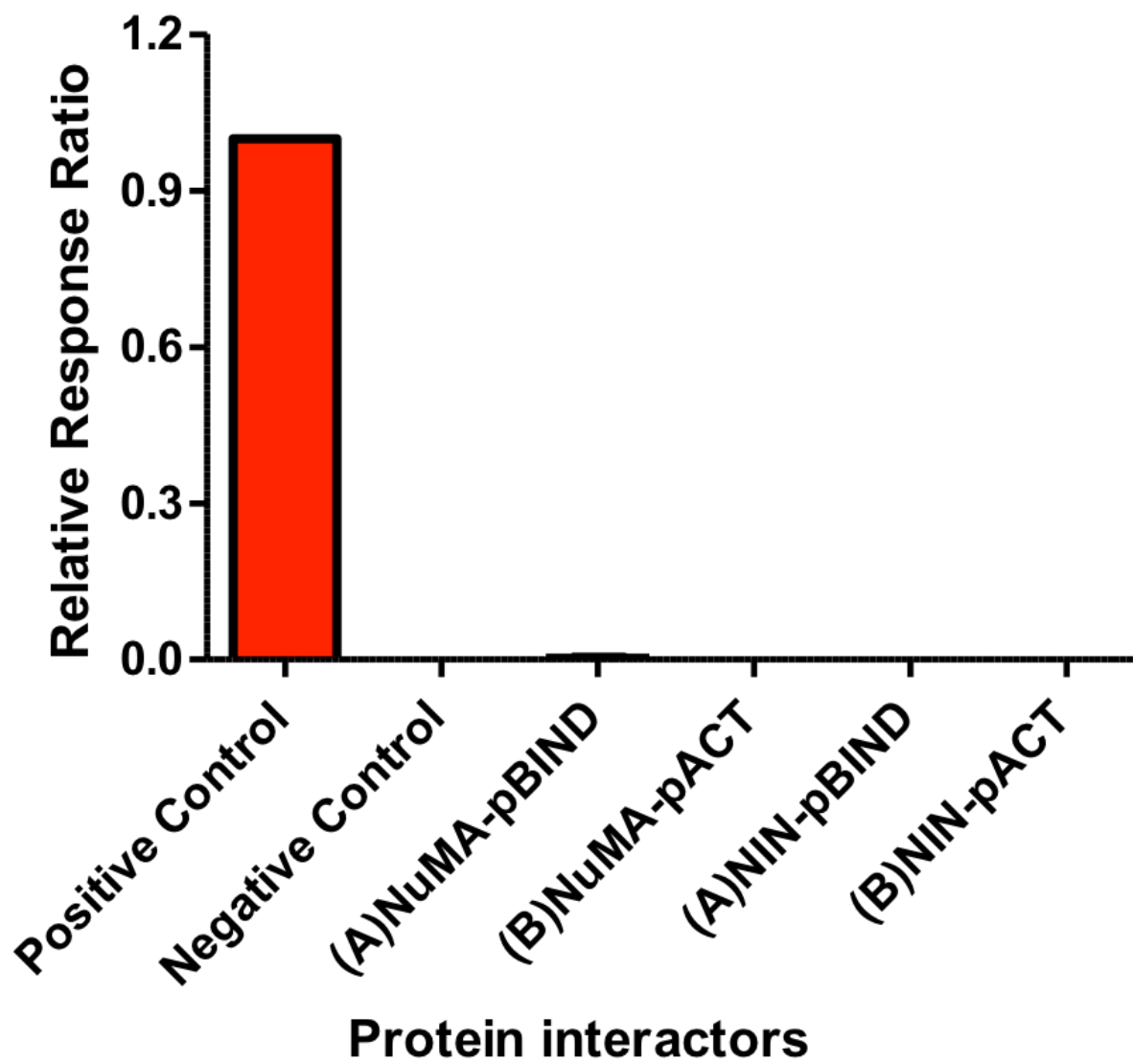


Figure 3.20.

Figure 3.20 (previous page). Mammalian Two-Hybrid luciferase assay results of mitosis-related gene of interest vector controls. DNA plasmids were made by subcloning genes of interest into the pACT and pBIND vectors. Both vectors, as well as the pG5luc vector, were then transiently transfected into HEK-293 cells and luminescence was measured to detect protein-protein interactions. (A) indicates that a gene has been subcloned into the pACT vector. (B) indicates that a gene has been subcloned into the pBIND vector. All data are presented as luciferase/Renilla output, which has been normalized to the positive and negative control values to produce a relative response ratio (RRR). Data are presented as mean \pm SEM of three independent experiments (N=3) performed in triplicate. Statistical analyses were done using one-way ANOVA followed by Tukey's Multiple Comparison test.

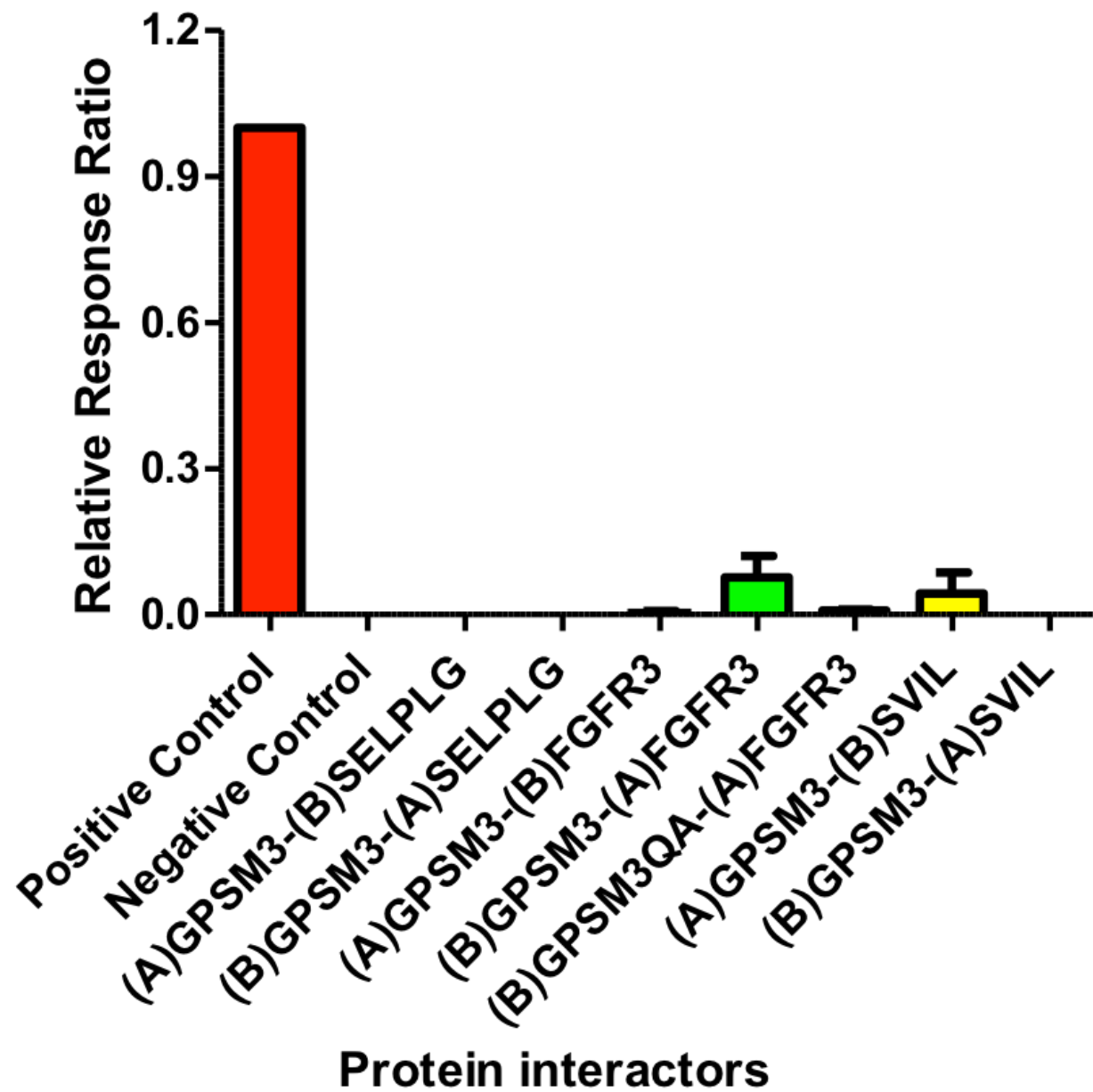


Figure 3.21.

Figure 3.21 (previous page). Mammalian Two-Hybrid luciferase assay results between GPSM3 and online database-predicted interactors. DNA plasmids were made by subcloning genes of interest into the pACT and pBIND vectors. Both vectors, as well as the pG5luc vector, were then transiently transfected into HEK-293 cells and luminescence was measured to detect protein-protein interactions. (A) indicates that the protein's corresponding gene has been subcloned into the pACT vector. (B) indicates that the protein's corresponding gene has been subcloned into the pBIND vector. All data are presented as luciferase/Renilla output, which has been normalized to the positive and negative control values to produce a relative response ratio (RRR). Data are presented as mean \pm SEM of three to five independent experiments ($N \geq 3$) performed in triplicate. Statistical analyses were done using one-way ANOVA followed by Tukey's Multiple Comparison test.

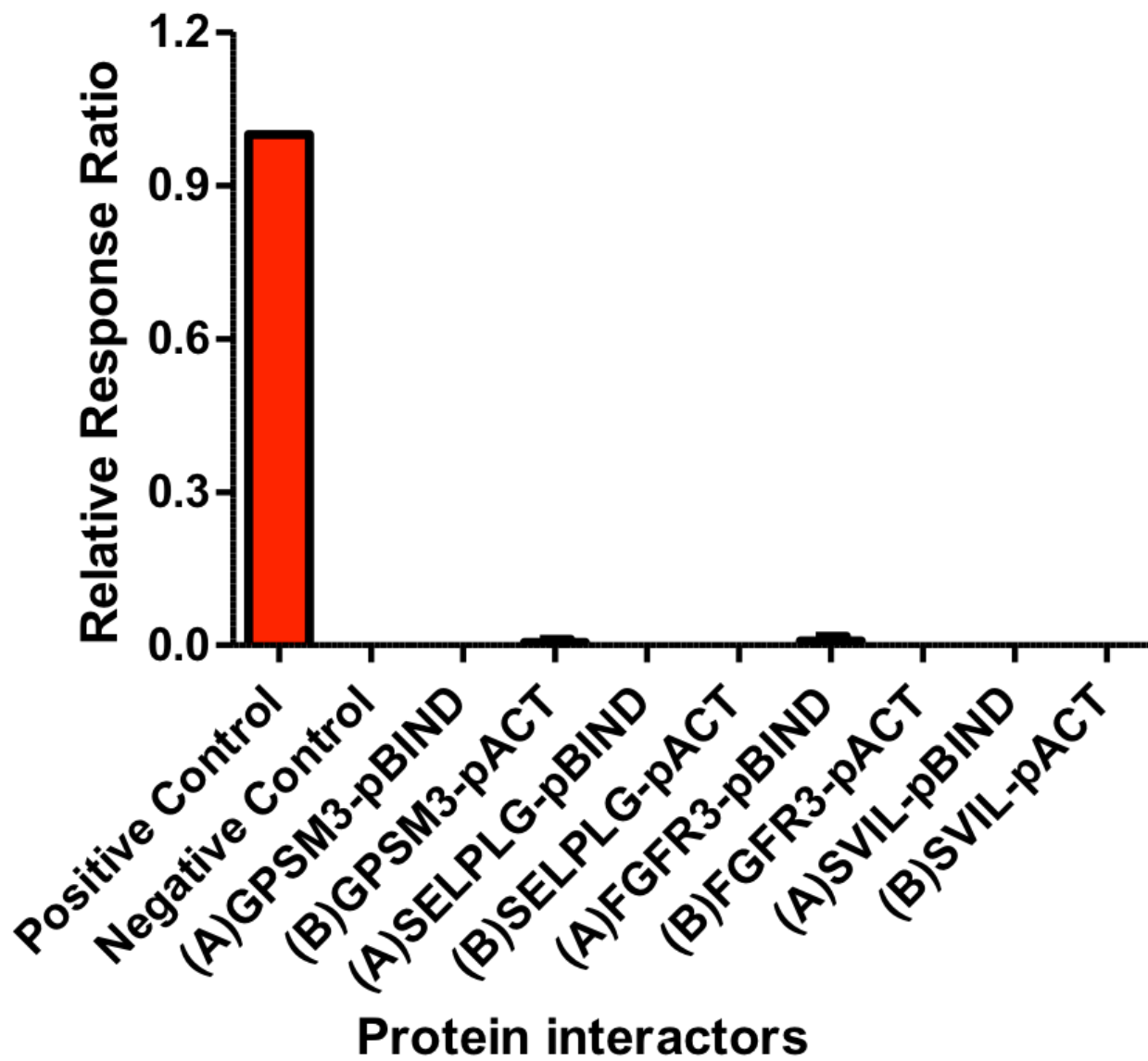


Figure 3.22.

Figure 3.22 (previous page). Mammalian Two-Hybrid luciferase assay results of online database-predicted interactor vector controls. DNA plasmids were made by subcloning genes of interest into the pACT and pBIND vectors. Both vectors, as well as the pG5luc vector, were then transiently transfected into HEK-293 cells and luminescence was measured to detect protein-protein interactions. (A) indicates that a gene has been subcloned into the pACT vector. (B) indicates that a gene has been subcloned into the pBIND vector. All data are presented as luciferase/Renilla output, which has been normalized to the positive and negative control values to produce a relative response ratio (RRR). Data are presented as mean \pm SEM of three independent experiments (N=3) performed in triplicate. Statistical analyses were done using one-way ANOVA followed by Tukey's Multiple Comparison test.

4 DISCUSSION

4.1 SUMMARY OF NOVEL FINDINGS

The functional role of GPSM3 in the cell remains poorly understood, especially compared to other components of the G protein-mediated signaling machinery. I hypothesized that GPSM3 plays a role in cell division, likely via an as yet undefined interaction with the mitotic spindle. In this study, GPSM3 transcript and protein levels were shown to be elevated in vascular smooth muscle cells (VSMCs) taken from spontaneously hypertensive (SHR) rats compared to those from normotensive Wistar-Kyoto (WKY) rats. In addition, a profile of GPSM3 transcript levels was compiled for the first time from rat tissues. SHR spleen tissue had higher levels of GPSM3 transcript compared to its WKY counterpart. GPSM3 transcript levels were also detected in aortic tissue at relatively high levels for the first time.

While heterotrimeric G protein subunits and GPSM motif-containing proteins have been linked to cell division, such a role for GPSM3 has not been reported in the literature. The results of the present study suggest that GPSM3 is indeed connected to the process of cell proliferation. In the SHR VSMCs with elevated GPSM3 expression, depriving cells of serum to promote cell cycle arrest resulted in decreased GPSM3 transcript and protein levels. Re-adding serum to these cells, allowing them to reenter the cell cycle, led to transcript and protein levels returning to control levels. GPSM3 expression seems to be linked to which stage of the cell cycle a cell is in. These results also suggest that GPSM3 expression is regulated at the level of transcription. Two independent experimental methods, an MTT assay and cell counting, showed that overexpression

of EYFP-GPSM3 in HEK-293 cells results in an increased proliferation rate. This indicates that changing GPSM3 expression is sufficient to significantly alter a cell's rate of proliferation.

Immunofluorescent labeling in WKY and SHR VSMCs revealed that GPSM3 co-localizes with β -tubulin during mitosis. During metaphase and anaphase, GPSM3 appears to localize to the microtubules as they attach to and pull apart chromatin. In cytokinetic cells, GPSM3 localizes to the microtubules in the midbody. These results suggest that GPSM3 functions in cell division via interaction with the mitotic spindle and could influence spindle orientation, spindle position, and chromosome segregation. Finally, the mammalian two-hybrid assay does not support previous observations that GPSM3 interacts with $G\beta 1$ and $G\alpha o$. The assay also provided evidence against a number of hypothesized protein-protein interactions involving GPSM3.

Ultimately, the results of this study support the hypothesis that GPSM3 is involved in the process of cell division. Expression of GPSM3 in VSMCs is linked to being in the cell cycle and increasing expression increases proliferation rate. GPSM3 likely exerts its function in cell division through an as yet undefined interaction with the mitotic spindle.

4.2 CONTRIBUTION OF RESEARCH TO CURRENT STATE OF KNOWLEDGE

Findings from this study have furthered our state of knowledge in three main categories: general knowledge about GPSM3, our understanding of cell division, and, to a lesser extent, our understanding of hypertension.

4.2.1 CONTRIBUTION TO OUR GENERAL KNOWLEDGE OF GPSM3

The expression profile compiled from GPSM3 transcript levels in WKY and SHR rat tissues (Figure 3.2) partially supports previously reported profiles from mouse and human tissues (Cao et al. 2004; Zhao et al. 2010). The finding that GPSM3 is moderately to highly expressed in spleen, lung and leukocytes is similar to mouse and human tissue. However, the finding that levels of GPSM3 mRNA in heart and liver are relatively low is at odds with reports from mouse and human tissues. For the first time, it is reported that GPSM3 transcript is present at high levels in aortic tissue as well. These findings also contradict the assertion by Billard et al. 2014 that GPSM3 expression is highly restricted to immune system cells.

Immunofluorescent labeling of vascular smooth muscle cells in interphase showed GPSM3 to be enriched in the nucleus and faintly detectable throughout the cytosol (Figure 3.9). Previous reports show GPSM3 mainly present in the cytosol or enriched at the plasma membrane (Cao et al. 2004; Giguère et al. 2013; Giguère, Laroche, Oestreich, Duncan, et al. 2012; Giguère, Laroche, Oestreich & Siderovski 2012; Willard et al. 2008; Zhao & Chidiac 2015). However, the COMPARTMENTS Subcellular localization database uses a sequence-based subcellular localization prediction method to predict that GPSM3 would be distributed similarly to the results seen in this study: enriched in the nucleus and present in the cytosol (Binder et al. 2014). It is worth noting that these cells were primed to divide by first serum starving them and then giving them serum-containing medium again in order to synchronize their cell cycles. This was not performed on any of the cells imaged in previous reports.

Regulation of GPSM3 expression has been studied very little. It has been reported that GPSM3 expression in immune cells changes in response to differentiation, but the underlying mechanism remains unclear (Giguère et al. 2013; Gall, Schroer, et al. 2016). Our finding that GPSM3 transcript and protein levels change to a similar degree in response to serum starvation and serum replacement (Figures 3.4 and 3.6) suggest that GPSM3 protein levels are modulated by transcriptional regulatory mechanisms rather than via translational or post-translational mechanisms, such as altered degradation. Two single nucleotide polymorphisms (SNPs) of the human GPSM3 gene result in decreased transcript abundance due to reduced promoter activity and these are inversely correlated with rheumatoid arthritis prevalence (Gall, Wilson, et al. 2016). Considering GPSM3 deficiency has been shown to act as a protective factor in a mouse model of inflammatory arthritis (Giguère et al. 2013), our finding that GPSM3 is likely transcriptionally regulated recalls the earlier report that GPSM3 SNPs that reduce transcript abundance result in decreased rheumatoid arthritis risk. It would be interesting to see if these polymorphisms are correlated with other disease states, especially hypertension and cancer.

In agreement with our findings (Figure 3.17), GPSM3 has been reported by multiple studies to interact with $G\alpha_i$ subunits while it does not interact with $G\alpha_s$ (Zhao et al. 2010; Cao et al. 2004; Kimple et al. 2004; Robichaux et al. 2015; Giguère, Laroche, Oestreich & Siderovski 2012; Giguère, Laroche, Oestreich, Duncan, et al. 2012; Oner, Maher, et al. 2010). However, unlike previous reports, our findings do not show that GPSM3 interacts with $G\alpha_o$ (Zhao et al. 2010) or $G\beta_1$ (Giguère, Laroche, Oestreich & Siderovski 2012). $G\alpha_o$ and a mutationally activated variant, $G\alpha_oQ205L$, were both tested and neither returned statistically significant signals. $G\alpha_oQ205L$ was used to mimic the fluoroaluminate-activated version of $G\alpha_o$ that Zhao et al. 2010 showed

was capable of interacting with GPSM3. G α Q205L has had a glutamine at position 205 mutated to become a leucine, and this is thought to result in persistent activation by inhibiting the GTPase activity of the protein (Kroll et al. 1992). On the other hand, fluoroaluminate activates G α subunits by binding to the GDP-binding site next to GDP and mimicking the role of the γ -phosphate of GTP (Bigay et al. 1985). The resulting structure more closely resembles that of the transition state for GTP hydrolysis than the ground state of an active G α subunit (Kleuss et al. 1994). Therefore, G α Q205L may be a more physiologically relevant model of activated G α and this could account for the different results of these two studies.

Giguère et al. 2012 reported that GPSM3 is capable of interacting with the G β subunits G β 1 to G β 4. Their study suggested that GPSM3 acts as a stabilizing chaperone of neosynthesized G β subunits during transport to the plasma membrane and that the binding site overlaps the N-terminal side of the first GPSM motif in GPSM3. Other than in that study, no GPSM motif-containing protein has yet been reported to interact with G β subunits. This finding could not be replicated using G β 1 in the mammalian two-hybrid assay. If GPSM3 does indeed act as a chaperone for G β subunits, the signal shuttling them to the plasma membrane could potentially interfere with the two-hybrid assay by preventing the DNA-binding domain from associating with the luciferase reporter gene, thereby precluding the promotion of luciferase protein synthesis by the transcriptional activation domain.

4.2.2 CONTRIBUTION TO OUR KNOWLEDGE OF HYPERTENSION

Increased GPSM3 expression in vascular smooth muscle cells from SHR rats relative to WKY rats (Figure 3.1) could be a protective factor in response to hypertensive conditions. Many pathological conditions of the cardiovascular system such as hypertension, hypertrophy, and heart failure have been linked to altered *Gai/o*-mediated signaling (Sato & Ishikawa 2010). This altered signaling is likely an adaptive response of the cardiovascular system. *Gai/o*-mediated signaling in the vasculature of SHR rats is reported to be elevated (Kost et al. 1999). Expression of *Gai2/3* in the heart and *Gai2* in the aorta were reported to be increased in SHR rats compared to WKY rats, while *Gas* was unchanged (Anand-Srivastava 1992). Hypertension in SHR rats can also be delayed by temporally inactivating *Gai/o*-mediated signaling via pertussis toxin treatment (Li & Anand-Srivastava 2002). Therefore, the inhibitory effect of GPSM3 on *Gai/o* activation could play a protective role in hypertension.

Increased GPSM3 expression in SHR VSMCs could also be a causative factor in the hypertensive phenotype of SHR rats. The transition of smooth muscle cells from a contractile to a proliferative, migratory phenotype is associated with cardiovascular disease (Dzau et al. 2002; Fingerle et al. 1989; Sandison et al. 2016). Changes in GPSM3 expression have been linked to differentiation, with higher GPSM3 levels associated with more mobile cell types (Giguère et al. 2013; Gall, Schroer, et al. 2016). Our finding that GPSM3 overexpression results in increased proliferation (Figures 3.7 and 3.8) suggests that elevated GPSM3 in SHR VSMCs could foster a more proliferative phenotype, thus leading to hypertension. Interestingly, blood pressure control mechanisms in GPSM1 null mice are altered, as sensitivity to the vasodilator sodium

nitroprusside (SNP) and baroreceptor reflex sensitivity were both reported to be elevated, while the ability to return to pre-SNP arterial pressure levels was impaired (Blumer et al. 2008).

Finally, I also found that GPSM3 transcript levels are increased in SHR spleen tissue.

Hypertension is associated with increased immune activity (Sun et al. 2006). As immune cells, particularly monocytes, are known to have relatively high GPSM3 expression, and the spleen has been shown to act as a reservoir for the majority of monocytes in the body, this could account for the higher levels of GPSM3 in SHR spleen tissue compared to spleen tissue from WKY rats (Giguère et al. 2013; Swirski et al. 2009). Alternatively, GPSM3 deficiency in mice has been linked to a decreased inflammatory response and decreased GPSM3 transcript levels in humans are linked with decreased arthritis risk (Giguère et al. 2013; Gall, Wilson, et al. 2016). The heart, brain, kidneys, and liver are reported to be inflamed in SHR rats (Sun et al. 2006). If the spleen is also inflamed in these rats, this could account for the increased levels of GPSM3 transcript.

4.2.3 CONTRIBUTION TO OUR KNOWLEDGE OF CELL DIVISION

G proteins and GPSM motif-containing proteins play essential roles in the process of cell division. Our data provide evidence of a role for GPSM3 in cell division for the first time. GPSM3 expression appears to be linked to the cell cycle (Figures 3.4 and 3.6). Depriving SHR VSMCs of serum in order to arrest the cell cycle resulted in GPSM3 mRNA levels significantly decreasing and GPSM3 protein levels following a similar trend. Reintroducing serum into the medium to allow re-entry into the cell cycle led to transcript and protein levels returning to normal. GPSM2 and Gai3 expression also change during the cell cycle, being upregulated during

metaphase in mammalian cells (Blumer et al. 2006). Expression of other protein classes, such as cyclins and cyclin-dependent kinases (CDKs), also vary throughout the cell cycle and can determine the proliferative fate of a cell (Yang et al. 2006; Shankland et al. 1996).

Overexpressing EYFP-tagged GPSM3 in HEK-293 cells resulted in an increased proliferation rate, as measured by both MTT assay and cell counting (Figures 3.7 and 3.8). Therefore higher levels of GPSM3 are correlated with higher rates of cell division, and increasing the expression of GPSM3 appears to be sufficient to increase proliferation rates. This could partly explain why SHR VSMCs, which have higher GPSM3 transcript and protein levels than WKY VSMCs (Figures 3.1, 3.5, and 3.6), divide at a rate approximately 1.75 times greater than their WKY counterparts (Hadrava et al. 1991). In addition, this could give insight into the elevated levels of GPSM3 in aortic tissue taken from abdominal aortic aneurism (AAA) (Lenk et al. 2007). AAA is associated with a decreased number of smooth muscle cells; therefore GPSM3 levels may be elevated in the smooth muscle cells in order to stimulate proliferation. However, an alternate explanation could be that the elevated levels of GPSM3 are a result of the immune cells known to infiltrate aortic tissue in AAA. GPSM3 expression is relatively high in immune cells and these cells could be responsible for the elevated GPSM3 levels reported.

The present findings may also indicate a role for GPSM3 in cancer biology. GPSM3 expression increases by greater than two-fold in prostate cancer models which mimic angiogenesis (Lapan et al. 2009). Furthermore, GPSM3 has been identified as a gene required for the proliferation of p53 human cancer cell lines (Xie et al. 2012). GPSM2 levels are elevated in most breast cancer cell lines and knocking down GPSM2 in those cells results in significant growth suppression and

incomplete cell division (Fukukawa et al. 2010b). Since elevated GPSM3 levels correlate with and may in fact cause increased rates of cell division, GPSM3 could be an attractive therapeutic target for cancer treatment.

GPSM3 was observed to co-localize with β -tubulin at the spindle fibers during metaphase and anaphase (Figures 3.10 and 3.11), and at the midbody during telophase (Figure 3.12). GPSM2 has been shown to localize to these same regions during these three stages of mitosis as well in breast cancer cells (Fukukawa et al. 2010b). G α o co-localizes with β -tubulin at the mitotic spindle in animal and human cell lines as well (Wu & Lin 1994), and G β subunits are incorporated into the mitotic spindle and interact with tubulin in bovine brain cells according to Wu et al. 1998. G α i2, on the other hand, has been reported to bind to the kinetochores of chromatin in 3T3 cells (Crouch & Simson 1997). Since GPSM2 has been reported to directly interact with G α o and that overexpression of G α o subunits are capable of redirecting localization of GPSM2 in the cell, it is likely that GPSM2 is being recruited to the spindle fibers by G α o (Kaushik et al. 2003). Our findings also suggest that GPSM3 interacts with G α i1 and G α i2 (Figure 3.17). Therefore GPSM3 may be recruited to the spindle fibers by one of the members of the G α i/o family.

Considering the many parallels between the findings of this study and previous reports on GPSM2, I propose that GPSM3 may function in a similar capacity to GPSM2. The tertiary complex consisting of G α i, GPSM2, and NuMA plays a critical role in the generation of pulling forces on the mitotic spindle and spindle pole orientation and positioning (Du & Macara 2004; Merdes et al. 2000; Tall & Gilman 2005). Rapid cycling of nucleotide exchange on the G α i

subunit is thought to contribute to these pulling forces, and is accomplished by GAP and GEF activity of accessory proteins (Tall & Gilman 2005; Dave et al. 2009). GPSM3 could be part of an alternative complex that plays a related but different role from GPSM2 in cell division. It is a particularly attractive candidate for such a role as its reported GEF activity could aid rapid cycling of nucleotide exchange (Zhao et al. 2010).

4.3 EXPERIMENTAL METHODS: NOTES AND LIMITATIONS

4.3.1 *SERUM STARVATION*

This study used serum starvation to induce reversible cell cycle arrest (Chen et al. 2012), which has been shown to not change overall RNA and protein synthesis in a cell (Zetterberg & Sköld 1969). Changes in GPSM3 transcript and protein levels were therefore thought to be the result of changes in the cell cycle. However, serum starvation is a potent cellular stress and it cannot be ruled out that GPSM3 expression changes in response to cellular stress. It should also be noted that serum starvation has been shown to induce transcriptional changes in pathways related to cancer, cell death, apoptosis, and the cell cycle in the LoVo colon cancer cell line (Zheng et al. 2016).

4.3.2 *EYFP-TAGGED GPSM3*

In the MTT assay and cell counting experiments, HEK-293 cells were transiently transfected with either EYFP-tagged GPSM3 or EYFP. The difference in proliferation rates between these two groups of cells was attributed to GPSM3. Since linking a fluorescent protein to a protein of

interest and the position of this linkage can affect the localization and functionality of that protein of interest (Snapp 2005), it is conceivable that the same effect would not occur using untagged GPSM3.

4.3.3 MAMMALIAN TWO-HYBRID ASSAY

I failed to identify any novel GPSM3 interactors using the mammalian two-hybrid assay. The proteins of interest that were tested were chosen for specific reasons. NuMA was chosen due to its functional role with GPSM2 and the many similarities between GPSM3 and GPSM2. Ninein was chosen because it plays a role in anchoring microtubules to the centrosome and due to its high expression in the vasculature of normal and pathological human tissues, making it an attractive target (Matsumoto et al. 2008; Mogensen et al. 2000). Neither of these proteins when tested produced statistically significant signals (Figure 3.19). Previously in our lab, a co-immunoprecipitation assay using His-tagged GPSM3 as bait and probing for β -tubulin failed to indicate that the two proteins directly interact or co-exist in a complex. For this reason, β -tubulin was not included in the list of proteins to test for interaction with GPSM3.

The remaining three proteins, FGFR3, supervillin, and SELPLG, were chosen because they were predicted as likely GPSM3 interactors by the web resource STRING (Search Tool for the Retrieval of INteracting Genes) database (Szklarczyk et al. 2015). In addition to making its own predictions, STRING also uses protein-protein interaction prediction data and resources from over twenty other online resources. GPSM motifs can be regulated via phosphorylation (Hollinger et al. 2003; Blumer et al. 2003; Fukukawa et al. 2010b) and FGFR3 contains a

cytosolic tyrosine kinase domain (Keegan et al. 1991; Bocharov et al. 2013). I therefore reasoned that FGFR3 could be regulating GPSM3 via its kinase activity. SELPLG shares many of the associations GPSM3 has, being linked to cardiovascular disease (Tregouet et al. 2003; Volcik et al. 2009), inflammation (Sun et al. 2016), and cell migration, and reported expression in immune cells (Luan et al. 2010). GPSM2 and NuMA require Afadin, an actin-binding protein, for proper cortical localization via direct interaction between GPSM2 and Afadin (Carminati, Gallini, et al. 2016; Carminati, Cecatiello, et al. 2016). Supervillin contains actin-binding sites and is associated with cell motility and cancer (Fedechkin et al. 2013). I predicted that supervillin might interact with GPSM3 in a role analogous to that of Afadin with GPSM2. None of these proposed interactions were confirmed by the mammalian two-hybrid assay (Figure 3.21). It should be noted that SELPLG no longer appears as a predicted GPSM3 interactor in the STRING database since it was updated. The intragenic microRNA database still lists SELPLG as a GPSM3 interactor, listing STRING as its source (miRAD 2016).

Mammalian Two-Hybrid assays have the potential to produce false negative results. First, the size and orientation of the proteins of interest could interfere with the ability of the fused DNA-binding domain and transcriptional activation domain from coming into close contact and promoting the synthesis of luciferase. Supervillin, ninein, and NuMA are all over 2000 amino acids in length, which could have interfered with the ability of the fused domains from coming into close contact. Second, the fused domains could sterically hinder the ability of the proteins of interest to associate (Lievens et al. 2009). These situations likely account for vector directionality, as observed with the tested interaction between GPSM3 and *Gai1/2* (Figure 3.17). Third, one or more of the proteins of interest may be tethered to a part of the cell preventing the

complex from coming into contact with the reporter gene. For example, supervillin may be tethered to actin filaments via its actin-binding domains. Finally, if the tested proteins are part of a larger complex, other components of the complex may need to be overexpressed as well in order for the complex to form and a signal to be produced.

4.4 FUTURE DIRECTIONS

The results of this study provide strong evidence of a role for GPSM3 in cell division. The specific function of GPSM3 and how it achieves that function remain to be elucidated.

Overexpression of GPSM3 was shown to increase the rate of proliferation of cells. Future studies should determine whether using siRNA to knockdown the level of GPSM3 in a cell produces the opposite effect, decreasing proliferation rate. If this is indeed the case, targeted gene therapy against GPSM3 could be a potential treatment for certain cancers. Knockdown of GPSM1 and GPSM2 homologues in *C. elegans* leads to incorrect spindle orientations and decreased spindle pulling forces (Srinivasan et al. 2003; Schneider & Bowerman 2003b). Overexpression of GPSM2 in kidney cells results in oscillations and rotations of the mitotic spindle which indicate strong pulling forces being exerted on astral microtubules (Du & Macara 2004). Future experiments should overexpress and knock down GPSM3 to determine whether a similar phenotype occurs.

GPSM3 null mice have been successfully bred (Giguère et al. 2013). Considering GPSM3 is elevated in SHR VSMCs and they divide at a faster rate than WKY VSMCs (Hadrava et al. 1991), measuring the proliferation rate in VSMCs taken from GPSM3 null mice would be

interesting. Spindle orientation and pulling forces should also be studied in the smooth muscle cells and compared to those that endogenously express GPSM3. If proliferation rate is indeed decreased in these VSMCS, overexpressing GPSM3 in these cells to rescue a normal division rate phenotype could strengthen the argument that GPSM3 levels are correlated with proliferation rate.

Coupling between GPSM motif-containing proteins and $G\alpha$ proteins is necessary for mitosis to occur properly. Blocking this interaction via a point mutation which prevents the GPSM motif from binding to $G\alpha$ results in cytokinetic defects and abnormal mitotic spindle rocking (Willard et al. 2008; Cho & Kehrl 2007). It is also possible to mutate the GPSM motifs in GPSM3 so that they are incapable of interacting with $G\alpha$ subunits (Zhao et al. 2010). Studying the mitotic spindle and cytokinesis in cells that have this mutation could help demystify the role GPSM3 plays in cell division.

Finally, like GPSM2, GPSM3 most likely interacts with other proteins in order to fulfill its role in cell division. Therefore identifying these interaction partners would be an important step in determining the function of GPSM3. This study suggests that despite sharing many similarities with GPSM2, GPSM3 may not interact with the same proteins. Online resource databases such as STRING also appear to struggle to correctly predict GPSM3 interactors. Therefore, a yeast two-hybrid assay could be used to screen a smooth muscle cell cDNA library for proteins that interact with GPSM3. Identifying GPSM3 interaction partners could be the turning point in ascertaining its function in cell division.

4.5 CONCLUSIONS

Our results provide evidence that GPSM3 plays a role in the process of cell division. GPSM3 levels are correlated with changes in the cell cycle of vascular smooth muscle cells from spontaneously hypertensive rats. Overexpression of EYFP-tagged GPSM3 in HEK-293 cells results in a significant increase in the proliferation rate of those cells. Furthermore, in vascular smooth muscle cells, GPSM3 co-localizes with β -tubulin at the mitotic spindle during metaphase and anaphase and at the midbody during telophase. Therefore, GPSM3 appears to play a role in the process of cell division, likely via interaction with the mitotic spindle.

5 REFERENCES

- Adhikari, A. & Sprang, S.R., 2003. Thermodynamic characterization of the binding of activator of G protein signaling 3 (AGS3) and peptides derived from AGS3 with G alpha i1. *The Journal of biological chemistry*, 278(51), pp.51825–32. Available at: <http://www.ncbi.nlm.nih.gov/pubmed/14530282> [Accessed June 5, 2016].
- Anand-Srivastava, M.B., 1992. Enhanced expression of inhibitory guanine nucleotide regulatory protein in spontaneously hypertensive rats. Relationship to adenylate cyclase inhibition. *The Biochemical journal*, 288 (Pt 1, pp.79–85. Available at: <http://www.pubmedcentral.nih.gov/articlerender.fcgi?artid=1132082&tool=pmcentrez&rendertype=abstract> [Accessed June 6, 2016].
- Anand-Srivastava, M.B., 1996. G-proteins and adenylyl cyclase signalling in hypertension. *Molecular and cellular biochemistry*, 157(1–2), pp.163–70. Available at: <http://www.ncbi.nlm.nih.gov/pubmed/8739243> [Accessed June 6, 2016].
- Barcellos, L.F. et al., 2009. High-density SNP screening of the major histocompatibility complex in systemic lupus erythematosus demonstrates strong evidence for independent susceptibility regions. *PLoS genetics*, 5(10), p.e1000696. Available at: <http://www.pubmedcentral.nih.gov/articlerender.fcgi?artid=2758598&tool=pmcentrez&rendertype=abstract> [Accessed May 28, 2016].
- Bernard, M.L. et al., 2001. Selective interaction of AGS3 with G-proteins and the influence of AGS3 on the activation state of G-proteins. *The Journal of biological chemistry*, 276(2), pp.1585–93. Available at: <http://www.ncbi.nlm.nih.gov/pubmed/11042168> [Accessed January 20, 2016].
- Bian, Y. et al., 2014. An enzyme assisted RP-RPLC approach for in-depth analysis of human liver phosphoproteome. *Journal of proteomics*, 96, pp.253–62. Available at: <http://www.ncbi.nlm.nih.gov/pubmed/24275569> [Accessed February 16, 2016].
- Biddlecome, G.H., Berstein, G. & Ross, E.M., 1996. Regulation of phospholipase C-beta1 by Gq and m1 muscarinic cholinergic receptor. Steady-state balance of receptor-mediated activation and GTPase-activating protein-promoted deactivation. *The Journal of biological chemistry*, 271(14), pp.7999–8007. Available at: <http://www.ncbi.nlm.nih.gov/pubmed/8626481> [Accessed May 31, 2016].
- Bigay, J. et al., 1985. Fluoroaluminates activate transducin-GDP by mimicking the gamma-phosphate of GTP in its binding site. *FEBS letters*, 191(2), pp.181–5. Available at: <http://www.ncbi.nlm.nih.gov/pubmed/3863758> [Accessed November 13, 2016].
- Billard, M.J. et al., 2014. G protein signaling modulator-3: a leukocyte regulator of inflammation in health and disease. *American journal of clinical and experimental immunology*, 3(2), pp.97–106. Available at:

<http://www.pubmedcentral.nih.gov/articlerender.fcgi?artid=4138133&tool=pmcentrez&rendertype=abstract> [Accessed January 20, 2016].

Binder, J.X. et al., 2014. COMPARTMENTS: unification and visualization of protein subcellular localization evidence. *Database : the journal of biological databases and curation*, 2014, p.bau012. Available at: <http://www.ncbi.nlm.nih.gov/pubmed/24573882> [Accessed November 13, 2016].

Blumer, J.B. et al., 2008. Activator of G protein signaling 3 null mice: I. Unexpected alterations in metabolic and cardiovascular function. *Endocrinology*, 149(8), pp.3842–9. Available at: <http://www.pubmedcentral.nih.gov/articlerender.fcgi?artid=2488243&tool=pmcentrez&rendertype=abstract> [Accessed June 6, 2016].

Blumer, J.B. et al., 2003. Interaction of activator of G-protein signaling 3 (AGS3) with LKB1, a serine/threonine kinase involved in cell polarity and cell cycle progression: phosphorylation of the G-protein regulatory (GPR) motif as a regulatory mechanism for the interaction of GP. *The Journal of biological chemistry*, 278(26), pp.23217–20. Available at: <http://www.ncbi.nlm.nih.gov/pubmed/12719437> [Accessed January 20, 2016].

Blumer, J.B. et al., 2006. The G-protein regulatory (GPR) motif-containing Leu-Gly-Asn-enriched protein (LGN) and Galpha3 influence cortical positioning of the mitotic spindle poles at metaphase in symmetrically dividing mammalian cells. *European journal of cell biology*, 85(12), pp.1233–40. Available at: <http://www.ncbi.nlm.nih.gov/pubmed/17000024> [Accessed June 11, 2016].

Blumer, J.B., Chandler, L.J. & Lanier, S.M., 2002. Expression analysis and subcellular distribution of the two G-protein regulators AGS3 and LGN indicate distinct functionality. Localization of LGN to the midbody during cytokinesis. *The Journal of biological chemistry*, 277(18), pp.15897–903. Available at: <http://www.ncbi.nlm.nih.gov/pubmed/11832491> [Accessed June 3, 2016].

Blumer, J.B., Smrcka, A. V & Lanier, S.M., 2007. Mechanistic pathways and biological roles for receptor-independent activators of G-protein signaling. *Pharmacology & therapeutics*, 113(3), pp.488–506. Available at: <http://www.pubmedcentral.nih.gov/articlerender.fcgi?artid=1978177&tool=pmcentrez&rendertype=abstract> [Accessed January 20, 2016].

Bocharov, E. V et al., 2013. Structure of FGFR3 transmembrane domain dimer: implications for signaling and human pathologies. *Structure (London, England : 1993)*, 21(11), pp.2087–93. Available at: <http://www.pubmedcentral.nih.gov/articlerender.fcgi?artid=3844157&tool=pmcentrez&rendertype=abstract> [Accessed March 28, 2016].

Boullaran, C. et al., 2014. Resistance to Inhibitors of Cholinesterase (RiC)-8A and Gai Contribute to Cytokinesis Abscission by Controlling Vacuolar Protein-Sorting (Vps)34

- Activity C. Prigent, ed. *PLoS ONE*, 9(1), p.e86680. Available at: <http://dx.plos.org/10.1371/journal.pone.0086680> [Accessed November 2, 2016].
- Bowers, M.S. et al., 2004. Activator of G protein signaling 3: a gatekeeper of cocaine sensitization and drug seeking. *Neuron*, 42(2), pp.269–81. Available at: <http://www.pubmedcentral.nih.gov/articlerender.fcgi?artid=3619420&tool=pmcentrez&rendertype=abstract> [Accessed June 3, 2016].
- Bøyum, A., 1968. Isolation of mononuclear cells and granulocytes from human blood. Isolation of mononuclear cells by one centrifugation, and of granulocytes by combining centrifugation and sedimentation at 1 g. *Scandinavian journal of clinical and laboratory investigation. Supplementum*, 97, pp.77–89. Available at: <http://www.ncbi.nlm.nih.gov/pubmed/4179068> [Accessed November 6, 2015].
- Burns, D.L., 1988. Subunit structure and enzymic activity of pertussis toxin. *Microbiological sciences*, 5(9), pp.285–7. Available at: <http://www.ncbi.nlm.nih.gov/pubmed/2908558> [Accessed May 28, 2016].
- Cao, X. et al., 2004. Identification and characterization of AGS4: a protein containing three G-protein regulatory motifs that regulate the activation state of G α . *The Journal of biological chemistry*, 279(26), pp.27567–74. Available at: <http://www.ncbi.nlm.nih.gov/pubmed/15096500> [Accessed January 20, 2016].
- Carminati, M., Gallini, S., et al., 2016. Concomitant binding of Afadin to LGN and F-actin directs planar spindle orientation. *Nature structural & molecular biology*, 23(2), pp.155–63. Available at: <http://www.ncbi.nlm.nih.gov/pubmed/26751642> [Accessed July 2, 2016].
- Carminati, M., Cecatiello, V. & Mapelli, M., 2016. Crystallization and X-ray diffraction of LGN in complex with the actin-binding protein afadin. *Acta Crystallographica Section F Structural Biology Communications*, 72(2), pp.145–151. Available at: <http://scripts.iucr.org/cgi-bin/paper?S2053230X16000807> [Accessed November 14, 2016].
- Chan, P. et al., 2011. Ric-8B is a GTP-dependent G protein alphas guanine nucleotide exchange factor. *The Journal of biological chemistry*, 286(22), pp.19932–42. Available at: <http://www.pubmedcentral.nih.gov/articlerender.fcgi?artid=3103368&tool=pmcentrez&rendertype=abstract> [Accessed May 31, 2016].
- Chang, W.-C. et al., 2012. ORAI1 genetic polymorphisms associated with the susceptibility of atopic dermatitis in Japanese and Taiwanese populations. *PloS one*, 7(1), p.e29387. Available at: <http://www.pubmedcentral.nih.gov/articlerender.fcgi?artid=3258251&tool=pmcentrez&rendertype=abstract> [Accessed January 8, 2016].

- Chen, M. et al., 2012. Serum starvation induced cell cycle synchronization facilitates human somatic cells reprogramming. *PloS one*, 7(4), p.e28203. Available at: <http://www.pubmedcentral.nih.gov/articlerender.fcgi?artid=3329488&tool=pmcentrez&rendertype=abstract> [Accessed January 18, 2016].
- Chidiac, P., 1998. Rethinking receptor-G protein-effector interactions. *Biochemical pharmacology*, 55(5), pp.549–56. Available at: <http://www.ncbi.nlm.nih.gov/pubmed/9515565> [Accessed February 10, 2016].
- Cho, H. & Kehrl, J.H., 2007. Localization of Gi alpha proteins in the centrosomes and at the midbody: implication for their role in cell division. *The Journal of cell biology*, 178(2), pp.245–55. Available at: <http://www.pubmedcentral.nih.gov/articlerender.fcgi?artid=2064444&tool=pmcentrez&rendertype=abstract> [Accessed January 21, 2016].
- Cho, H., Kim, D.-U. & Kehrl, J.H., 2005. RGS14 is a centrosomal and nuclear cytoplasmic shuttling protein that traffics to promyelocytic leukemia nuclear bodies following heat shock. *The Journal of biological chemistry*, 280(1), pp.805–14. Available at: <http://www.ncbi.nlm.nih.gov/pubmed/15520006> [Accessed June 11, 2016].
- Coleman, D.E. et al., 1994. Structures of active conformations of Gi alpha 1 and the mechanism of GTP hydrolysis. *Science (New York, N.Y.)*, 265(5177), pp.1405–12. Available at: <http://www.ncbi.nlm.nih.gov/pubmed/8073283> [Accessed May 31, 2016].
- Comuzzie, A.G. et al., 2012. Novel genetic loci identified for the pathophysiology of childhood obesity in the Hispanic population. *PloS one*, 7(12), p.e51954. Available at: <http://www.pubmedcentral.nih.gov/articlerender.fcgi?artid=3522587&tool=pmcentrez&rendertype=abstract> [Accessed December 15, 2015].
- Cornwell, T.L. & Lincoln, T.M., 1989. Regulation of intracellular Ca²⁺ levels in cultured vascular smooth muscle cells. Reduction of Ca²⁺ by atriopeptin and 8-bromo-cyclic GMP is mediated by cyclic GMP-dependent protein kinase. *The Journal of biological chemistry*, 264(2), pp.1146–55. Available at: <http://www.ncbi.nlm.nih.gov/pubmed/2536016> [Accessed November 16, 2016].
- Corona, E., Dudley, J.T. & Butte, A.J., 2010. Extreme evolutionary disparities seen in positive selection across seven complex diseases. *PloS one*, 5(8), p.e12236. Available at: <http://www.pubmedcentral.nih.gov/articlerender.fcgi?artid=2923198&tool=pmcentrez&rendertype=abstract> [Accessed January 20, 2016].
- Crouch, M.F., Osborne, G.W. & Willard, F.S., 2000. The GTP-binding protein G(ialpha) translocates to kinetochores and regulates the M-G(1) cell cycle transition of Swiss 3T3 cells. *Cellular signalling*, 12(3), pp.153–63. Available at: <http://www.ncbi.nlm.nih.gov/pubmed/10704822> [Accessed November 3, 2016].

- Crouch, M.F. & Simson, L., 1997. The G-protein G(i) regulates mitosis but not DNA synthesis in growth factor-activated fibroblasts: a role for the nuclear translocation of G(i). *FASEB journal : official publication of the Federation of American Societies for Experimental Biology*, 11(2), pp.189–98. Available at: <http://www.ncbi.nlm.nih.gov/pubmed/9039962> [Accessed October 17, 2016].
- Dave, R.H. et al., 2009. Heterotrimeric G-Proteins Interact Directly with Cytoskeletal Components to Modify Microtubule-Dependent Cellular Processes. *Neurosignals*, 17(1), pp.100–108. Available at: <http://www.pubmedcentral.nih.gov/articlerender.fcgi?artid=2836952&tool=pmcentrez&rendertype=abstract> [Accessed January 11, 2016].
- DeWire, S.M. et al., 2007. Beta-arrestins and cell signaling. *Annual review of physiology*, 69, pp.483–510. Available at: <http://www.ncbi.nlm.nih.gov/pubmed/17305471> [Accessed January 20, 2016].
- Du, Q. & Macara, I.G., 2004. Mammalian Pins is a conformational switch that links NuMA to heterotrimeric G proteins. *Cell*, 119(4), pp.503–16. Available at: <http://www.ncbi.nlm.nih.gov/pubmed/15537540> [Accessed May 3, 2016].
- Dzau, V.J., Braun-Dullaeus, R.C. & Sedding, D.G., 2002. Vascular proliferation and atherosclerosis: New perspectives and therapeutic strategies. *Nature Medicine*, 8(11), pp.1249–1256. Available at: <http://www.nature.com/doi/10.1038/nm1102-1249> [Accessed November 2, 2016].
- Van Eps, N. et al., 2015. The guanine nucleotide exchange factor Ric-8A induces domain separation and Ras domain plasticity in Gai1. *Proceedings of the National Academy of Sciences*, 112(5), pp.1404–1409. Available at: <http://www.pnas.org/lookup/doi/10.1073/pnas.1423878112> [Accessed November 2, 2016].
- Fedechkin, S.O. et al., 2013. An N-terminal, 830 residues intrinsically disordered region of the cytoskeleton-regulatory protein supervillin contains Myosin II- and F-actin-binding sites. *Journal of Biomolecular Structure and Dynamics*, 31(10), pp.1150–1159. Available at: <http://www.tandfonline.com/doi/abs/10.1080/07391102.2012.726531> [Accessed November 14, 2016].
- Ferguson, S.S., 2001. Evolving concepts in G protein-coupled receptor endocytosis: the role in receptor desensitization and signaling. *Pharmacological reviews*, 53(1), pp.1–24. Available at: <http://www.ncbi.nlm.nih.gov/pubmed/11171937> [Accessed January 20, 2016].
- Fingerle, J. et al., 1989. Role of platelets in smooth muscle cell proliferation and migration after vascular injury in rat carotid artery. *Proceedings of the National Academy of Sciences of the United States of America*, 86(21), pp.8412–6. Available at: <http://www.ncbi.nlm.nih.gov/pubmed/2813399> [Accessed October 18, 2016].

- Fukukawa, C. et al., 2010a. Critical roles of LGN/GPSM2 phosphorylation by PBK/TOPK in cell division of breast cancer cells. *Genes, chromosomes & cancer*, 49(10), pp.861–72. Available at: <http://www.ncbi.nlm.nih.gov/pubmed/20589935> [Accessed June 2, 2016].
- Fukukawa, C. et al., 2010b. Critical roles of LGN/GPSM2 phosphorylation by PBK/TOPK in cell division of breast cancer cells. *Genes, chromosomes & cancer*, 49(10), pp.861–72. Available at: <http://www.ncbi.nlm.nih.gov/pubmed/20589935> [Accessed October 11, 2016].
- Gall, B.J., Wilson, A., et al., 2016. Genetic variations in GPSM3 associated with protection from rheumatoid arthritis affect its transcript abundance. *Genes and immunity*. Available at: <http://www.ncbi.nlm.nih.gov/pubmed/26821282> [Accessed February 1, 2016].
- Gall, B.J., Schroer, A.B., et al., 2016. Reduction of GPSM3 expression akin to the arthritis-protective SNP rs204989 differentially affects migration in a neutrophil model. *Genes and immunity*. Available at: <http://www.ncbi.nlm.nih.gov/pubmed/27307211> [Accessed June 22, 2016].
- Ghosh, M. et al., 2003. Receptor- and nucleotide exchange-independent mechanisms for promoting G protein subunit dissociation. *The Journal of biological chemistry*, 278(37), pp.34747–50. Available at: <http://www.ncbi.nlm.nih.gov/pubmed/12881533> [Accessed January 20, 2016].
- Gibson, D.G. et al., 2009. Enzymatic assembly of DNA molecules up to several hundred kilobases. *Nature methods*, 6(5), pp.343–5. Available at: <http://www.ncbi.nlm.nih.gov/pubmed/19363495> [Accessed July 14, 2014].
- Giguère, P.M. et al., 2013. G-protein signaling modulator-3, a gene linked to autoimmune diseases, regulates monocyte function and its deficiency protects from inflammatory arthritis. *Molecular immunology*, 54(2), pp.193–8. Available at: <http://www.pubmedcentral.nih.gov/articlerender.fcgi?artid=3563835&tool=pmcentrez&rendertype=abstract> [Accessed January 20, 2016].
- Giguère, P.M., Laroche, G., Oestreich, E.A. & Siderovski, D.P., 2012. G-protein signaling modulator-3 regulates heterotrimeric G-protein dynamics through dual association with G β and G α i protein subunits. *The Journal of biological chemistry*, 287(7), pp.4863–74. Available at: <http://www.pubmedcentral.nih.gov/articlerender.fcgi?artid=3281645&tool=pmcentrez&rendertype=abstract> [Accessed January 20, 2016].
- Giguère, P.M. et al., 2014. G Protein signaling modulator-3 inhibits the inflammasome activity of NLRP3. *The Journal of biological chemistry*, 289(48), pp.33245–57. Available at: <http://www.pubmedcentral.nih.gov/articlerender.fcgi?artid=4246083&tool=pmcentrez&rendertype=abstract>

ez&rendertype=abstract [Accessed January 20, 2016].

- Giguère, P.M., Laroche, G., Oestreich, E.A., Duncan, J.A., et al., 2012. Regulation of the subcellular localization of the G-protein subunit regulator GPSM3 through direct association with 14-3-3 protein. *The Journal of biological chemistry*, 287(37), pp.31270–9. Available at: <http://www.pubmedcentral.nih.gov/articlerender.fcgi?artid=3438958&tool=pmcentrez&rendertype=abstract> [Accessed January 20, 2016].
- Gilman, A.G., 1987. G proteins: transducers of receptor-generated signals. *Annual review of biochemistry*, 56, pp.615–49. Available at: <http://www.ncbi.nlm.nih.gov/pubmed/3113327> [Accessed October 19, 2015].
- Goldstein, B., 2003. Asymmetric division: AGS proteins position the spindle. *Current biology : CB*, 13(22), pp.R879-80. Available at: <http://www.ncbi.nlm.nih.gov/pubmed/14614844> [Accessed January 20, 2016].
- Gönczy, P., 2008. Mechanisms of asymmetric cell division: flies and worms pave the way. *Nature reviews. Molecular cell biology*, 9(5), pp.355–66. Available at: <http://www.ncbi.nlm.nih.gov/pubmed/18431399> [Accessed January 21, 2016].
- Gotta, M. & Ahringer, J., 2001. Distinct roles for Galpha and Gbetagamma in regulating spindle position and orientation in *Caenorhabditis elegans* embryos. *Nature cell biology*, 3(3), pp.297–300. Available at: <http://www.ncbi.nlm.nih.gov/pubmed/11231580> [Accessed June 7, 2016].
- Granderath, S. et al., 1999. loco encodes an RGS protein required for *Drosophila* glial differentiation. *Development (Cambridge, England)*, 126(8), pp.1781–91. Available at: <http://www.ncbi.nlm.nih.gov/pubmed/10079238> [Accessed January 20, 2016].
- Hadrava, V. et al., 1991. Vascular smooth muscle cell proliferation and its therapeutic modulation in hypertension. *American heart journal*, 122(4 Pt 2), pp.1198–203. Available at: <http://www.ncbi.nlm.nih.gov/pubmed/1927887> [Accessed June 27, 2016].
- Hampoelz, B. & Knoblich, J.A., 2004. Heterotrimeric G proteins: new tricks for an old dog. *Cell*, 119(4), pp.453–6. Available at: <http://www.ncbi.nlm.nih.gov/pubmed/15537535> [Accessed January 20, 2016].
- Hollinger, S., Ramineni, S. & Hepler, J.R., 2003. Phosphorylation of RGS14 by protein kinase A potentiates its activity toward G alpha i. *Biochemistry*, 42(3), pp.811–9. Available at: <http://www.ncbi.nlm.nih.gov/pubmed/12534294> [Accessed June 2, 2016].
- Iiri, T., Farfel, Z. & Bourne, H.R., 1998. G-protein diseases furnish a model for the turn-on switch. *Nature*, 394(6688), pp.35–8. Available at: <http://www.ncbi.nlm.nih.gov/pubmed/9665125> [Accessed May 31, 2016].

- Jacoby, E. et al., 2006. The 7 TM G-protein-coupled receptor target family. *ChemMedChem*, 1(8), pp.761–82. Available at: <http://www.ncbi.nlm.nih.gov/pubmed/16902930> [Accessed November 30, 2015].
- Jastrzebska, B., 2013. GPCR: G protein complexes--the fundamental signaling assembly. *Amino acids*, 45(6), pp.1303–14. Available at: <http://www.pubmedcentral.nih.gov/articlerender.fcgi?artid=3845202&tool=pmcentrez&rendertype=abstract> [Accessed January 20, 2016].
- Jia, M. et al., 2012. Crystal structures of the scaffolding protein LGN reveal the general mechanism by which GoLoco binding motifs inhibit the release of GDP from Gai. *The Journal of biological chemistry*, 287(44), pp.36766–76. Available at: <http://www.pubmedcentral.nih.gov/articlerender.fcgi?artid=3481280&tool=pmcentrez&rendertype=abstract> [Accessed June 5, 2016].
- Johnston, C.A. et al., 2009. Identification of an Aurora-A/PinsLINKER/Dlg spindle orientation pathway using induced cell polarity in S2 cells. *Cell*, 138(6), pp.1150–63. Available at: <http://www.pubmedcentral.nih.gov/articlerender.fcgi?artid=2789599&tool=pmcentrez&rendertype=abstract> [Accessed January 20, 2016].
- Kamakura, S. et al., 2013. The cell polarity protein mInsc regulates neutrophil chemotaxis via a noncanonical G protein signaling pathway. *Developmental cell*, 26(3), pp.292–302. Available at: <http://www.ncbi.nlm.nih.gov/pubmed/23891662> [Accessed October 18, 2016].
- Kaushik, R. et al., 2003. Subcellular localization of LGN during mitosis: evidence for its cortical localization in mitotic cell culture systems and its requirement for normal cell cycle progression. *Molecular biology of the cell*, 14(8), pp.3144–55. Available at: <http://www.ncbi.nlm.nih.gov/pubmed/12925752> [Accessed October 17, 2016].
- Kaye, R.G. et al., 2011. Helix 8 of the M1 muscarinic acetylcholine receptor: scanning mutagenesis delineates a G protein recognition site. *Molecular pharmacology*, 79(4), pp.701–9. Available at: <http://www.ncbi.nlm.nih.gov/pubmed/21247934> [Accessed November 14, 2016].
- Keegan, K. et al., 1991. Isolation of an additional member of the fibroblast growth factor receptor family, FGFR-3. *Proceedings of the National Academy of Sciences of the United States of America*, 88(4), pp.1095–9. Available at: <http://www.ncbi.nlm.nih.gov/pubmed/1847508> [Accessed June 16, 2016].
- Khafizov, K., 2009. GoLoco motif proteins binding to Galpha(i1): insights from molecular simulations. *Journal of molecular modeling*, 15(12), pp.1491–9. Available at: <http://www.pubmedcentral.nih.gov/articlerender.fcgi?artid=2847169&tool=pmcentrez&rendertype=abstract> [Accessed January 20, 2016].

- Kimble, R.J. et al., 2004. Guanine nucleotide dissociation inhibitor activity of the triple GoLoco motif protein G18: alanine-to-aspartate mutation restores function to an inactive second GoLoco motif. *The Biochemical journal*, 378(Pt 3), pp.801–8. Available at: <http://www.pubmedcentral.nih.gov/articlerender.fcgi?artid=1224015&tool=pmcentrez&rendertype=abstract> [Accessed January 20, 2016].
- Kimble, R.J., Kimble, M.E., et al., 2002. Structural determinants for GoLoco-induced inhibition of nucleotide release by Galpha subunits. *Nature*, 416(6883), pp.878–81. Available at: <http://www.ncbi.nlm.nih.gov/pubmed/11976690> [Accessed January 20, 2016].
- Kimble, R.J., Willard, F.S. & Siderovski, D.P., 2002. The GoLoco motif: heralding a new tango between G protein signaling and cell division. *Molecular interventions*, 2(2), pp.88–100. Available at: <http://www.ncbi.nlm.nih.gov/pubmed/14993354> [Accessed January 20, 2016].
- Kinoshita-Kawada, M., Oberdick, J. & Xi Zhu, M., 2004. A Purkinje cell specific GoLoco domain protein, L7/Pcp-2, modulates receptor-mediated inhibition of Cav2.1 Ca²⁺ channels in a dose-dependent manner. *Brain research. Molecular brain research*, 132(1), pp.73–86. Available at: <http://www.ncbi.nlm.nih.gov/pubmed/15548431> [Accessed May 4, 2016].
- Kleuss, C. et al., 1992. Different β -subunits determine G-protein interaction with transmembrane receptors. *Nature*, 358(6385), pp.424–426. Available at: <http://www.nature.com/doifinder/10.1038/358424a0> [Accessed November 15, 2016].
- Kleuss, C. et al., 1994. Mechanism of GTP hydrolysis by G-protein alpha subunits. *Proceedings of the National Academy of Sciences of the United States of America*, 91(21), pp.9828–31. Available at: <http://www.ncbi.nlm.nih.gov/pubmed/7937899> [Accessed November 13, 2016].
- Kleuss, C. et al., 1993. Selectivity in signal transduction determined by gamma subunits of heterotrimeric G proteins. *Science (New York, N.Y.)*, 259(5096), pp.832–4. Available at: <http://www.ncbi.nlm.nih.gov/pubmed/8094261> [Accessed November 15, 2016].
- Kobilka, B.K., 2007. G protein coupled receptor structure and activation. *Biochimica et biophysica acta*, 1768(4), pp.794–807. Available at: <http://www.ncbi.nlm.nih.gov/pubmed/17188232> [Accessed October 17, 2016].
- Kost, C.K. et al., 1999. Pertussis toxin-sensitive G-proteins and regulation of blood pressure in the spontaneously hypertensive rat. *Clinical and experimental pharmacology & physiology*, 26(5–6), pp.449–55. Available at: <http://www.ncbi.nlm.nih.gov/pubmed/10386237> [Accessed June 6, 2016].

- Kroll, S.D. et al., 1992. The Q205LGo-alpha subunit expressed in NIH-3T3 cells induces transformation. *The Journal of biological chemistry*, 267(32), pp.23183–8. Available at: <http://www.ncbi.nlm.nih.gov/pubmed/1429665> [Accessed November 13, 2016].
- Lambert, N.A. et al., 2010. Regulators of G-protein signaling accelerate GPCR signaling kinetics and govern sensitivity solely by accelerating GTPase activity. *Proceedings of the National Academy of Sciences of the United States of America*, 107(15), pp.7066–71. Available at: <http://www.pubmedcentral.nih.gov/articlerender.fcgi?artid=2872438&tool=pmcentrez&rendertype=abstract> [Accessed April 28, 2016].
- Lambright, D.G. et al., 1994. Structural determinants for activation of the alpha-subunit of a heterotrimeric G protein. *Nature*, 369(6482), pp.621–8. Available at: <http://www.ncbi.nlm.nih.gov/pubmed/8208289> [Accessed February 19, 2016].
- Lapan, P. et al., 2009. Image-based assessment of growth and signaling changes in cancer cells mediated by direct cell-cell contact. *PloS one*, 4(8), p.e6822. Available at: <http://www.ncbi.nlm.nih.gov/pubmed/19774227> [Accessed June 14, 2016].
- Lehner, B. et al., 2004. Analysis of a high-throughput yeast two-hybrid system and its use to predict the function of intracellular proteins encoded within the human MHC class III region. *Genomics*, 83(1), pp.153–67. Available at: <http://www.ncbi.nlm.nih.gov/pubmed/14667819> [Accessed February 15, 2016].
- Lenarczyk, M. et al., 2015. Localization and expression profile of Group I and II Activators of G-protein Signaling in the kidney. *Journal of molecular histology*, 46(2), pp.123–36. Available at: <http://www.ncbi.nlm.nih.gov/pubmed/25533045> [Accessed January 20, 2016].
- Lenk, G.M. et al., 2007. Whole genome expression profiling reveals a significant role for immune function in human abdominal aortic aneurysms. *BMC Genomics*, 8(1), p.237. Available at: <http://bmcbgenomics.biomedcentral.com/articles/10.1186/1471-2164-8-237> [Accessed November 5, 2016].
- Leung, S.B. et al., 2016. Attenuation of blood pressure in spontaneously hypertensive rats by acupuncture was associated with reduction oxidative stress and improvement from endothelial dysfunction. *Chinese Medicine*, 11(1), p.38. Available at: <http://cmjournal.biomedcentral.com/articles/10.1186/s13020-016-0110-0> [Accessed November 3, 2016].
- Li, X. et al., 2013. Biolistic transfection of human embryonic kidney (HEK) 293 cells. *Methods in molecular biology (Clifton, N.J.)*, 940, pp.119–32. Available at: <http://www.ncbi.nlm.nih.gov/pubmed/23104338> [Accessed May 30, 2016].
- Li, Y. & Anand-Srivastava, M.B., 2002. Inactivation of enhanced expression of G(i) proteins by pertussis toxin attenuates the development of high blood pressure in

- spontaneously hypertensive rats. *Circulation research*, 91(3), pp.247–54. Available at: <http://www.ncbi.nlm.nih.gov/pubmed/12169651> [Accessed June 6, 2016].
- Lievens, S., Lemmens, I. & Tavernier, J., 2009. Mammalian two-hybrids come of age. *Trends in Biochemical Sciences*, 34(11), pp.579–588. Available at: <http://linkinghub.elsevier.com/retrieve/pii/S0968000409001583> [Accessed November 14, 2016].
- Liu, W. & Northup, J.K., 1998. The helical domain of a G protein alpha subunit is a regulator of its effector. *Proceedings of the National Academy of Sciences of the United States of America*, 95(22), pp.12878–83. Available at: <http://www.pubmedcentral.nih.gov/articlerender.fcgi?artid=23639&tool=pmcentrez&rendertype=abstract> [Accessed May 28, 2016].
- Lu, M.S., Mauser, J.F. & Prehoda, K.E., 2012. Ultrasensitive synthetic protein regulatory networks using mixed decoys. *ACS synthetic biology*, 1(2), pp.65–72. Available at: <http://www.pubmedcentral.nih.gov/articlerender.fcgi?artid=3358930&tool=pmcentrez&rendertype=abstract> [Accessed January 20, 2016].
- Luan, S.-L. et al., 2010. Primary effusion lymphoma: genomic profiling revealed amplification of SELPLG and CORO1C encoding for proteins important for cell migration. *The Journal of Pathology*, 222(2), pp.166–179. Available at: <http://doi.wiley.com/10.1002/path.2752> [Accessed November 14, 2016].
- Mapelli, M. & Gonzalez, C., 2012. On the inscrutable role of Inscuteable: structural basis and functional implications for the competitive binding of NuMA and Inscuteable to LGN. *Open biology*, 2(8), p.120102. Available at: <http://www.pubmedcentral.nih.gov/articlerender.fcgi?artid=3438535&tool=pmcentrez&rendertype=abstract> [Accessed January 20, 2016].
- Matsumoto, T. et al., 2008. Ninein is expressed in the cytoplasm of angiogenic tip-cells and regulates tubular morphogenesis of endothelial cells. *Arteriosclerosis, thrombosis, and vascular biology*, 28(12), pp.2123–30. Available at: <http://www.ncbi.nlm.nih.gov/pubmed/18772498> [Accessed October 18, 2016].
- McIntire, W.E., 2009. Structural determinants involved in the formation and activation of G protein betagamma dimers. *Neuro-Signals*, 17(1), pp.82–99. Available at: <http://www.pubmedcentral.nih.gov/articlerender.fcgi?artid=2836951&tool=pmcentrez&rendertype=abstract> [Accessed February 21, 2016].
- Merdes, A. et al., 2000. Formation of spindle poles by dynein/dynactin-dependent transport of NuMA. *The Journal of cell biology*, 149(4), pp.851–62. Available at: <http://www.ncbi.nlm.nih.gov/pubmed/10811826> [Accessed June 11, 2016].
- Miller, K.G. & Rand, J.B., 2000. A role for RIC-8 (Synembryn) and GOA-1 (G(o)alpha) in regulating a subset of centrosome movements during early embryogenesis in

- Caenorhabditis elegans. *Genetics*, 156(4), pp.1649–60. Available at: <http://www.ncbi.nlm.nih.gov/pubmed/11102364> [Accessed June 7, 2016].
- miRAD, 2016. Gene | GPSM3. Available at: https://www.bioinfo.mochsl.org.br/miriad/gene/GPSM3/?pi_table_page=4 [Accessed January 1, 2016].
- Mittal, V. & Linder, M.E., 2006. Biochemical characterization of RGS14: RGS14 activity towards G-protein alpha subunits is independent of its binding to Rap2A. *The Biochemical journal*, 394(Pt 1), pp.309–15. Available at: <http://www.pubmedcentral.nih.gov/articlerender.fcgi?artid=1386029&tool=pmcentrez&rendertype=abstract> [Accessed June 1, 2016].
- Mixon, M.B. et al., 1995. Tertiary and quaternary structural changes in Gi alpha 1 induced by GTP hydrolysis. *Science (New York, N.Y.)*, 270(5238), pp.954–60. Available at: <http://www.ncbi.nlm.nih.gov/pubmed/7481799> [Accessed February 27, 2016].
- Mogensen, M.M. et al., 2000. Microtubule minus-end anchorage at centrosomal and non-centrosomal sites: the role of ninein. *Journal of cell science*, pp.3013–23. Available at: <http://www.ncbi.nlm.nih.gov/pubmed/10934040> [Accessed November 10, 2016].
- Mukhopadhyay, S. & Ross, E.M., 1999. Rapid GTP binding and hydrolysis by G(q) promoted by receptor and GTPase-activating proteins. *Proceedings of the National Academy of Sciences of the United States of America*, 96(17), pp.9539–44. Available at: <http://www.pubmedcentral.nih.gov/articlerender.fcgi?artid=22244&tool=pmcentrez&rendertype=abstract> [Accessed February 6, 2016].
- Natochin, M. & Artemyev, N.O., 2000. Mutational analysis of functional interfaces of transducin. *Methods in enzymology*, 315, pp.539–54. Available at: <http://www.ncbi.nlm.nih.gov/pubmed/10736725> [Accessed June 2, 2016].
- Nebi, T. et al., 2002. Proteomic analysis of a detergent-resistant membrane skeleton from neutrophil plasma membranes. *The Journal of biological chemistry*, 277(45), pp.43399–409. Available at: <http://www.ncbi.nlm.nih.gov/pubmed/12202484> [Accessed June 12, 2016].
- Neves, S.R., Ram, P.T. & Iyengar, R., 2002. G protein pathways. *Science (New York, N.Y.)*, 296(5573), pp.1636–9. Available at: <http://www.ncbi.nlm.nih.gov/pubmed/12040175> [Accessed January 20, 2016].
- Noel, J.P., Hamm, H.E. & Sigler, P.B., 1993. The 2.2 Å crystal structure of transducin-alpha complexed with GTP gamma S. *Nature*, 366(6456), pp.654–63. Available at: <http://www.ncbi.nlm.nih.gov/pubmed/8259210> [Accessed May 31, 2016].
- Oldham, W.M. & Hamm, H.E., 2006. Structural basis of function in heterotrimeric G proteins. *Quarterly reviews of biophysics*, 39(2), pp.117–66. Available at:

- <http://www.ncbi.nlm.nih.gov/pubmed/16923326> [Accessed May 31, 2016].
- Oner, S.S., Maher, E.M., et al., 2010. Receptor-regulated interaction of activator of G-protein signaling-4 and Galphai. *The Journal of biological chemistry*, 285(27), pp.20588–94. Available at: <http://www.pubmedcentral.nih.gov/articlerender.fcgi?artid=2898320&tool=pmcentrez&rendertype=abstract> [Accessed January 20, 2016].
- Oner, S.S., An, N., et al., 2010. Regulation of the AGS3·G α i signaling complex by a seven-transmembrane span receptor. *The Journal of biological chemistry*, 285(44), pp.33949–58. Available at: <http://www.pubmedcentral.nih.gov/articlerender.fcgi?artid=2962495&tool=pmcentrez&rendertype=abstract> [Accessed June 2, 2016].
- Oner, S.S. et al., 2013. Regulation of the G-protein regulatory-G α i signaling complex by nonreceptor guanine nucleotide exchange factors. *The Journal of biological chemistry*, 288(5), pp.3003–15. Available at: <http://www.pubmedcentral.nih.gov/articlerender.fcgi?artid=3561525&tool=pmcentrez&rendertype=abstract> [Accessed January 20, 2016].
- Overington, J.P., Al-Lazikani, B. & Hopkins, A.L., 2006. How many drug targets are there? *Nature reviews. Drug discovery*, 5(12), pp.993–6. Available at: <http://www.ncbi.nlm.nih.gov/pubmed/17139284> [Accessed November 4, 2014].
- Pathan, S. et al., 2009. Confirmation of the novel association at the BTNL2 locus with ulcerative colitis. *Tissue antigens*, 74(4), pp.322–9. Available at: <http://www.ncbi.nlm.nih.gov/pubmed/19659809> [Accessed May 28, 2016].
- Pattingre, S. et al., 2003. The G-protein regulator AGS3 controls an early event during macroautophagy in human intestinal HT-29 cells. *The Journal of biological chemistry*, 278(23), pp.20995–1002. Available at: <http://www.ncbi.nlm.nih.gov/pubmed/12642577> [Accessed June 6, 2016].
- Peterson, Y.K. et al., 2002. Identification of structural features in the G-protein regulatory motif required for regulation of heterotrimeric G-proteins. *The Journal of biological chemistry*, 277(9), pp.6767–70. Available at: <http://www.ncbi.nlm.nih.gov/pubmed/11756403> [Accessed January 20, 2016].
- Peterson, Y.K. et al., 2000. Stabilization of the GDP-bound Conformation of Gi by a Peptide Derived from the G-protein Regulatory Motif of AGS3. *Journal of Biological Chemistry*, 275(43), pp.33193–33196. Available at: <http://www.ncbi.nlm.nih.gov/pubmed/10969064> [Accessed January 8, 2016].
- Pizzinat, N., Takesono, A. & Lanier, S.M., 2001. Identification of a truncated form of the G-protein regulator AGS3 in heart that lacks the tetratricopeptide repeat domains. *The Journal of biological chemistry*, 276(20), pp.16601–10. Available at:

- <http://www.ncbi.nlm.nih.gov/pubmed/11278352> [Accessed January 20, 2016].
- Popov, S.G. et al., 2000. Ca²⁺/Calmodulin reverses phosphatidylinositol 3,4, 5-trisphosphate-dependent inhibition of regulators of G protein-signaling GTPase-activating protein activity. *The Journal of biological chemistry*, 275(25), pp.18962–8. Available at: <http://www.ncbi.nlm.nih.gov/pubmed/10747990> [Accessed May 31, 2016].
- Preininger, A.M. & Hamm, H.E., 2004. G protein signaling: insights from new structures. *Science's STKE : signal transduction knowledge environment*, 2004(218), p.re3. Available at: <http://www.ncbi.nlm.nih.gov/pubmed/14762218> [Accessed May 28, 2016].
- Purcell, E.S. & Gattone, V.H., 1992. Immune system of the spontaneously hypertensive rat. I. Sympathetic innervation. *Experimental neurology*, 117(1), pp.44–50. Available at: <http://www.ncbi.nlm.nih.gov/pubmed/1618286> [Accessed November 3, 2016].
- Rhee, S.G. & Bae, Y.S., 1997. Regulation of phosphoinositide-specific phospholipase C isozymes. *The Journal of biological chemistry*, 272(24), pp.15045–8. Available at: <http://www.ncbi.nlm.nih.gov/pubmed/9182519> [Accessed January 20, 2016].
- Riss, T., 2006. Is Your MTT Assay Really the Best Choice. *Scientific Style and Format, 7th edition*. Available at: <https://www.promega.ca/resources/pubhub/is-your-mtt-assay-really-the-best-choice/>.
- Robichaux, W.G. et al., 2015. Direct Coupling of a Seven-Transmembrane-Span Receptor to a Gai G-Protein Regulatory Motif Complex. *Molecular pharmacology*, 88(2), pp.231–7. Available at: <http://www.ncbi.nlm.nih.gov/pubmed/25972449> [Accessed January 20, 2016].
- Ross, E.M. & Wilkie, T.M., 2000. GTPase-activating proteins for heterotrimeric G proteins: regulators of G protein signaling (RGS) and RGS-like proteins. *Annual review of biochemistry*, 69, pp.795–827. Available at: <http://www.ncbi.nlm.nih.gov/pubmed/10966476> [Accessed April 20, 2016].
- Sanada, K. & Tsai, L.-H., 2005. G protein betagamma subunits and AGS3 control spindle orientation and asymmetric cell fate of cerebral cortical progenitors. *Cell*, 122(1), pp.119–31. Available at: <http://www.ncbi.nlm.nih.gov/pubmed/16009138> [Accessed June 7, 2016].
- Sandison, M.E., Dempster, J. & McCarron, J.G., 2016. The transition of smooth muscle cells from a contractile to a migratory, phagocytic phenotype: direct demonstration of phenotypic modulation. *The Journal of Physiology*, 594(21), pp.6189–6209. Available at: <http://doi.wiley.com/10.1113/JP272729> [Accessed November 2, 2016].
- Sato, M. & Ishikawa, Y., 2010. Accessory proteins for heterotrimeric G-protein: Implication

- in the cardiovascular system. *Pathophysiology : the official journal of the International Society for Pathophysiology / ISP*, 17(2), pp.89–99. Available at: <http://www.ncbi.nlm.nih.gov/pubmed/19501489> [Accessed June 6, 2016].
- Schneider, S.Q. & Bowerman, B., 2003a. Cell polarity and the cytoskeleton in the *Caenorhabditis elegans* zygote. *Annual review of genetics*, 37, pp.221–49. Available at: <http://www.ncbi.nlm.nih.gov/pubmed/14616061> [Accessed June 10, 2016].
- Schneider, S.Q. & Bowerman, B., 2003b. Cell polarity and the cytoskeleton in the *Caenorhabditis elegans* zygote. *Annual review of genetics*, 37, pp.221–49. Available at: <http://www.ncbi.nlm.nih.gov/pubmed/14616061> [Accessed June 9, 2016].
- Scott, J.K. et al., 2001. Evidence that a protein-protein interaction “hot spot” on heterotrimeric G protein betagamma subunits is used for recognition of a subclass of effectors. *The EMBO journal*, 20(4), pp.767–76. Available at: <http://www.pubmedcentral.nih.gov/articlerender.fcgi?artid=145424&tool=pmcentrez&rendertype=abstract> [Accessed January 20, 2016].
- Shankland, S.J. et al., 1996. Changes in cell-cycle protein expression during experimental mesangial proliferative glomerulonephritis. *Kidney international*, 50(4), pp.1230–9. Available at: <http://www.ncbi.nlm.nih.gov/pubmed/8887282> [Accessed November 13, 2016].
- Shu, F. et al., 2007. Selective interactions between Gi alpha1 and Gi alpha3 and the GoLoco/GPR domain of RGS14 influence its dynamic subcellular localization. *Cellular signalling*, 19(1), pp.163–76. Available at: <http://www.ncbi.nlm.nih.gov/pubmed/16870394> [Accessed June 11, 2016].
- Siderovski, D.P., Diversé-Pierluissi, M. a & De Vries, L., 1999. The GoLoco motif: a Galphai/o binding motif and potential guanine-nucleotide exchange factor. *Trends in biochemical sciences*, 24(9), pp.340–1. Available at: <http://www.ncbi.nlm.nih.gov/pubmed/10470031> [Accessed January 20, 2016].
- Siderovski, D.P. & Willard, F.S., 2005. The GAPs, GEFs, and GDIs of heterotrimeric G-protein alpha subunits. *International journal of biological sciences*, 1(2), pp.51–66. Available at: <http://www.pubmedcentral.nih.gov/articlerender.fcgi?artid=1142213&tool=pmcentrez&rendertype=abstract> [Accessed January 8, 2016].
- Sirota, M. et al., 2009. Autoimmune disease classification by inverse association with SNP alleles. *PLoS genetics*, 5(12), p.e1000792. Available at: <http://www.pubmedcentral.nih.gov/articlerender.fcgi?artid=2791168&tool=pmcentrez&rendertype=abstract> [Accessed January 20, 2016].
- Smith, N.R. & Prehoda, K.E., 2011. Robust spindle alignment in *Drosophila* neuroblasts by ultrasensitive activation of pins. *Molecular cell*, 43(4), pp.540–9. Available at: <http://www.pubmedcentral.nih.gov/articlerender.fcgi?artid=3161515&tool=pmcentrez&rendertype=abstract>

ez&rendertype=abstract [Accessed January 20, 2016].

Smrcka, A. V., 2008. G protein $\beta\gamma$ subunits: central mediators of G protein-coupled receptor signaling. *Cellular and molecular life sciences : CMLS*, 65(14), pp.2191–214. Available at:

<http://www.pubmedcentral.nih.gov/articlerender.fcgi?artid=2688713&tool=pmcentrez&rendertype=abstract> [Accessed January 4, 2016].

Snapp, E., 2005. Design and use of fluorescent fusion proteins in cell biology. *Current protocols in cell biology*, Chapter 21, p.Unit 21.4. Available at:

<http://www.ncbi.nlm.nih.gov/pubmed/18228466> [Accessed November 14, 2016].

Sondek, J. et al., 1994. GTPase mechanism of Gproteins from the 1.7-A crystal structure of transducin alpha-GDP-AIF-4. *Nature*, 372(6503), pp.276–9. Available at:

<http://www.ncbi.nlm.nih.gov/pubmed/7969474> [Accessed May 31, 2016].

Srinivasan, D.G. et al., 2003. A complex of LIN-5 and GPR proteins regulates G protein signaling and spindle function in *C elegans*. *Genes & development*, 17(10), pp.1225–39. Available at: <http://www.ncbi.nlm.nih.gov/pubmed/12730122> [Accessed June 7, 2016].

Sun, D.-S., Ho, P.-H. & Chang, H.-H., 2016. Soluble P-selectin rescues viper venom-induced mortality through anti-inflammatory properties and PSGL-1 pathway-mediated correction of hemostasis. *Scientific Reports*, 6, p.35868. Available at:

<http://www.nature.com/articles/srep35868> [Accessed November 14, 2016].

Sun, L. et al., 2006. Inflammation of different tissues in spontaneously hypertensive rats.

Sheng li xue bao : [Acta physiologica Sinica], 58(4), pp.318–23. Available at:

<http://www.ncbi.nlm.nih.gov/pubmed/16906331> [Accessed December 15, 2016].

Swirski, F.K. et al., 2009. Identification of splenic reservoir monocytes and their deployment to inflammatory sites. *Science (New York, N.Y.)*, 325(5940), pp.612–6.

Available at: <http://www.ncbi.nlm.nih.gov/pubmed/19644120> [Accessed December 15, 2016].

Szklarczyk, D. et al., 2015. STRING v10: protein-protein interaction networks, integrated over the tree of life. *Nucleic Acids Research*, 43(D1), pp.D447–D452. Available at:

<http://nar.oxfordjournals.org/lookup/doi/10.1093/nar/gku1003> [Accessed November 14, 2016].

Takesono, A. et al., 1999. Receptor-independent activators of heterotrimeric G-protein signaling pathways. *The Journal of biological chemistry*, 274(47), pp.33202–5.

Available at: <http://www.ncbi.nlm.nih.gov/pubmed/10559191> [Accessed March 4, 2016].

Tall, G.G., 2013. Ric-8 regulation of heterotrimeric G proteins. *Journal of receptor and signal*

- transduction research*, 33(3), pp.139–43. Available at: <http://www.pubmedcentral.nih.gov/articlerender.fcgi?artid=3870196&tool=pmcentrez&rendertype=abstract> [Accessed January 21, 2016].
- Tall, G.G. & Gilman, A.G., 2005. Resistance to inhibitors of cholinesterase 8A catalyzes release of Galphai-GTP and nuclear mitotic apparatus protein (NuMA) from NuMA/LGN/Galphai-GDP complexes. *Proceedings of the National Academy of Sciences of the United States of America*, 102(46), pp.16584–9. Available at: <http://www.pubmedcentral.nih.gov/articlerender.fcgi?artid=1283842&tool=pmcentrez&rendertype=abstract> [Accessed January 20, 2016].
- Taymans, J.-M., Kia, H.K. & Langlois, X., 2006. Activator of G protein signaling type 3 mRNA is widely distributed in the rat brain and is particularly abundant in the subventricular zone-olfactory bulb system of neural precursor cell proliferation, migration and differentiation. *Neuroscience Letters*, 391(3), pp.116–121. Available at: <http://linkinghub.elsevier.com/retrieve/pii/S0304394005009754> [Accessed November 2, 2016].
- Thomas, C.J. et al., 2008. Ric-8A catalyzes guanine nucleotide exchange on G alpha1 bound to the GPR/GoLoco exchange inhibitor AGS3. *The Journal of biological chemistry*, 283(34), pp.23150–60. Available at: <http://www.pubmedcentral.nih.gov/articlerender.fcgi?artid=2516996&tool=pmcentrez&rendertype=abstract> [Accessed January 20, 2016].
- Tompkins, J.D. et al., 2012. Epigenetic stability, adaptability, and reversibility in human embryonic stem cells. *Proceedings of the National Academy of Sciences of the United States of America*, 109(31), pp.12544–9. Available at: <http://www.pubmedcentral.nih.gov/articlerender.fcgi?artid=3411986&tool=pmcentrez&rendertype=abstract> [Accessed May 2, 2016].
- Tregouet, D.A. et al., 2003. SELPLG gene polymorphisms in relation to plasma SELPLG levels and coronary artery disease. *Annals of human genetics*, 67(Pt 6), pp.504–11. Available at: <http://www.ncbi.nlm.nih.gov/pubmed/14641238> [Accessed November 11, 2016].
- Trzaskowski, B. et al., 2012. Action of molecular switches in GPCRs--theoretical and experimental studies. *Current medicinal chemistry*, 19(8), pp.1090–109. Available at: <http://www.pubmedcentral.nih.gov/articlerender.fcgi?artid=3343417&tool=pmcentrez&rendertype=abstract> [Accessed September 23, 2015].
- Tse, M.K. et al., 2015. Activator of G protein signaling 3 forms a complex with resistance to inhibitors of cholinesterase-8A without promoting nucleotide exchange on Gai3. *Molecular and Cellular Biochemistry*, 401(1–2), pp.27–38. Available at: <http://link.springer.com/10.1007/s11010-014-2289-7> [Accessed November 2, 2016].
- Volcik, K.A. et al., 2009. SELP and SELPLG Genetic Variation Is Associated with Cell Surface

- Measures of SELP and SELPLG: The Atherosclerosis Risk in Communities Carotid MRI Study. *Clinical Chemistry*, 55(6), pp.1076–1082. Available at: <http://www.clinchem.org/cgi/doi/10.1373/clinchem.2008.119487> [Accessed November 11, 2016].
- Wang, J. et al., 2009. Evidence for a second, high affinity Gbetagamma binding site on Galphai1(GDP) subunits. *The Journal of biological chemistry*, 284(25), pp.16906–13. Available at: <http://www.pubmedcentral.nih.gov/articlerender.fcgi?artid=2719327&tool=pmcentrez&rendertype=abstract> [Accessed January 20, 2016].
- Warner, D.R. et al., 1998. A novel mutation in the switch 3 region of Gsalph in a patient with Albright hereditary osteodystrophy impairs GDP binding and receptor activation. *The Journal of biological chemistry*, 273(37), pp.23976–83. Available at: <http://www.ncbi.nlm.nih.gov/pubmed/9727013> [Accessed May 31, 2016].
- Webb, C.K. et al., 2005. D2 dopamine receptor activation of potassium channels is selectively decoupled by Galpha-specific GoLoco motif peptides. *Journal of neurochemistry*, 92(6), pp.1408–18. Available at: <http://www.ncbi.nlm.nih.gov/pubmed/15748159> [Accessed June 1, 2016].
- Weinstein, L.S. et al., 2004. Minireview: GNAS: normal and abnormal functions. *Endocrinology*, 145(12), pp.5459–64. Available at: <http://www.ncbi.nlm.nih.gov/pubmed/15331575> [Accessed March 16, 2016].
- Whitfield, M.L. et al., 2002. Identification of genes periodically expressed in the human cell cycle and their expression in tumors. *Molecular biology of the cell*, 13(6), pp.1977–2000. Available at: <http://www.pubmedcentral.nih.gov/articlerender.fcgi?artid=117619&tool=pmcentrez&rendertype=abstract> [Accessed March 4, 2016].
- Willard, F.S. et al., 2008. A point mutation to Galphai selectively blocks GoLoco motif binding: direct evidence for Galpha.GoLoco complexes in mitotic spindle dynamics. *The Journal of biological chemistry*, 283(52), pp.36698–710. Available at: <http://www.pubmedcentral.nih.gov/articlerender.fcgi?artid=2605979&tool=pmcentrez&rendertype=abstract> [Accessed January 20, 2016].
- Willard, F.S. et al., 2007. Differential G-alpha interaction capacities of the GoLoco motifs in Rap GTPase activating proteins. *Cellular signalling*, 19(2), pp.428–38. Available at: <http://www.ncbi.nlm.nih.gov/pubmed/16949794> [Accessed May 4, 2016].
- Willard, F.S., Kimple, R.J. & Siderovski, D.P., 2004. Return of the GDI: the GoLoco motif in cell division. *Annual review of biochemistry*, 73, pp.925–51. Available at: <http://www.ncbi.nlm.nih.gov/pubmed/15189163> [Accessed January 21, 2016].
- Willard, F.S., McCudden, C.R. & Siderovski, D.P., 2006. G-protein alpha subunit interaction

- and guanine nucleotide dissociation inhibitor activity of the dual GoLoco motif protein PCP-2 (Purkinje cell protein-2). *Cellular signalling*, 18(8), pp.1226–34. Available at: <http://www.ncbi.nlm.nih.gov/pubmed/16298104> [Accessed May 4, 2016].
- Windh, R.T. & Manning, D.R., 2002. Analysis of G protein activation in Sf9 and mammalian cells by agonist-promoted [³⁵S]GTP gamma S binding. *Methods in enzymology*, 344, pp.3–14. Available at: <http://www.ncbi.nlm.nih.gov/pubmed/11771391> [Accessed May 31, 2016].
- Wiser, O. et al., 2006. Modulation of basal and receptor-induced GIRK potassium channel activity and neuronal excitability by the mammalian PINS homolog LGN. *Neuron*, 50(4), pp.561–73. Available at: <http://www.ncbi.nlm.nih.gov/pubmed/16701207> [Accessed January 20, 2016].
- Wu, H.C., Huang, P.H. & Lin, C.T., 1998. G protein beta subunit is closely associated with microtubules. *Journal of cellular biochemistry*, 70(4), pp.553–62. Available at: <http://www.ncbi.nlm.nih.gov/pubmed/9712152> [Accessed November 13, 2016].
- Wu, H.C. & Lin, C.T., 1994. Association of heterotrimeric GTP binding regulatory protein (Go) with mitosis. *Laboratory investigation; a journal of technical methods and pathology*, 71(2), pp.175–81. Available at: <http://www.ncbi.nlm.nih.gov/pubmed/8078296> [Accessed October 17, 2016].
- Xie, L. et al., 2012. A synthetic interaction screen identifies factors selectively required for proliferation and TERT transcription in p53-deficient human cancer cells. *PLoS genetics*, 8(12), p.e1003151. Available at: <http://www.pubmedcentral.nih.gov/articlerender.fcgi?artid=3527276&tool=pmcentrez&rendertype=abstract> [Accessed February 16, 2016].
- Yang, K., Hitomi, M. & Stacey, D.W., 2006. Variations in cyclin D1 levels through the cell cycle determine the proliferative fate of a cell. *Cell division*, 1, p.32. Available at: <http://www.ncbi.nlm.nih.gov/pubmed/17176475> [Accessed November 13, 2016].
- Zetterberg, A. & Sköld, O., 1969. The effect of serum starvation on DNA, RNA and protein synthesis during interphase in L-cells. *Experimental cell research*, 57(1), pp.114–8. Available at: <http://www.ncbi.nlm.nih.gov/pubmed/5810923> [Accessed January 20, 2016].
- Zhao, P. et al., 2013. Fine-tuning of GPCR signals by intracellular G protein modulators. *Progress in molecular biology and translational science*, 115, pp.421–53. Available at: <http://www.ncbi.nlm.nih.gov/pubmed/23415100> [Accessed January 20, 2016].
- Zhao, P., 2011. *Regulation of G Protein Signaling by GoLoco Motif Containing Proteins*. The University of Western Ontario. Available at: <http://ir.lib.uwo.ca/etd/218>.
- Zhao, P. & Chidiac, P., 2015. Regulation of RGS5 GAP activity by GPSM3. *Molecular and*

cellular biochemistry, 405(1–2), pp.33–40. Available at:
<http://www.ncbi.nlm.nih.gov/pubmed/25842189> [Accessed January 20, 2016].

Zhao, P., Nguyen, C.H. & Chidiac, P., 2010. The proline-rich N-terminal domain of G18 exhibits a novel G protein regulatory function. *The Journal of biological chemistry*, 285(12), pp.9008–17. Available at:
<http://www.pubmedcentral.nih.gov/articlerender.fcgi?artid=2838322&tool=pmcentrez&rendertype=abstract> [Accessed January 20, 2016].

Zheng, N. et al., 2016. Effects of ADMA on gene expression and metabolism in serum-starved LoVo cells. *Scientific Reports*, 6, p.25892. Available at:
<http://www.nature.com/articles/srep25892> [Accessed November 14, 2016].

Zhong, H. et al., 2003. A spatial focusing model for G protein signals. Regulator of G protein signaling (RGS) protein-mediated kinetic scaffolding. *The Journal of biological chemistry*, 278(9), pp.7278–84. Available at:
<http://www.ncbi.nlm.nih.gov/pubmed/12446706> [Accessed May 31, 2016].

Zwaal, R.R. et al., 1996. G proteins are required for spatial orientation of early cell cleavages in *C. elegans* embryos. *Cell*, 86(4), pp.619–29. Available at:
<http://www.ncbi.nlm.nih.gov/pubmed/8752216> [Accessed January 20, 2016].

6 APPENDIX 1

5.1 SUPPLEMENTAL FIGURES

Localization of GPSM3 during mitosis was first investigated by transfecting HEK-293 cells with EYFP-tagged GPSM3 plasmid and labeling β -tubulin using anti- β -tubulin primary antibody and AlexaFluor 555 goat anti-rabbit secondary antibody (Figure 5.1). During metaphase, EYFP-GPSM3 and β -tubulin appear to co-localize. However, it was difficult to resolve how specific this co-localization was. Additionally, capturing cells undergoing mitosis was difficult using this protocol as cells first needed to be transfected and allowed to recover before having their cell cycles synced via removal and re-addition of serum-containing medium. For these reasons, successive experiments labeled endogenous GPSM3 using an anti-GPSM3 primary antibody and AlexaFluor 488 goat anti-rabbit secondary antibody. β -tubulin was stained using anti- β -tubulin primary antibody and AlexaFluor 568 goat anti-mouse secondary antibody.

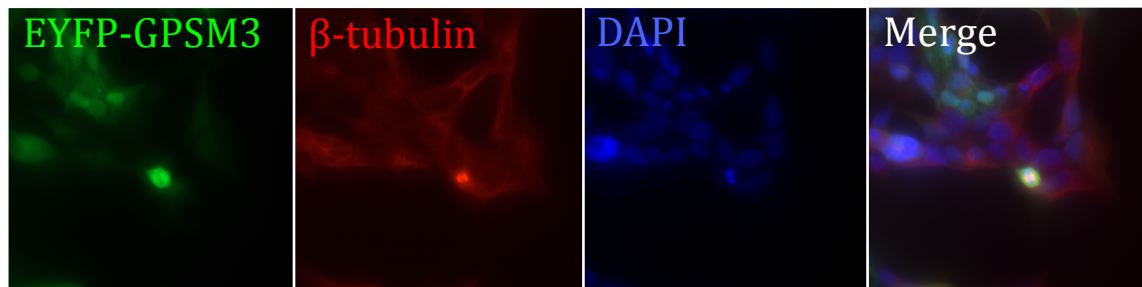


Figure 5.1. Localization of EYFP-tagged GPSM3 during mitosis in HEK-293 cells. HEK-293 cells were transfected with 1 μ g EYFP-GPSM3 DNA plasmid. Cells were serum starved for 24 hours, and 20 hours after serum replacement cells were fixed and subjected to immunofluorescent labeling. Cells were probed with anti- β -tubulin primary antibody (1:500), followed by AlexaFluor 555 goat anti-rabbit secondary antibody (1:500). Nuclei were stained using DAPI. Panels labeled in top left corners. N=3.

5.2 ANIMAL PROTOCOL APPROVAL FORM

Wednesday, November 30, 2016 at 12:05:45 PM Eastern Standard Time

Subject: eSirius Notification - Annual Protocol Renewal APPROVED by the AUS 2013-007::3
Date: Monday, July 11, 2016 at 2:44:34 PM Eastern Daylight Time
From: eSiriusWebServer
To: Robert Gros
CC: [REDACTED]



2013-007::3:

AUP Number: 2013-007

AUP Title: Elucidating molecular mechanisms in vascular signalling

Yearly Renewal Date: 07/01/2016

The YEARLY RENEWAL to Animal Use Protocol (AUP) 2013-007 has been approved, and will be approved for one year following the above review date.

1. This AUP number must be indicated when ordering animals for this project.
2. Animals for other projects may not be ordered under this AUP number.
3. Purchases of animals other than through this system must be cleared through the ACVS office. Health certificates will be required.

REQUIREMENTS/COMMENTS

Please ensure that individual(s) performing procedures on live animals, as described in this protocol, are familiar with the contents of this document.

The holder of this Animal Use Protocol is responsible to ensure that all associated safety components (biosafety, radiation safety, general laboratory safety) comply with institutional safety standards and have received all necessary approvals. Please consult directly with your institutional safety officers.

Submitted by: Kinchlea, Will D
on behalf of the Animal Use Subcommittee

[REDACTED]

5.3 FIGURE REPRINTING PERMISSIONS

License Details

This Agreement between Drew Wallace ("You") and Nature Publishing Group ("Nature Publishing Group") consists of your license details and the terms and conditions provided by Nature Publishing Group and Copyright Clearance Center.

[printable details](#)

License Number	3997760869333
License date	Nov 28, 2016
Licensed Content Publisher	Nature Publishing Group
Licensed Content Publication	Nature
Licensed Content Title	Structural determinants for GoLoco-induced inhibition of nucleotide release by G α subunits
Licensed Content Author	Randall J. Kimple, Michelle E. Kimple, Laurie Betts, John Sondek, David P. Siderovski
Licensed Content Date	Apr 25, 2002
Licensed Content Volume	416
Licensed Content Issue	6883
Type of Use	reuse in a dissertation / thesis
Requestor type	academic/educational
Format	print and electronic
Portion	figures/tables/illustrations
Number of figures/tables/illustrations	1
High-res required	no
Figures	Figure 1: α 1 GDP in complex with the RGS14 GoLoco region.
Author of this NPG article	no
Your reference number	
Title of your thesis / dissertation	Evidence of a role for G protein signaling modulator 3 in cell division
Expected completion date	Dec 2016
Estimated size (number of pages)	150
Total	0.00 CAD

License Details

This Agreement between Drew Wallace ("You") and Cambridge University Press ("Cambridge University Press") consists of your license details and the terms and conditions provided by Cambridge University Press and Copyright Clearance Center.

[printable details](#)

License Number	4012130358461
License date	Nov 28, 2016
Licensed Content Publisher	Cambridge University Press
Licensed Content Publication	Quarterly Reviews of Biophysics
Licensed Content Title	Structural basis of function in heterotrimeric G proteins
Licensed Content Author	William M. Oldham, Heidi E. Hamm
Licensed Content Date	Mar 30, 2005
Licensed Content Volume	39
Licensed Content Issue	2
Start page	117
End page	166
Type of Use	Dissertation/Thesis
Requestor type	Not-for-profit
Portion	Full article
Order reference number	
Territory for reuse	North America Only
Title of your thesis / dissertation	Evidence of a role for G protein signaling modulator 3 in cell division
Expected completion date	Dec 2016
Estimated size(pages)	150
Publisher Tax ID	123258667RT0001
Total	0.00 CAD

CURRICULUM VITAE
DREW WALLACE

EDUCATION

M.Sc. Candidate – Developmental Biology 2013 – 2016
 University of Western Ontario – degree expected in December 2016 London, ON
 ➤ Thesis – Evidence of a role for G protein signaling modulator 3 in cell division

B.Sc. – Honors Specialization Biology, Psychology Minor 2008 – 2013
 University of Western Ontario London, ON
 ➤ 4th Year Thesis – The Mouse Diversity Genotyping Array identifies copy number variants to infer phylogenetic relationships among *Mus musculus* strains

RELATED WORK EXPERIENCE

Teaching Assistant – First Year Biology, Department of Biology 2013 – 2015
 University of Western Ontario London, ON
 ➤ Led tutorials for first year biology courses. Mastered biological concepts in order to teach and demonstrate concepts to 200 undergraduate students. Helped increase course average ~3% by contributing to introduction of a new collaborative examination method. Developed guidelines for evaluating exams and counseled 30+ graduate teaching assistants during the marking process.

Research Assistant – Hill Lab, Department of Biology 2012
 University of Western Ontario London, ON
 ➤ Assisted with data analysis of single nucleotide polymorphisms in the mouse genome. Secured a position to perform my 4th year thesis project with the same supervisor.

Student Mentor – Department of Physiology & Pharmacology 2013 – 2016
 University of Western Ontario London, ON
 ➤ Graduate student supervision – Aneta Surmanski
 Project: G protein signaling modulator 3 in kidney disease states
 ➤ Physiology Pharmacology 4980 Honors Research Project supervision – Nicole Arseneau
 Project: G protein signaling modulator 3 expression profile in a model of hypertension
 ➤ High school Co-op student supervision – Jiyun Han

SCHOLARSHIPS AND ACHIEVEMENTS

- **Western Entrance Scholarship** – M.Sc.
- **Western Entrance Scholarship** – B.Sc.
- **Dean's Honor List** – B.Sc.

SKILLS

- **Cell biology:** basic cell culture, transient transfection, bacterial transformation
- **Molecular techniques:** subcloning, mutagenesis
- **DNA, RNA, and protein techniques:** RNA extraction, Reverse Transcriptase PCR, real-time PCR, protein extraction, SDS page, immunoblotting, protein-protein interaction assay (mammalian two-hybrid), fixation and immunofluorescent labeling of cells
- **Other:** confocal microscopy

CONFERENCES AND PRESENTATIONS

Cardiovascular Journal Club – London, ON October 19, 2016

- Title of seminar presentation: “Evidence of a role for G protein signaling modulator 3 in cell division of vascular smooth muscle cells.”

17th Annual Great Lakes GPCR Retreat – Chicago, IL October 13-15, 2016

- Title of poster presented: “Evidence of a role for G protein signaling modulator 3 in cell division.”

16th Annual Great Lakes GPCR Retreat – Mono, ON October 22-24, 2015

- Title of poster presented: “The role of G protein signaling modulator 3 (GPSM3) in cell division.”

London Health Research Day 2015 – London, ON April 1, 2015

- Title of poster presented: “GPSM3 and its role in cell division.”

OTHER WORK EXPERIENCE

Teaching Assistant – Geography of Tourism, Department of Geography 2015
University of Western Ontario London, ON

- Responsible for quickly and efficiently marking 180+ creative student assignments (PowerPoint presentations, website designs) and 90+ essay-format exams. Held regular office hours and worked closely with students to ensure they understood assignment expectations and how they could improve on past submissions

Summer Student Event Administrator 2013
Canadian Hearing Society Waterloo, ON

- Organized annual golf tournament and auction fundraising event. Increased funds raised by 5% from previous year by recruiting new sponsors and securing new donors for auction prizes and other event services. Return every summer for the annual fundraiser.

COMMUNITY CONTRIBUTIONS AND INVOLVEMENT

Chair and Co-Founder

2016

Lend an Ear London

London, ON

- Founded a student-run organization with the goal of improving communication accessibility for the hearing impaired community of London Ontario. Raised \$500 in our first year to create the Communication Advocacy Scholarship. Communicated with Audiologists and Itinerant teachers associated with the Thames Valley District School Board to raise awareness about the scholarship we provide.

Chair – Community Development Council

2013 – 2015

Canadian Hearing Society

London, ON

- Member of the Community Development Council for 2 years. Helped raise over \$1500 in the first year and over \$2500 in the second. Elected as Chair of the council after first year.

Team Leader – “The Stache Squad”

2014, 2015

Movember Foundation

- Staff members in the Physiology & Pharmacology Department at UWO came together to form "The Stache Squad". We raised \$3408 to contribute to men's health research. Led my team "The Three Mo's touches" the previous year by raising \$505 of our team's \$945 total.

Volunteer

2012 – 2013

Alzheimer's Society

London, ON

- Recognized for supportive skills and positive impact when helping individuals build daily skills through the First Link programs and services. Tasked with interactive activities to build confidence in individuals and their family caregivers through preparing meals, arts and crafts, and gardening. Served as liaison to family, patients and staff for the learning series program.